

SPILL ALERT DEVICE
FOR EARTH DAM FAILURE WARNING

by

Robert M. Koerner and
Arthur E. Lord, Jr.
Drexel University
Philadelphia, Pennsylvania 19104

Grant No. R-602511

Project Officer

John E. Brugger

Oil & Hazardous Materials Spills Branch
Municipal Environmental Research Laboratory
Edison, New Jersey 08837

MUNICIPAL ENVIRONMENTAL RESEARCH LABORATORY
OFFICE OF RESEARCH AND DEVELOPMENT
U.S. ENVIRONMENTAL PROTECTION AGENCY
CINCINNATI, OHIO 45268

DISCLAIMER

This report has been reviewed by the Municipal Environmental Research Laboratory, U. S. Environmental Protection Agency, and approved for publication. Approval does not signify that the contents necessarily reflect the views and policies of the U. S. Environmental Protection Agency, nor does mention of trade names or commercial products constitute endorsement or recommendation for use.

FOREWORD

The U.S. Environmental Protection Agency was created because of increasing public and government concern about the dangers of pollution to the health and welfare of the American people. Noxious air, foul water, and spoiled land are tragic testimonies to the deterioration of our natural environment. The complexity of that environment and the interplay of its components require a concentrated and integrated attack on the problem.

Research and development is that necessary first step in problem solution; it involves defining the problem, measuring its impact, and searching for solutions. The Municipal Environmental Research Laboratory develops new and improved technology and systems to prevent, treat, and manage wastewater and solid and hazardous waste pollutant discharges from municipal and community sources, to preserve and treat public drinking water supplies, and to minimize the adverse economic, social, health, and aesthetic effects of pollution. This publication is one of the products of that research and provides a most vital communications link between the researcher and the user community.

The subject of this report is the development of a spill-alert device for earth dam safety warning systems to identify dams that are in danger of failing and emptying their contents into downstream waters. For those dams that are in need of repair, the device can also act as a construction design aid to identify the adequacy of these repairs. This report will be valuable to governmental (Federal, state, and local), industrial, and private owners and operators of earth dams, dikes, embankments, lagoons, and impoundments that contain liquid materials and semi-solid sludge. The impounded material can be of any type, but the work described in this report focuses on liquid hazardous materials. The report is also of interest to researchers investigating the fundamental aspects of soil strength in relation to its "noise" generation during stressing. These noises, or more appropriately, acoustic emissions, are at the heart of this detection system. Further information on the subject may be obtained by contacting the Oil and Hazardous Materials Spills Branch of the Municipal Environmental Research Laboratory (Cincinnati) at Edison, N. J. 08837.

Francis T. Mayo, Director
Municipal Environmental
Research Laboratory

ABSTRACT

A spill alert device for determining earth dam safety based on the monitoring of the acoustic emissions generated in a deforming soil mass was developed and field tested. The acoustic emissions are related to the basic mechanisms from which soils derive their strength. Laboratory feasibility tests, conducted under widely varying conditions, have resulted in an instrument package consisting of a wave guide (a steel rod projecting into the earth mass), a transducer (to convert the mechanical waves transmitted from the deforming soil into an electrical signal), an amplifier (to increase the signal level), and a counter (to quantify the signal). The resulting monitoring system has been field tested at 19 field sites and found to portray accurately the stability of the particular site in question. Additional detail has been added that enables the following categorization of the relative stability of the soil mass being monitored:

No emissions: soil mass is at equilibrium and safe.

Low emissions: continue to monitor soil mass.

High emissions: soil mass requires remedial work.

Very high emissions: this situation requires evacuation of downstream residents.

This report was submitted in fulfillment of EPA Grant No. R-802511 by Drexel University under the sponsorship of the U. S. Environmental Protection Agency. This report covers the period from July 1, 1973, to June 30, 1979, and work was completed as of June 30, 1979.

CONTENTS

Foreword.	iii
Abstract.	iv
Figures	vi
Tables.	xi
Acknowledgements.	xii
1. Introduction.	1
2. Conclusions	2
3. Recommendations	3
4. Background and Project Design	4
5. Acoustic Emissions Fundamentals	7
6. Fundamentals of Acoustic Emissions in Soils	14
7. Applications of Acoustic Emissions in Soils	51
8. Spill Alert Device Details.	74
References.	81
Appendices.	86
A. Published and/or submitted technical papers on acoustic emission monitoring	86
B. Spill alert device users manual	89
C. Application of acoustic emission monitoring in seepage.	95
D. Application of acoustic emission monitoring in pipelines.	100
E. Application of acoustic emission monitoring in concrete	109
F. Glossary	116

FIGURES

<u>Number</u>	<u>Page</u>
1 Schematic diagram of acoustic emission monitoring system showing typical oscilloscope trace of series of emissions.....	8
2 Frequency distribution for silty sand soil tested in (a) unconfined compression and (b) triaxial shear at 69 kN/m ² (10 psi) confining pressure.....	16
3 Frequency versus attenuation response of dry granular soils using various techniques indicated.....	18
4 Granular soils tested.....	21
5 Schematic diagram and photograph of acoustic emission monitoring setup on stressed soil specimen tested in triaxial shear.....	22
6 Isostatic test results (time versus acoustic emission in units of 10,000 counts) for four granular soils listed in Table 2.....	23
7 Triaxial shear test results (deviator stress versus acoustic emission in units of 100,000 counts) for four granular soils listed in Table 2.....	25
8 Triaxial shear test results (deviator stress versus acoustic emission in units of 100,000 counts) for four granular soils listed in Table 2.....	27
9 Average amplitude of acoustic emissions (measured as peak signal voltage output) for various soils as function of percentage failure stress in triaxial creep at 34 kN/m ² (5 psi) confining pressure.....	32
10 Frequency distribution of acoustic emissions from kaolinite clay (soil No. 6) tested in unconfined compression at 33% water content.....	33
11 Attenuation of acoustic emissions in clayey silt (soil No. 5) at varying water contents at frequency of about 1 kHz.....	35

<u>Number</u>		<u>Page</u>
12	Triaxial creep response of clayey silt (soil No. 5) at varying confining pressures.....	36
13	Triaxial creep response of kaolinite clay (soil No. 6) at varying confining pressures.....	37
14	Stress/acoustic emission response of clayey silt (soil No. 5) at varying water contents in unconfined compression.....	39
15	Stress/acoustic emission response of four cohesive soils in triaxial creep tests showing significance of plasticity index.....	40
16	Unconfined compression test results for undisturbed sample of silty clay (soil No. 7) at 56% water content.....	41
17	One-dimensional consolidation response of sandy, silty clay at constant pressure on log-time scale.....	43
18	One-dimensional consolidation response of sandy silty clay over range of pressures showing strain and acoustic emission responses.....	44
19	Effect of varying parameters in Equation (10) to observe behavior in maximum acceleration of emissions.....	49
20	Experimental setup and location of wave guide/accelerometer's first resonance as a function of length considering different diameter and geometry of steel rods.....	53
21	Elevation and plan views of site 3 near McCook, Nebraska, showing horizontal wave guide location scheme.....	57
22	Elevation view of site 5 in Philadelphia, Pa., showing surcharge load and compressible soil along with different types of wave guides.....	59
23	Time/settlement and time/acoustic emission response curves from site No. 5.....	60
24	Acoustic emission count rate versus time of cut for site No. 13 showing failure after fourth cut.....	63

<u>Number</u>		<u>Page</u>
25	Schematic diagram of site No. 14 showing approximate boundaries of five cuts made and photographs after Cut Nos. 1 and 4.....	65
26	Acoustic emission response after Cut No. 1.....	67
27	Acoustic emission response after Cut No. 2.....	67
28	Acoustic emission response after Cut No. 3.....	68
29	Acoustic emission response after Cut No. 4.....	68
30	Acoustic emission response after Cut No. 5.....	69
31	Summary of acoustic emission rates after each cut.....	71
32	Settlement and acoustic emission response curves from site No. 18, showing response at various locations along slide area.....	73
33	Photograph of acoustic emission field system.....	75
34	Photograph of acoustic emission field system.....	76
35	Photograph of acoustic emission laboratory system.....	77
36	Photograph of acoustic emission laboratory system.....	78
37	Photograph of acoustic emission laboratory system.....	79
B-1	Photographs of spill alert device components.....	90
B-2	Details of wave guides used in acoustic emission monitoring.....	92
B-3	Sample monitoring sheet.....	94
C-1	Flow rates and acoustic emission rates compared for seepage study at site No. 15.....	97
C-2	Experimental setup for study of acoustic emission results from soil void seepage.....	98

<u>Number</u>		<u>Page</u>
C-3	Acoustic emission rates for flow of water through a column of Ottawa sand.....	99
D-1	Acoustic emission count rate versus internal pipe pressure for air leaking from 15.2-cm (6-in.) diameter pipe.....	102
D-2	Acoustic emission counts versus internal pipe pressure for water leaking from 15.2-cm (6-in.) diameter pipe.....	103
D-3	Acoustic emission counts versus internal pipe pressure for oil leaking from 15.2-cm (6-in.) diameter pipe.....	104
D-4	Field results of signal amplitude and acoustic emission count rate for a constant-source leak in a 7.6-cm (3-in.) diameter pipeline as a function of distance from the leak.....	106
D-5	Field results of acoustic emission count rate for a pulsating leak in a 7.6-cm (3-in.) diameter pipeline as a function of distance from the leak and on both sides of the leak.....	107
D-6	Data of Figure D-5 replotted to illustrate the method of leak source location using the acoustic emission monitoring technique.....	108
E-1	Load versus acoustic emission response of 3-day-old concrete specimens showing effect of load cycling on acoustic emissions.....	111
E-2	Acoustic emission response of concrete cylinders as a function of age (curing time) at various percentages of ultimate fracture load.....	112
E-3	Acoustic emission versus time response for creep tests (sustained-load tests) at various percentages of ultimate failure load.....	113

<u>Number</u>		<u>Page</u>
E-4	Acoustic emission rate versus time response for creep tests (sustained-load tests) at various percentages of ultimate failure load over long-term monitoring.....	114
E-5	Load versus acoustic emission response of concrete beams tested in three-point loading tests (flexure tests) with transducer mounted either on the compression face or on the tension face.....	115

TABLES

<u>Number</u>		<u>Page</u>
1	Categorization of Acoustic Emission Level as Obtained from Spill Alert Device on Numerous Earth Dams.....	2
2	Effect of Particle Characteristics on Acoustic Emission in Granular Soil	20
3	Properties of Cohesive Soils Used in this Study.....	30
4	Influence of Medium Surrounding Wave Guide on Frequency and Amplitude of First Resonance.....	54
5	Overview of Sites Being Monitored Using the Acoustic Emission Method.....	56
6	Acoustic Emission from Neb-200 Dam Site.....	58
7	Commercially Available Acoustic Emission Equipment.....	80

ACKNOWLEDGEMENTS

The authors express their sincere appreciation to all those who contributed so generously to the completion of this project. Special thanks are due to John E. Brugger, EPA Project Officer, Ira Wilder, Oil & Hazardous Materials & Spills Branch Chief, and W. Martin McCabe, Research Assistant, Drexel University, for their excellent cooperation, interest, and enthusiasm.

The laboratory work was performed mainly by W. Martin McCabe, John W. Curran, Shirley L. McMaster, and John V. Lima, with technical assistance by Albert Bangs and Kenneth Whitlock.

The difficult and costly field work aspects of the study would not have been possible without the cooperation of the following public and private organizations.

USDA Soil Conservation Service

Bethlehem Steel Corporation

City of Philadelphia, Division of Aviation

Site Engineers, Inc., Cherry Hill, N. J.

Les Mines Madeleine, Ltd., Quebec, Canada

Borough of Boyertown, Boyertown, Pa.

City of Hopewell, Va.

U. S. Coast Guard

Thomas M. Durkin and Sons, Inc., Philadelphia, Pa.

Raymond International, Inc., Soiltech Division

Our thanks are also expressed to Sidney Mathues and Richard Spotts of the General Electric Co. (Philadelphia), who lent and/or donated instrumentation to Drexel University.

The preparation of this report was accomplished through the efforts of John J. McElroy, who drew all figures, and Elizabeth T. Fox, who typed the manuscript; to them, we express our sincere thanks.

SECTION 1

INTRODUCTION

A research and development program was undertaken to understand the fundamentals, investigate the feasibility, and refine the development of a field device--based on the detection and measurement of acoustic emissions--to monitor the stability of earth dams. This program included the laboratory investigation of a wide range of soil types (sands, silts, and clays) under varying conditions (density, moisture, stress state, etc.) in relation to acoustic emission behavior. After this information was acquired and analyzed, a field-use system was assembled that met the combined objectives of portability, ease-of-use, rapid data acquisition and analysis, and low cost. This system is known as a spill alert device and consists of a steel rod wave guide, transducer, amplifier, and counter. Included in this report are the essential elements of the laboratory program (Sections 5 and 6), the field program (Section 7), and the final unit as currently used (Section 8).

Parallel studies that have spun off from this project (e. g., acoustic emission monitoring of seepage, pipelines, and concrete) are included as appendices.

SECTION 2

CONCLUSIONS

The principle of the spill alert device described in this report is based on the detection and analysis of the acoustic emissions generated by a deforming soil mass. These internal sub-surface acoustic emissions are brought to the ground surface by a steel rod wave guide, converted to an electrical signal by a transducer, amplified, shaped, and finally counted on a frequency counter. The acoustic emission counts are directly related to the stability of the earthen mass being monitored (Table 1). With the acoustic emission count level known, the stability assessment is immediately available--a major goal of the study. Other goals of the study were also realized in that the device is portable (all components are battery operated), is lightweight (less than 18 kg (40 pounds)), consists of commercially available components that are reasonably priced (the entire system cost about \$2,000 in 1979), is rapid (each monitoring station requires only 3 to 10 min), and yields easy-to-interpret data.

TABLE 1. CATEGORIZATION OF ACOUSTIC EMISSION LEVEL AS OBTAINED FROM SPILL ALERT DEVICE ON NUMEROUS EARTH DAMS*

Acoustic emission level (counts/min.)	Soil deformation	Relative safety	Recommendation
Negligible (0 to 10)	None	Good	Visit periodically
Low (10 to 100)	Slight	Marginal	Continue to monitor
High (100 to 1,000)	Large	Poor	Remedial measures required
Very high (greater than 1,000)	Very large	None	Evacuate downstream

* These results are based strictly on the monitoring done in the project.

SECTION 3

RECOMMENDATIONS

As a result of this 6-year project, the spill alert device is based on a firm technical background. Its feasibility has been verified by numerous small-scale laboratory tests and by extensive work in the field. Nineteen sites have been; or are in the process of being, monitored by the techniques. Persons and organizations other than EPA or Drexel University are being encouraged to use the system to assess its utility and to discover its limitations and/or flaws. To this end, we have been actively publishing, lecturing, and making the equipment available to those with valid uses for such a monitoring system. Thus, technology transfer to the intended user remains as the final, currently identifiable goal of this project.

Among other candidates for acoustic emission monitoring are above-grade stockpiles of non-soil, industrial materials (e.g., tailings, fly ash, phosphate residues (slimes), gypsum). Such mounds can yield or fail during or following rainstorms. Additionally, certain above-grade sanitary landfills and poorly engineered dumps (both of which have large non-soil components) are subject to disintegration for which advance warning can be obtained by acoustic emission methods.

The detailed relationship between flow patterns and acoustic emissions of water-rich clays, silts, and thixotropic materials should be further investigated.

Additional lab and field work should be done on the use of sound-attenuating jackets or shields bonded to the metal waveguides so that emissions will be only transmitted from the stratum where the soil or other material is in contact with the uncovered rod.

To keep potential and actual users of acoustic emission techniques in dike integrity assessments current with the state-of-the-art, the convening of topical conferences and symposia (preferably with published proceedings) should be fostered.

Consideration should be given to the development by ASTM or similar associations of guidelines or, better, standards for the use of acoustic emission in soil applications.

Acoustic emission techniques are recommended for (and in some instances, have already been applied to) slope stability of cuts and fills, subsurface seepage (piping), and related civil engineering concerns.

SECTION 4

BACKGROUND AND PROJECT DESIGN

The problem of earth dam failures, which includes earthen dikes, holding ponds, lagoons, embankments, etc., is ageless, but it probably entered the technical literature in 1889 with the failure of the South Fork Dam in Pennsylvania, which caused so much death and destruction in Johnstown. Since that time, so many earth dam failures have occurred that a categorization is possible: 30% of failures were structural, 40% were seepage, and 30% were hydraulic (1). The problem is far from being solved. Since 1972, when the authors began working in this area, four major failures have occurred, all of which have been widely publicized by the news media. These failures included Buffalo Creek, West Virginia (February 26, 1972); Grand Teton, Idaho (June 5, 1976); Johnstown (Laurel Run), Pennsylvania (July 20, 1977), and Toccoa, Georgia (November 4, 1977).

Along with the failures of these major dams have been the failures of innumerable small dams of both private and public ownership. The latter category (small dams) has received little attention, since such failures have usually produced no loss of life and only minor property damage. Their environmental damage, however, has often been devastating. This is particularly the case with failure of dams containing hazardous materials or industrial wastes, which cause extensive fish kills and water pollution, depending on the original water quality of the receiving stream or river. The category of small earth dams is the one focused on by this research and development project, but the results are applicable to all types of unstable earth masses.

Initial feasibility tests on acoustic emission generation in soils were carried out in 1970 and 1971 and published in a short paper in January 1972. By July 1, 1973, the first part of a 6-year research and development effort was funded by the U. S. Environmental Protection Agency (EPA). This report summarizes this effort.

Work carried out under the project has been brought to the attention of the technical community through publications in various journals and conference proceedings. In all, 30 papers have been written by the principal investigators on the subject. The complete reference list is given in Appendix A of this report.

The most significant achievement is that the effort resulted in the fabrication of a usable and workable earth-mass monitoring system known as an earth dam spill alert device. The device has been field tested and calibrated, and it is available for both government and private use. The

system consists of components that are all commercially available and easy to assemble, install, and use. The version of a user's manual is given in Appendix B of this report.

Several industrially engineered and packaged acoustic emission-based systems for field use in dam and soil stability evaluations are now available commercially. We are convinced that the monitoring system resulting from this research and development program will find widespread use in evaluating the stability of earth masses in the near future.

In 1977, the acoustic emission system was entered in the prestigious IR-100 competition, in which awards are made annually on the basis of the 100 most significant advances in industrial research and development. The ceremony is held at Chicago's Museum of Science and Industry and the winning entries are on display for a month. The contest is sponsored by INDUSTRIAL RESEARCH (now INDUSTRIAL RESEARCH AND DEVELOPMENT), a widely distributed publication that reports on those advances in R&D that have special and practical application to industrial problems.

Koerner and Lord began their joint work (which ultimately led to the work described here) by studying the relation between acoustics and soils in 1970. The first research covered measuring the strength of the returned ultrasonic echo from an Al_2O_3 /soil interface as the soil dried. They expected to detect the shrinkage limit, etc. in this manner. Results were poor. The next project was an attempt to measure the dynamic Young's modulus of a soil in the composite resonator (bending mode vibration of steel strip plus soil layer) apparatus of Bruel and Kjaer. Again, results were inconclusive.

Fortunately, the next joint venture was quite productive from the start. Transducers and amplifiers most sensitive in the kilohertz region were kindly loaned to the authors by Sidney Mathues and Richard Spotts of the General Electric Company of Philadelphia.

Soil samples were axially loaded to failure, and the receiving transducer picked up the generated noises throughout the deformation process, up to and including failure. When the transducer output was fed into an amplifier, shaped, and then counted on a frequency counter, the response revealed a basic similarity to the typical stress-versus-strain response. A series of tests at varying water contents on clayey silt soil samples (locally called Delaware River silt) resulted in logical trends, since the lower the water content, the greater the emissions and also the greater the strength. These data and the resulting family of curves were reported in a paper which was published as a Technical Note (2) in the Geotechnical Engineering Division Journal of the American Society of Civil Engineers in January, 1972.

Applications of this newly found phenomenon seemed numerous, since soil masses are known to deform before reaching a failure state. Such problems are encountered with retaining walls, footing foundations, pile deformations, underground tunnels, pipelines, etc. and were all reasonable target areas for application. None seemed so promising as the slope stability area in general and earth dams in particular. During the proposal

writing stage, we became aware that our "noise" monitoring of soils had much in common with microseismic monitoring of rock by geologists and geophysicists and the acoustic emission monitoring for flaws of pressure vessels and metals by metallurgists and aerospace engineers. This parallel body of literature was reported in a state-of-the-art review by Lord (3), which was in preparation at about the same time that a sponsoring agency was being sought. The information that follows in this report was all done under EPA sponsorship and, for the most part, is taken from various sections of the papers listed in Appendix A, particularly references 4, 5, 6, and 7.

SECTION 5

ACOUSTIC EMISSION FUNDAMENTALS

Introduction

Acoustic emissions are the internally generated sounds that a material produces when it is placed under certain stress conditions. Sometimes these sounds are audible (wood cracking, tin crying, ice expanding, soil and rock particles abrading against one another, etc.), but more often they are not heard by humans, either because of their low magnitude or high frequency or both.

Normally a piezoelectric sensor (an accelerometer or transducer) is used to detect the acoustic emissions. These sensors, when mechanically stimulated, produce an electrical signal. (The casual reader may note a similarity to what is commonly called a microphone). The signal is then amplified, filtered, shaped, counted, and displayed or recorded. Figure 1 shows a schematic drawing of a typical acoustic emission monitoring system being used as a stress is applied to a soil sample in unconfined compression. Also shown is an oscilloscope trace of a typical set of acoustic emission bursts from a stressed soil sample. The counts or recordings of the emissions are then related to the basic material characteristics to determine the relative stability of the specimen being tested. (Counts refer to electric pulses above a threshold level.) When no acoustic emissions are present, the material is in equilibrium and thus stable under that condition. When emissions are observed, however, a nonequilibrium situation is present that, if continued, can ultimately lead to specimen failure.

Literature Survey

With respect to Figure 1, it should be noted that two types of soil strength tests are commonly performed; one called unconfined compression tests, the other, triaxial shear tests. Some explanation of these tests may be of value. The soil sample is usually in the form of right circular cylinder. It is taken from the sampling tube (or made in the laboratory) and placed on a metal base especially prepared for such tests. (The test is an ASTM Standard.) The upper base plate is placed on top of the sample and the assembly is then fitted with a thin rubber membrane and made leakproof using O-rings. A plastic cylinder of approximately twice the diameter of the sample is then installed and the chamber is bolted together to the upper assembly which has a free moving piston in it. Water is next introduced into the plastic chamber surrounding the rubber membrane encased soil sample. When the sample comes to equilibrium, the pressures are ready to be imposed.

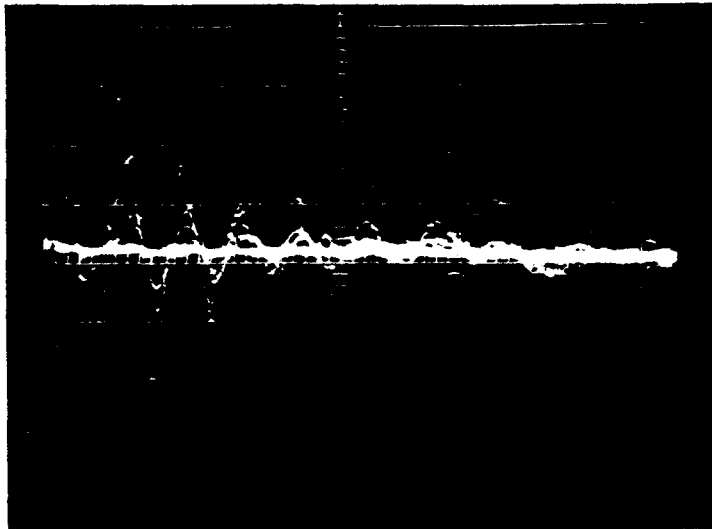
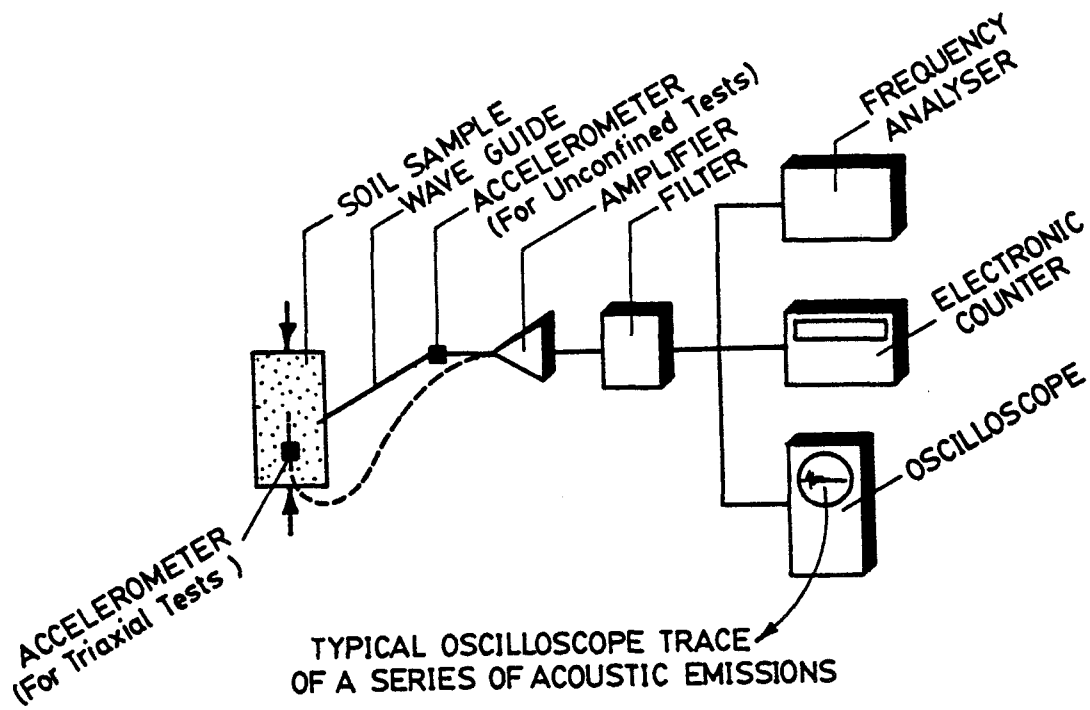


Figure 1. Schematic diagram of acoustic emission monitoring system showing typical oscilloscope trace of series of emissions.

If no confining pressure is applied (the weight of the water is almost negligible), the piston imposes vertical load to the sample until it eventually fails. The vertical load divided by the sample area is the major principal stress (σ_1). Since there is not confining pressure, the horizontal stress, called the minor principal stress (σ_3), is zero. (In these tests, the intermediate principal stress (σ_2) is always equal to the minor principal stress (σ_3)). Hence the test is called an "unconfined compression" test. It is often performed without water in the chamber and without a rubber jacket surrounding the sample, i.e., just an axial load on the sample until it fails.

The "triaxial shear" test is intended to simulate the effect of in-situ horizontal stresses acting on the soil. Prepared as described above, the test consists of a two-part process. First, air pressure is applied to the water in the chamber, which in turn stresses the rubber membrane and the soil contained within it. This stress is truly hydrostatic, hence isotropic, and its magnitude should be representative of conditions in the soil as they exist. Being isostatic, there are no principal stresses, and the magnitude is often designated σ_0 . After equilibrium of the soil to this stress is established, the second part of the test begins.

Axial load from the piston is now initiated. Immediately, σ_0 conditions are lost. Now, the constant value of cell pressure on the water becomes the minor principal stress (σ_3), which is numerically equivalent to the former value of σ_0 . The difference is that the axial load piston is now at a higher stress magnitude which, in fact, is the major principal stress, σ_1 . The test continues by gradually increasing the axial load piston, i.e., increasing the σ_1 stress, until shear failure of the soil sample occurs. Throughout the test the lateral stress remains at the same magnitude. This particular test, the triaxial shear test, is the premier soils test for determining:

- o modules of elasticity
- o strain at failure
- o shear strength

When a series of such tests are performed on different soil samples, at different confining stresses, the shear strength parameters " c " and " ϕ " can be obtained, where

- c = cohesion (soil strength at zero confinement)
- ϕ = angle of shearing resistance (friction angle)

These values are routinely used in the design and analysis of problems involving stability of soil masses.

To return to Figure 1, in the unconfined tests, the accelerometer wave guide can merely touch the surface or be inserted in a small drilled hole. A core of natural material or a shaped compacted cylinder can be used. In the triaxial test, the accelerometer and short wave guide are embedded in the sample. The accelerometer + guide can be embedded during sample forming or can be inserted in a hole that is subsequently packed full with the test material. (More details are provided in Figure 5, which will not be discussed at this point.)

Historically, acoustic emission work began in the mining industry to detect instability in mine roof, face, and pillar rock to predict when failure might occur. This work was initiated by Obert (8), and Obert and Duvall (9) in the United States, and by Hodgson (10,11) in Canada. Their monitoring of rock emissions, which they called microseisms, began in the early 1930's and has continued to the present by the Bureau of Mines' scientists (12) and others (13,14). Although these pioneering workers were hampered by a lack of sophisticated and reliable equipment, their ideas and goals were certainly in the right direction and set the tone (no pun intended!) for many modern projects.

Beginning in the 1950's, acoustic emission research was initiated in the metals area. Kaiser (15,16) worked with steel, copper, aluminum, lead, and zinc. He discovered many fundamental properties that relate stress behavior to acoustic emissions. Tatro and Liptai, (17,18) in the early 1960's, used the technique as a yield detector in metals and also did pioneering work in analyzing the fundamental characteristics of acoustic emissions in metals. Recently, the most active acoustic emission work has been in the area of nuclear pressure vessel proof-testing (19,20). A large number of transducers are placed on the vessel, which is pressurized. Any flaws that may be present are detected and evaluated by their acoustic emission response. These flaws can be source-located to within inches of their actual locations.

While the previously mentioned materials (rocks and metals) have been the major subjects of acoustic emission research, other materials have also been evaluated. These include composites, concrete, ceramics, ice, and wood, and the results have been summarized in a number of review articles written by Liptai et al (21), Dunegan and Tatro (22), Knill et al (23), and Lord (3). In addition, a recent bibliography on the subject has been compiled by Drouillard (24).

Information regarding the acoustic emission response of soils is noticeably lacking in the literature. The original soils reference, stemming from a rock monitoring program (25), appears to have been by Cadman and Goodman (26), who addressed soils, per se, in a relatively preliminary manner. Subsequent work has been done by the authors at Drexel University over the past 6 years and is summarized in this report.

ACOUSTIC EMISSION SOURCES

To familiarize the reader with the concept of acoustic emission, it is important to examine the initiation or source of the emissions in stress materials of different types (including metals, single crystals, and rocks) and to hypothesize behavior in granular and cohesive soils.

Metals

A wide variety of mechanisms can generate acoustic emissions in metals. According to Pollock (27), the formation and propagation of dislocations (defined by Van Vlack (28) as highly stressed crystalline

imperfections usually appearing as line defects) and the fracture of brittle, dissimilar particles locked within the crystalline structure (i.e., inclusions (29)) can produce weak signals. Stronger signals are produced by initiation and propagation of macroscopic cracks (i.e., those greater than 0.01 mm (3.9×10^{-4} in.) in length). Though metallurgists generally agree on the foregoing as being probable acoustic emission sources, substantiation of this theory is difficult since few controlled experiments of a fundamental nature have been conducted.

Ionic Crystals

Engle (30) used single crystals of lithium fluoride oriented for minimum resistance to displacement. Acoustic emission and displacement as small as 10^{-7} cm (4×10^8 in.) were measured during stress application. In general, he found that acoustic emission activity was directly related to the cause and nature of piled up dislocations.

Sedgwick (31) tested both lithium fluoride and potassium chloride in compression within the elastic range. He found that the rapid dislocation movement that occurs in hard lithium fluoride crystals produced greater acoustic emission activity than the typically slow dislocation movement occurring in the softer potassium chloride crystals. In addition, his analysis of the acoustic emission distribution formed the basis for a macroscopic deformation model for lithium fluoride. The model predicts values of dislocation strain, dislocation density, and ultrasonic attenuation that agree well with the experimental data.

Additional aspects of the study of acoustic emission initiation in metals and crystals can be found in the review article by Lord (3).

Rock

Audible noises from cracking pillars and roofs in mines provided the initial impetus for acoustic emission monitoring by Obert (8).

Laboratory testing of rock specimens convinced Scholz (32) that the first signals received after the application of stress were caused by crack and pore closure. Both the amplitude and number of emissions recorded then increased continuously as macroscopic cracks were initiated and propagated in first a stable, then an unstable manner. He finally concluded that, when rupture of the specimen was near, friction along crack surfaces--as well as crack propagation and coalescence--were contributing to the acoustic emission activity.

Mineral and lithological differences among rock specimens have been shown by Knill et al (23) to affect the amount of acoustic emission activity recorded. Chugh et al (33) have noted changes in the nature of emissions caused by varying moisture and stress conditions. The effects of factors such as these will be addressed later in this study.

Soils

The mechanisms responsible for the shear strength of soils appear to be the basic generators of acoustic emissions in soils. These mechanisms in granular soils are the fundamental components of the angle of shearing resistance, including sliding and rolling friction, degradation, and dilation (34,35). In simple cases, sandy (non-cohesive) soils, the angle of shearing resistance, ϕ , is defined by the equation: shear strength (τ) = normal effective stress on the failure surface (σ_n) multiplied by $\tan \phi$; in the case of a cohesive (clay) soil, a term "c", cohesion, in stress units is added to the right side of the equation.) Evidence for such a conclusion will be provided here to show that conditions producing the greatest number of interparticle and therefore frictional contacts (i.e., well-graded soils) also produce the greatest level of acoustic emission activity. The tendency of a granular soil to generate more emissions with higher confining pressures and consequently higher frictional forces is further evidence of a friction-based emission source.

Horn and Deere (36) have shown that the frictional characteristics of soil particles vary with mineral type. One would then logically conclude that mineral type will also affect acoustic emission activity, although this hypothesis has not yet been tested.

The strength mechanisms for most cohesive soils in a drained test include both friction and cohesion. Some perspective on the relative contribution of these mechanisms to the acoustic emission behavior of soils will be discussed later.

ACOUSTIC EMISSION APPLICATION WITH EMPHASIS ON CIVIL ENGINEERING

The civil engineering community has recently taken an interest in the acoustic emission technique and is nondestructively monitoring a wide variety of structures. This activity is important since this particular group is the most likely user of the earth dam warning system developed in this project; the greater their familiarity with the technique, the more favorable will be their response.

Continuing with the classic work originated in rock monitoring, Hardy and Khair (37,38) have adapted the technique to determine the safety of over-pressurizing underground gas storage facilities, and Mearns and Hoover (14) have continued a long-term project of monitoring the stability of rock highway slopes begun by Goodman and Blake (25). Closely related is the work of Wisecarver et al. (39), who have used the technique to determine the stability of large, open-pit mine walls and concluded that the technique is a satisfactory means for monitoring slope stability in rock and for determining the adequacy of corrective measures.

Liptai (40) and Hutton (41) report use of the technique to inspect the safety of large crane rails and wooden roof trusses, and the compression effects of tendons in prestressed concrete beams and even in bridges. Regarding highway bridge inspection, Galambos and McGogney (42) include

acoustic emission monitoring as a possible nondestructive testing method in their recent state-of-the-art review.

With rapid growth predicted in materials transportation by pipeline (43), leak detection and overstressing (44) become significant economic and environmental problems. Acoustic emission techniques have been used with considerable success on buried (45) and underwater pipelines (46) to determine whether they are leaking and to determine the actual location of the leak.

Another area recently studied using the acoustic emission technique is that of monitoring stressed wire rope (47,48). Tensile tests have shown that there is a direct correspondence between wire breakage and acoustic emission events, and that damaged cables are more emissive at a given load than undamaged ones (49).

SECTION 6

FUNDAMENTALS OF ACOUSTIC EMISSION IN SOILS

In this project, soils were broadly classified as sandy soils and cohesive soils.

Sand is a soil composed largely of siliceous particles ranging in nominal diameter from 0.074 mm (74 microns = 0.003 in. = retained by No. 200 sieve) to 4.76 mm (ca. 0.2 in. = passed by No. 4 sieve) and thus covering a ratio of diameters (largest:smallest) of 65 : 1. The sands studied included the following types: round (Ottawa sand), subround (beach sand), angular (concrete-making sand), and subangular (sand drain soil).

Cohesive soils include clays, silty clays, and clayey silts. Clays are soils capable of remaining in a plastic state over a relatively wide range of water contents. A silt is a fine-grained soil of low plasticity. Commonly, a silt is a fine sand that can float in a watercourse, but the term is sometimes indicative of organic content.

In this study, all cohesive soils passed a No. 200 sieve (-200 mesh). In classifying the cohesive soils, an important parameter is the liquid limit, which is defined as the water content of a cohesive soil in which a cut closes under specified test conditions. "L" means less than 50% water; "H", greater than 50% water. Soils are also classified as "M" (silts and silty clays), "C" (clays), and other types of no interest here. The cohesive soils tested included a clayey silt (ML); a kaolinite clay (MH) (kaolin is a white clay of low plasticity); a silty clay (CL); and a Bentonite clay (CH)--(Bentonite is highly plastic, results from decomposition of volcanic ash, and swells considerably on wetting).

Additional description and characterization is included in the text of this report (vide infra).

GRANULAR SOILS

This section describes the behavior of velocity, frequency, and attenuation in granular soils such as gravels and sands and the effects of several important physical properties of these soils.

Velocity of Acoustic Emissions (Elastic Waves) in Granular Soils

Although the subject of velocity of elastic waves in soils is not used directly in our acoustic emission studies, it is of significance to know how fast such waves travel from their source to the pickup accelerometer or wave guide.

Velocity measurements in soils were made in the following manner: a small hammer regulated by a timing device was used to generate an impulsive mechanical wave in a large tank containing silty sand. This reasonably reproducible signal was then monitored by using two strategically placed accelerometers from which the wave velocity was computed. This test was actually developed to determine soil attenuation as obtained from the difference in magnitudes of the two accelerometer responses, a topic that will be examined more fully later in this section. Measurements in the granular soil produced velocity values from 120 to 240 m/s (400 to 800 ft/s), depending on density and water content. These values are consistent with the literature, which is quite abundant on this particular topic. Thus, only one general reference by Hardin (50) is cited.

For the acoustic emission study presented here, this velocity information leads to the conclusion that detection of wave pulses in small laboratory samples is essentially simultaneous with their initiation. Furthermore, the pulses are probably accumulations of all types of waves (P, S, and R) generated at the individual sites with the soil mass, where P = longitudinal elastic wave (primary wave); S = shear elastic wave (secondary wave), and R = Rayleigh surface elastic wave (see Glossary).

Frequency of Acoustic Emissions in Granular Soils

Of considerable interest with regard to accelerometer selection, sensitivity, monitoring procedure, etc., are the predominant frequencies of waves emanating from stressed soil samples. To determine the frequency composition, a series of unconfined compression creep tests was performed on dry, silty sands 70 mm (2.8 in.) in diameter and 150-mm (6.0-in.) high. The emissions were converted to electric analogs, taped, and then played back through a Bruel and Kjaer octave band filter. Tests resulted in the response shown in Figure 2(a), where emissions are predominantly in the 500-Hz to 2-kHz region (Hz = cycles per second).

In addition, triaxial shear creep tests were performed on the same soil at 17% water content and at a 69 kN/m^2 (kilo-Newtons per square meter) ($10 \text{ lb/in}^2 = 10 \text{ psi}$) confining pressure. Figure 2(b) shows this response, where the dominant frequencies are now in the 4- and 8-kHz bands. The mode of generation of the acoustic emissions has thus changed. Our tentative explanation is that densification as a result of confinement has allowed more of the higher frequency signals to pass through the soil structure in a less attenuated manner than with loose density soils. Thus the dominant frequencies have shifted upward.

Additional tests led to the conclusion that accelerometers having a band width from 500 Hz to 15 kHz are adequate for acoustic emission studies in soils. At frequencies lower than 500 Hz, background noise becomes very troublesome whereas, at higher frequencies, essentially no undamped emissions are present.

Attenuation of Acoustic Emission in Granular Soils

Although the tendency of soils to attenuate stress waves (especially

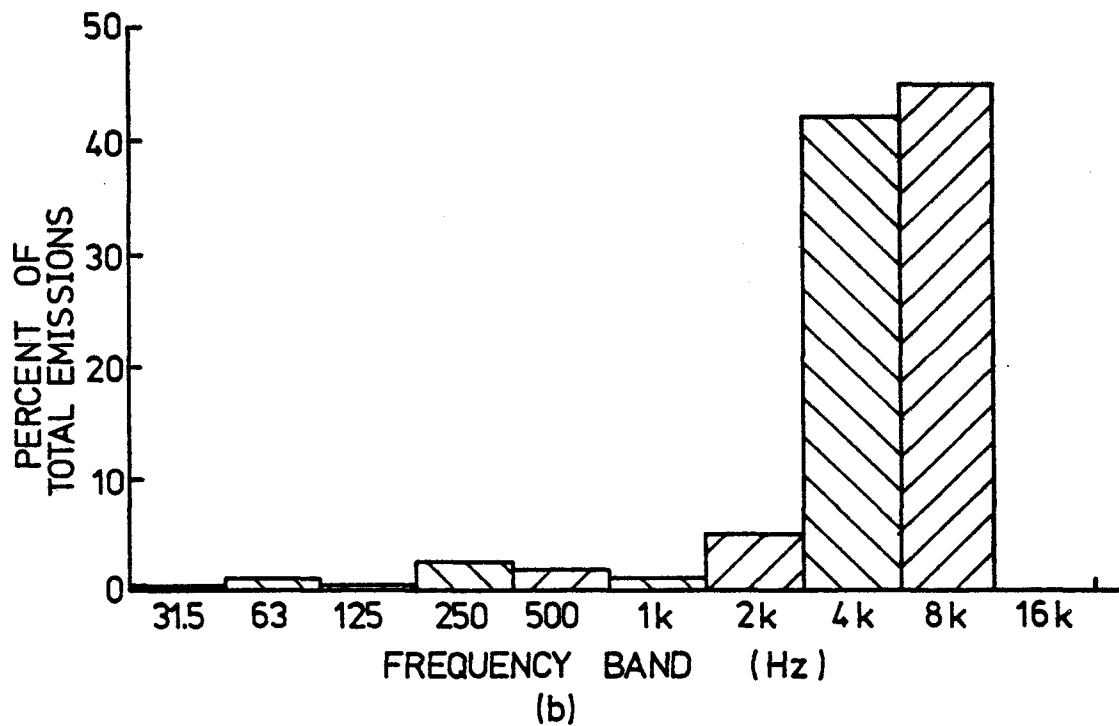
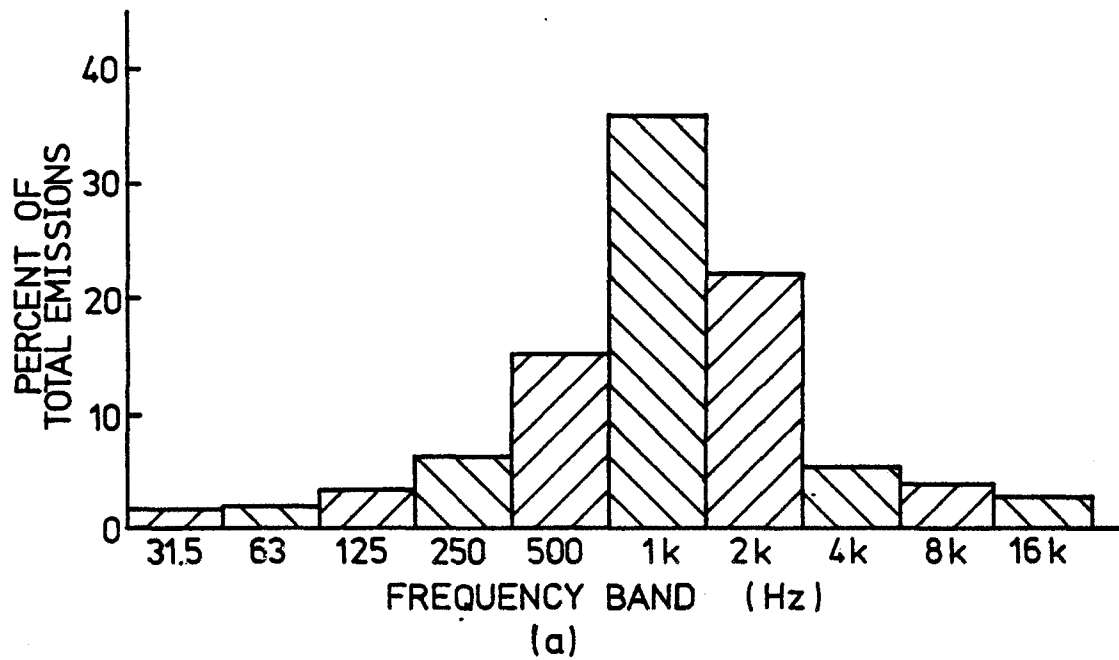


Figure 2. Frequency distribution for silty sand soil tested in (a) unconfined compression and (b) triaxial shear at 69 kN/m^2 (10 psi) confining pressure

in comparison to other construction materials) is generally known, the actual values of attenuation and their dependence on frequency are largely unknown and of great importance in this study, since high attenuation decreases the volume of soil from which emissions can be transferred to the wave guide rod and thus requires the use of more rod and/or greater signal amplification. At the low frequency range, Hardin's (51) logarithmic decrement data on sands (obtained in resonant column tests) can be converted to attenuation of approximately 0.007 dB/cm (0.2 dB/ft) at 200 Hz. Further review of the literature shows that Cadman and Goodman (26) measured attenuation of approximately 0.09 dB/cm (2.7 dB/ft) at 500 Hz using a sand embankment model in which failure (sand movement) was produced by tilting the supporting surface. These differences suggest a frequency dependence that must be explored further, considering the frequency range of soil emissions previously analyzed.

Mentioned in the section on velocity (vide supra) was a soil tank assembly wherein a pulse was generated and multiple signal pickups were used to compute attenuation values. Tests conducted at a frequency of approximately 1,000 Hz on a dry, silty sand resulted in an attenuation of approximately 1.3 dB/cm (40 dB/ft).

A test setup described by Nyborg, Rudnick, and Shilling (52) was duplicated to determine attenuation values at still higher frequencies. In this method, a loudspeaker generates a continuous signal. A layer of soil is placed between this loudspeaker and a microphone pickup. The microphone response, measured in decibels as a function of soil layer thickness, thus determines the attenuation in the soil. The frequency capability of this system ranges from a few kilohertz up to the frequency limits of the transducer system (limited by the speaker), which is about 18 to 20 kHz. Frequencies of 1 to 2 kHz and below cannot be reliably tested because of the large physical dimensions of the frame required at these long wave lengths.

Initial tests using the loudspeaker/microphone technique compared favorably with the published results of Nyborg et al (52), and use of the method was extended into the frequency regime of our interest. In general, the attenuation values are very high and quite sensitive to changes in water content. For example, a change in water content from 0% to 12% decreased attenuation in silty sand by approximately 200%. The approximate attenuation recorded by using this method varied from 5 dB/cm (150 dB/ft) at 4 kHz, to 10 dB/cm (300 dB/ft) at 16 kHz, which are the highest values observed in this investigation.

After considering the various methods used to determine attenuation (each of which has been determined in a different regime), it is possible to look at frequency versus attenuation on a unified basis. Figure 3 shows the approximate response curve for granular soils. A pronounced difference in behavior is to be noted at approximately 1 kHz. Below this level, attenuation is relatively low, and above it it is high. Since most of the acoustic emissions are in the 500 Hz to 8 kHz region, the pickup accelerometer must be placed directly at the source of the emissions in laboratory specimens; but special treatment will be required when dealing with the

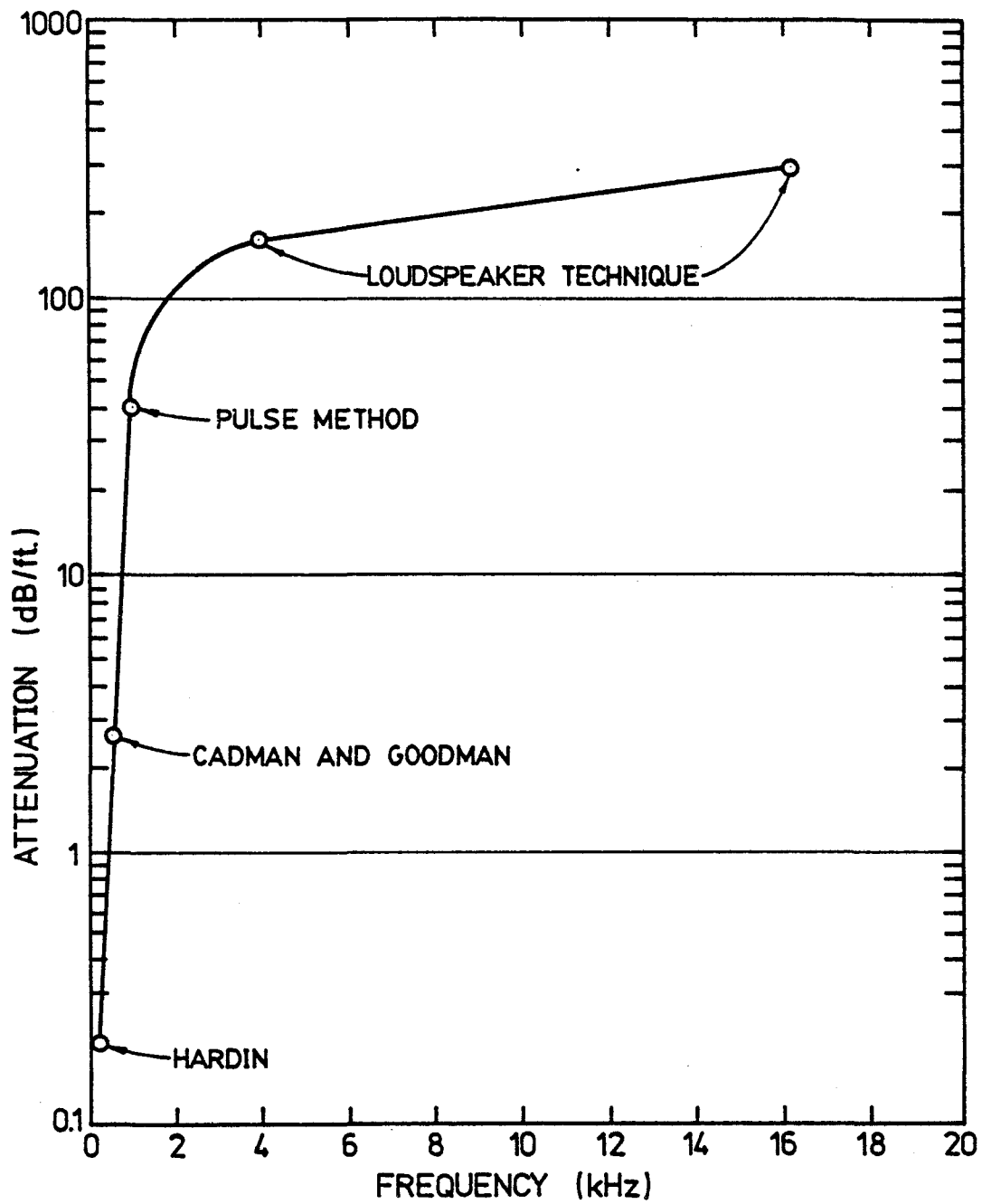


Figure 3. Frequency versus attenuation response of dry granular soils using various techniques.

monitoring of large earth masses in the field. When acoustic emissions are monitored in the field, metal rod wave guides must be used to conduct the emissions to the ground surface, where they can be monitored and recorded.

Effects of Physical Characteristics on Acoustic Emissions in Granular Soils

During this phase of the study, four granular soils with different physical characteristics were tested under drained (no excess pore water pressure) conditions in both isostatic and triaxial creep modes. The samples were tested in the creep (sustained stress) mode so that, compared to conventional strength testing, machine noise would be eliminated. (Refer to Appendix F. for definitions.) The soils varied in shape, uniformity, and size. Table 2 lists the physical characteristics of the granular soils tested (Figure 4).

All tests were performed on 70 mm-(2.8-in.) diameter by 150-mm (6.0-in.) high samples in a consolidated, drained condition. The pickup accelerometer was 12.7 mm (1/2-in.) in diameter by 19 mm (3/4-in.) in length and was embedded in the center of the sample as it was prepared (Figure 5) (see Glossary). The connecting coaxial cable was taken out through a port in the cell to an amplifier and counter. The gains were set equal for all tests in this series so that acoustic emission levels could be compared. Stress and strain data were taken in a conventional manner.

In the first series of tests, hydrostatic pressure was applied to the specimen, producing isostatic conditions. Cumulative acoustic emission counts were recorded with time after the pressure increment was applied. Figure 6 shows the response curves for these tests. Other than the final level of acoustic emission counts (see Table 2), the time for the acoustic emissions to cease (i.e., equilibrium of particle reorientation) varied primarily with particle shape. Samples containing the rounder particles (soil labeled No. 2 and No. 4) ceased emitting much before those with angular particles. Further comparisons will be deferred until later in this section.

Using the same soil samples and experimental test setup as with the isostatic test results just covered, a series of triaxial shear creep tests was performed. The deviator stress (or principal stress difference) versus strain behavior is given in Figure 7, and the deviator stress versus acoustic emission behavior is given in Figure 8 for the four soils under consideration. Note the almost identical behavioral patterns of stress/strain and stress/acoustic emission curves at all levels of confining pressure. This behavior indicates a basic relationship between strain and acoustic emission, the determination of which was a fundamental goal noted earlier. In addition to listing the limiting acoustic emission counts at failure (last column of Table 2), a modulus of emittivity was also calculated. This is the slope of the initial portion of the deviator stress vs. acoustic emission curves shown in Figure 8. The value listed in Table 2, however, is the inverse of the slope and is expressed in units of counts per kilo-Newtons per square meter (kN/m^2) since the value is intuitively more helpful on a unit stress basis. It is designated as the coefficient of emittivity and has potential use in field monitoring studies.

TABLE 2. EFFECT OF PARTICLE CHARACTERISTICS ON ACOUSTIC EMISSION IN GRANULAR SOIL

Soil Number and type	Particle shape ^a	Coefficient of uniformity ^b	Effective size ^c	Friction angle, °	Cell pressure $\frac{\text{kN}}{\text{m}^2}$	AE _{iso} ^d ($\times 10^4$)	E _T ^e ($\times 10^2$)	AE _{TRIAX} ^f ($\times 10^5$)
Sand drain soil No. 1	Subangular	8.4	0.45	35	34.5	1.7	16.1	2
					69.0	7.0	6.5	3
					138.0	15.0	6.5	12
Ottawa sand No. 2	Round	2.0	0.20	35	34.5	0.2	5.2	2
					69.0	0.5	5.2	3
					138.0	1.2	2.5	4
Concrete sand No. 3	Angular	2.4	0.21	39	34.5	0.04	8.1	8
					69.0	0.2	5.5	9
					138.0	1.8	4.8	14
Beach sand No. 4	Subround	1.5	0.24	42	34.5	0.01	1.0	1
					69.0	0.10	1.0	2
					138.0	0.38	0.87	4

^aBased on a relative scale of angular, subangular, subround, round, or very round.

^bDefined as $CU = d_{60}/d_{10}$.

^c d_{10} , the particle size at which 10% of the entire sample is finer, given in millimeters.

^dCumulative acoustic emission counts under isostatic conditions at cell pressure equilibrium.

^eCoefficient of emittivity, i. e., slope of initial portion of AE versus deviator stress curve in units of counts/ $\frac{\text{kN}}{\text{m}^2}$.

^fCumulative acoustic emission counts under triaxial creep conditions at failure.

1 $\frac{\text{kN}}{\text{m}^2}$ = 6.895 psi 25.4 mm = 1 in.

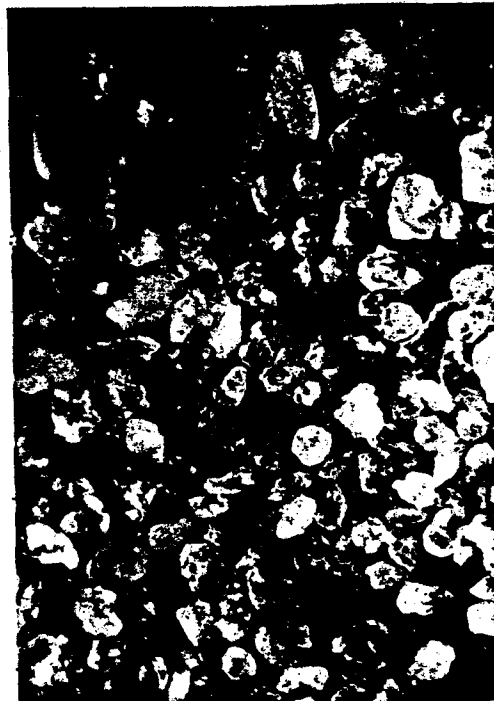
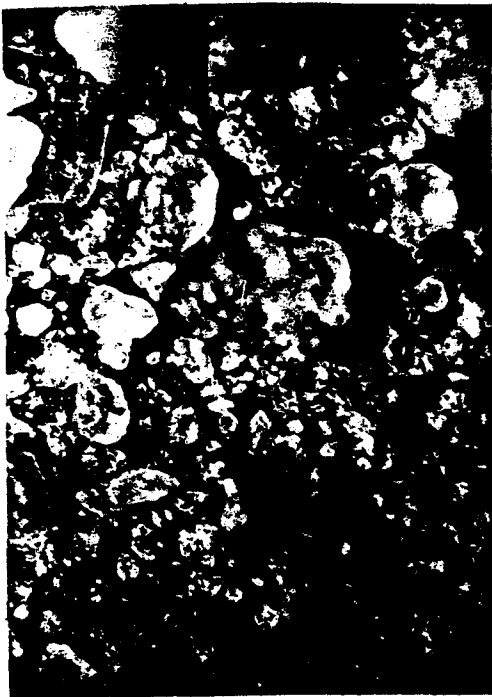
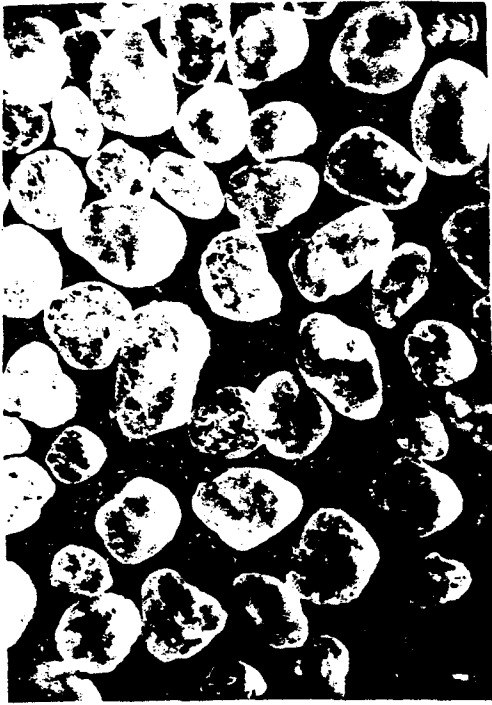


Figure 4. Granular soils tested: upper left, sand drain soil; upper right, Ottawa sand; lower left, concrete sand; lower right, beach sand.

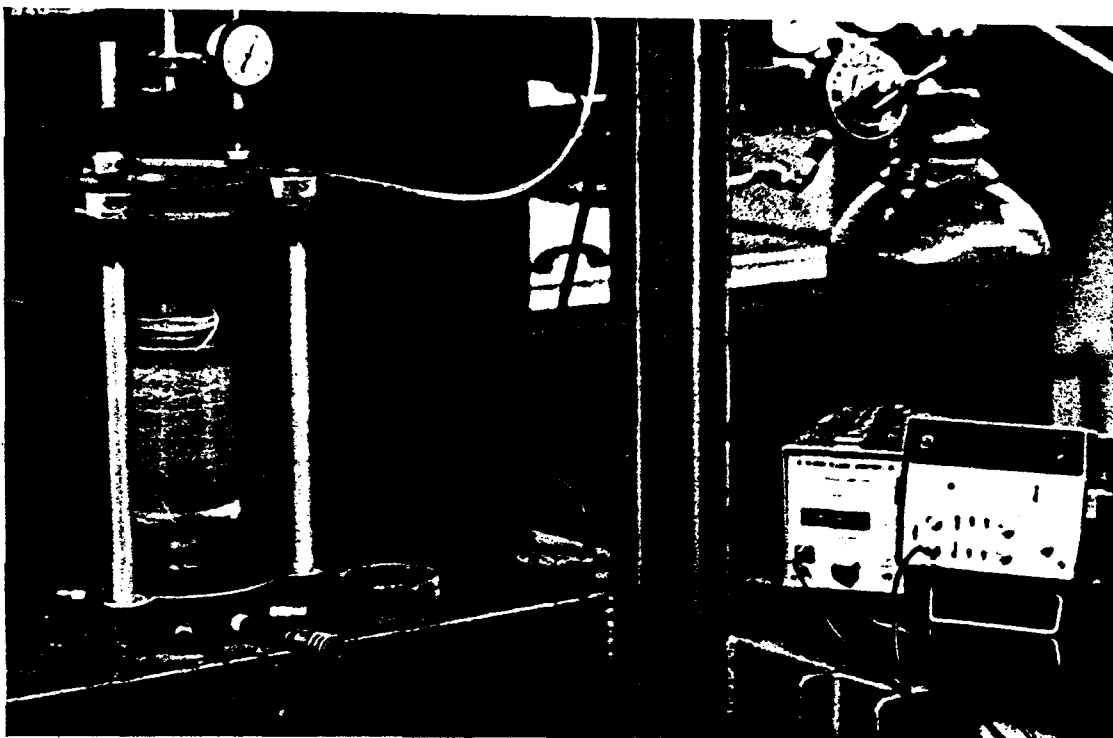
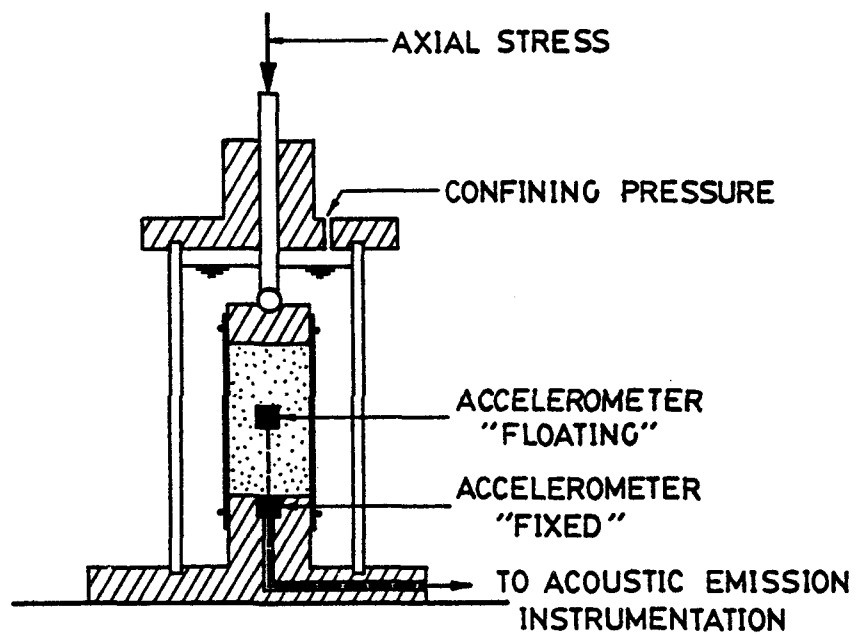


Figure 5. Schematic diagram and photograph of acoustic emission monitoring setup on stressed soil specimen tested in triaxial shear.

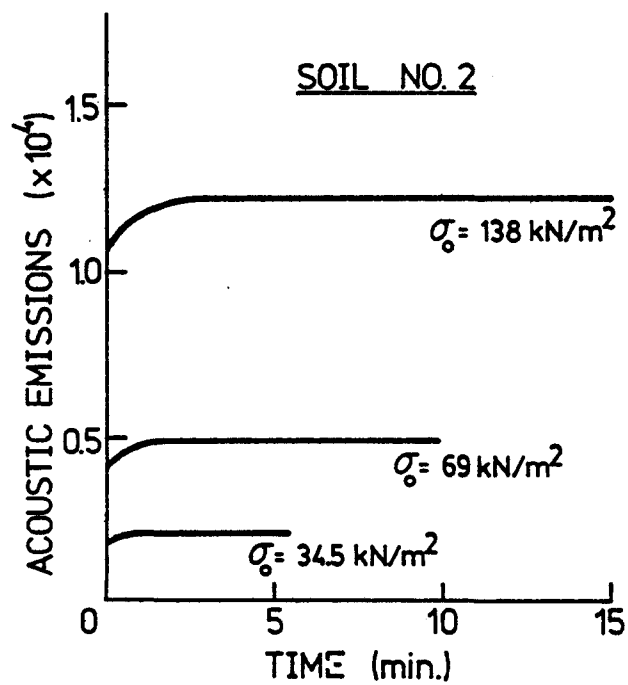
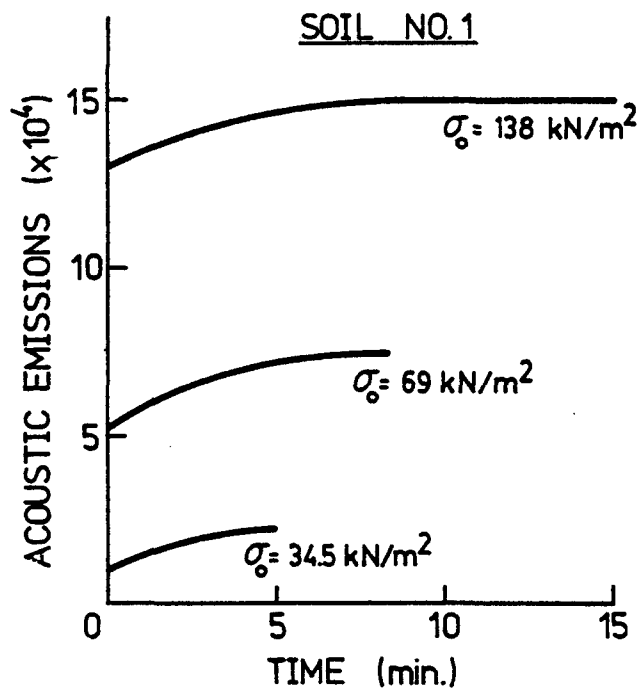


Figure 6. Isostatic test results (time versus acoustic emission in units of 10,000 counts) for four granular soils listed in Table 2.

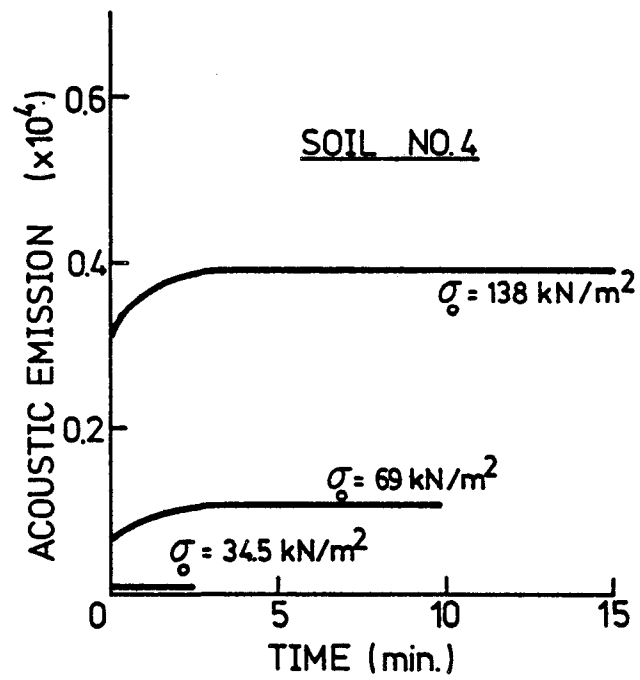
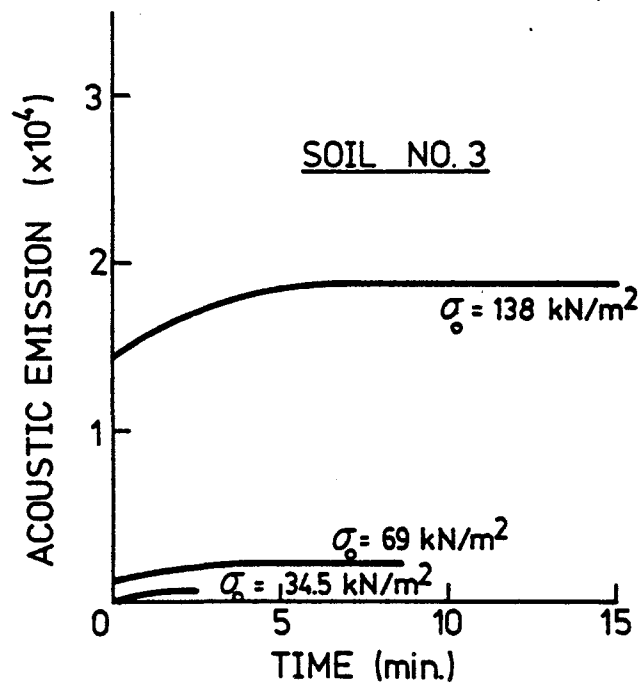


Figure 6. Continued

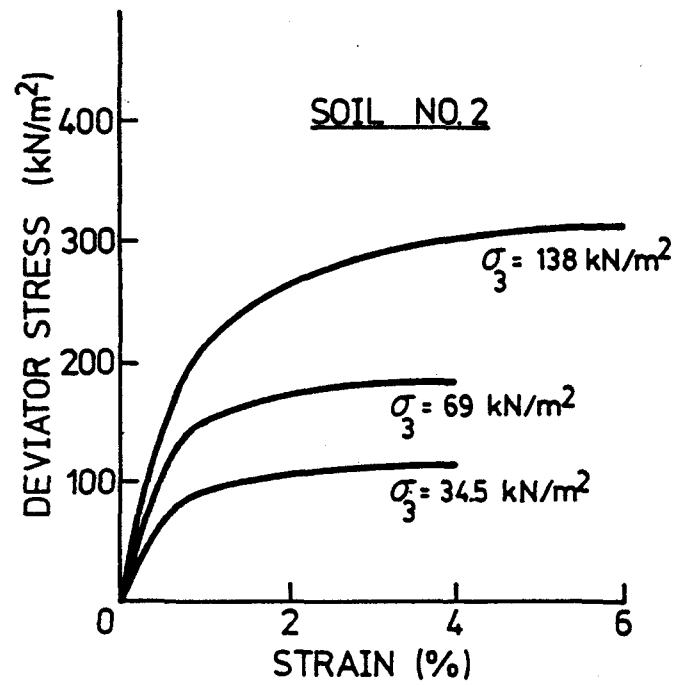
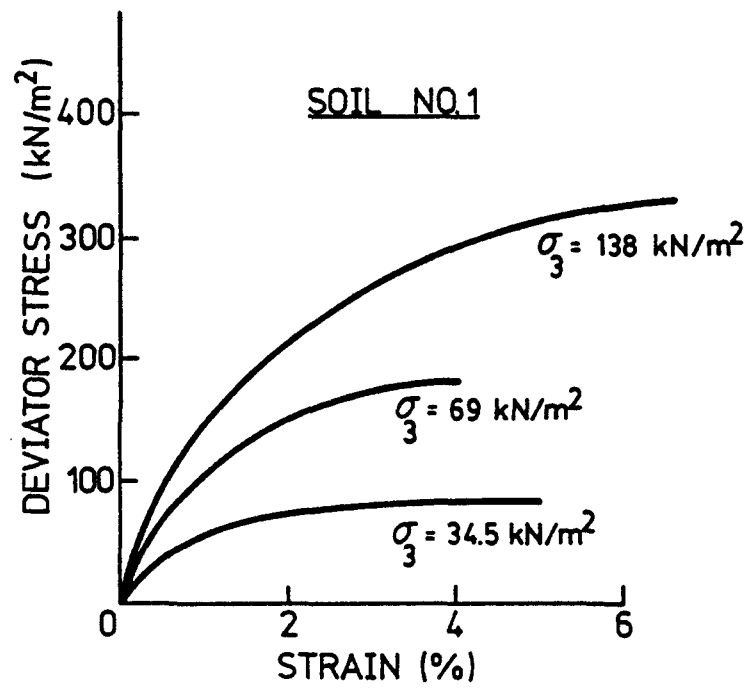


Figure 7. Triaxial shear test results (deviator stress versus strain) for four granular soils listed in Table 2.

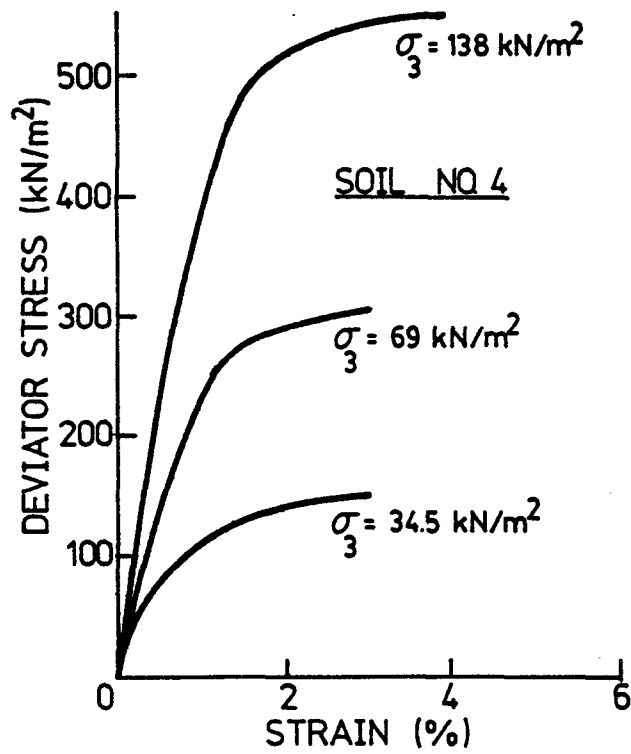
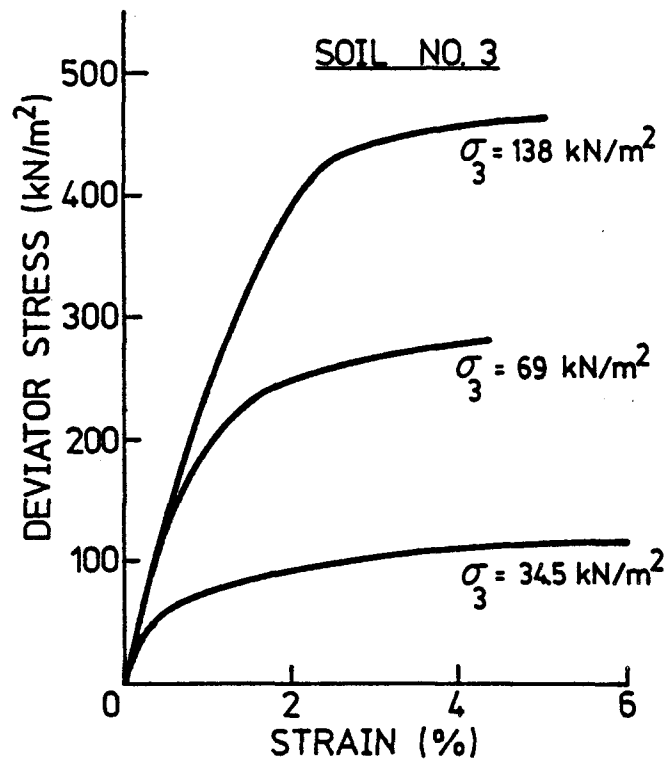


Figure 7. Continued

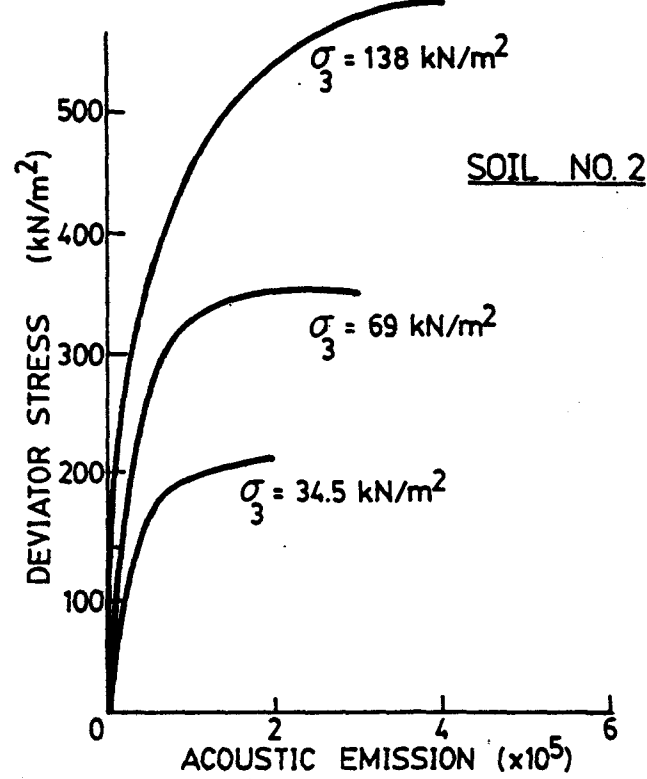
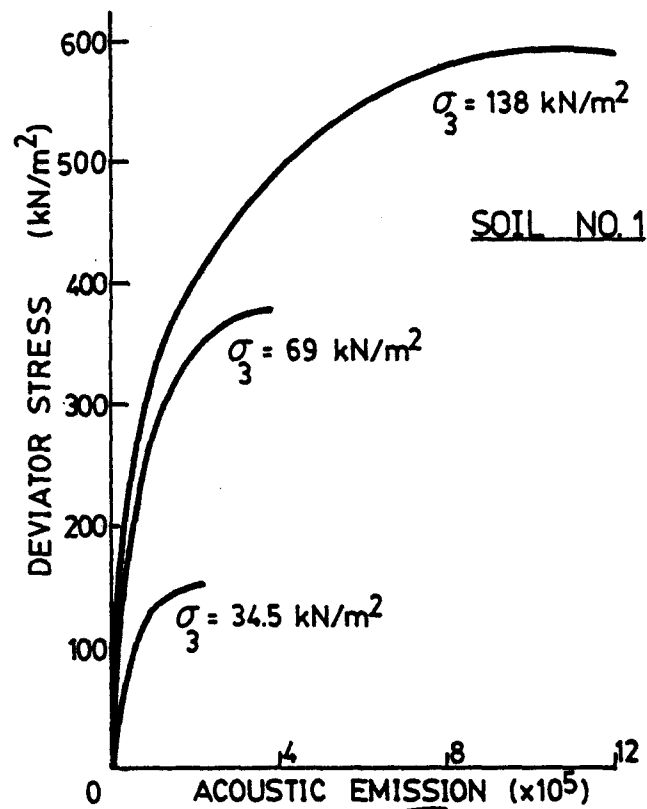


Figure 8. Triaxial shear test results (deviator stress versus acoustic emission in units of 100,000 counts) for four granular soils listed in Table 2.

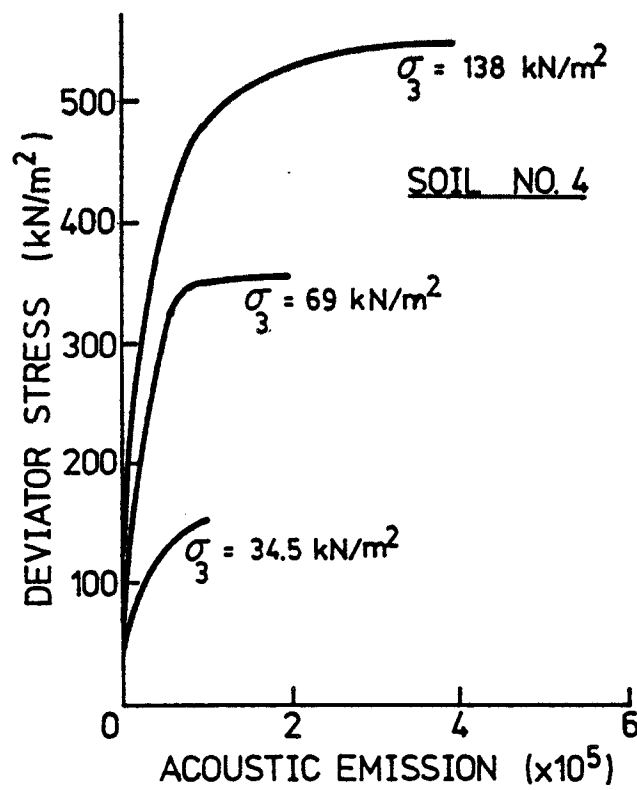
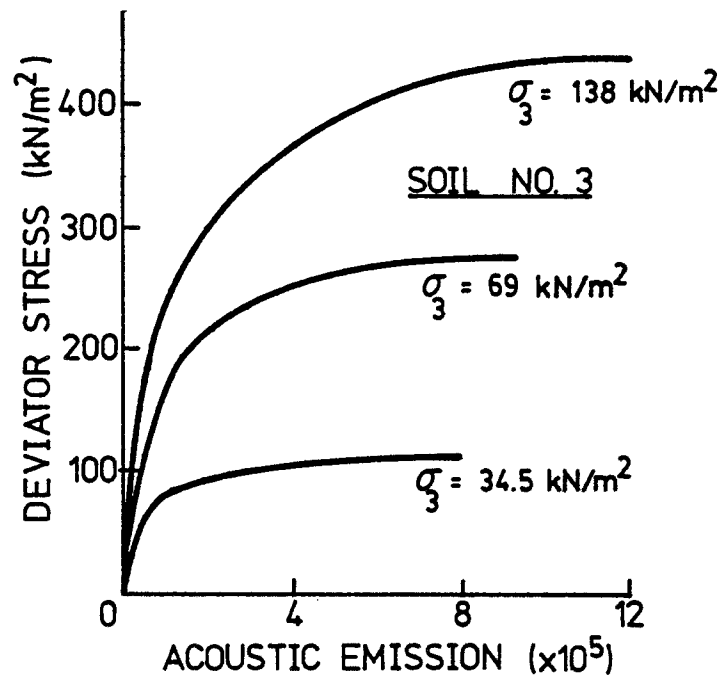


Figure 8. Continued

Because this portion of the project was aimed at the effect of particle characteristics on acoustic emission generation in stressed soil samples, a comparison can now be made. The comments that follow are made after a review of the data in Table 2 and Figures 6 and 8, and after observations made during the actual testing and subsequent data evaluation.

Particle Shape--

- The more angular the soil particles contained within the total sample, the more emissive is the sample under stress. Samples Nos. 3 and 1 (angular and subangular, respectively) are significantly more emissive in both the initial and final stages of triaxial testing than the other two samples. In general, the isostatic behavior of these angular soils particularly of soil No. 1, is also more emissive. As previously noted, the time for them to reach equilibrium is significantly longer than for those samples having rounded soil particles.

Coefficient of Uniformity--

- As the coefficient of uniformity increases, so does the level of cumulative acoustic emissions. This is a strong conclusion for the triaxial test behavior and is in nearly perfect agreement with the isostatic test results. However, the more angular soils also happen to have the highest coefficient of uniformity. The actual cause of greater emissions may therefore be a combined effect.

Effective Size--

Because the range of effective size is quite limited (0.20 mm to 0.45 mm (0.0079 to 0.0177 in), little in the way of a firm conclusion can be stated.

COHESIVE SOILS: CLAYS, SILTY CLAYS, CLAYEY SILTS

This section describes the behavior of amplitude, frequency, and attenuation of acoustic emissions in cohesive soils as listed in Table 3 along with the effects of many macroscopic variables that influence fine-grained, i.e., cohesive soil behavior.

Signal Amplitude in Cohesive Soils

Of primary interest is the comparison of levels of acoustic emission signals emanating from three different soil types (soil No. 2 and 3 (granular) and No. 6 (cohesive)). The soils to be evaluated were tested in triaxial shear at a confining pressure of 34 kN/m² (5 psi). The output signal from an embedded Columbia 476-R accelerometer range in kHz was amplified at a gain of approximately 30 dB (0.01 "g" sensitivity setting, where "g" is the acceleration due to gravity) for all tests and fed directly into an oscilloscope. The peak signal level was measured in volts at different levels of axial stress, and an average was calculated for signals observed at each stress level. For each load increment in both granular and cohesive soils, both the rate and amplitude of observed

TABLE 3. PROPERTIES OF COHESIVE SOILS USED IN THIS STUDY^a

Soil number ^b	Soil description	Type ^c	Liquid limit (% water) (w_l)	Plastic limit (% water) (w_p)	Plasticity index (%) ($w_l - w_p$)	Specific gravity of solids (g/cm^3)	Optimum water Content(%)	Cohesion (kN/m^2)	Friction ^d angle (ϕ)
5	Clayey silt	ML	47	37	10	2.62	23	41	29
6	Kaolinite clay	MH	52	33	19	2.60	29	28	29
7	Silty clay	CL	43	24	19	2.64	34	48	10
8	Bentonite clay	CH	570	58	512	2.20	43	62	5

^a All soils passed No. 200 sieve, unit weights varied slightly according to test series (see text).

^b Soils 1 through 4 are found in Table 2.

^c Unified Soil Classification System.

$$1 \frac{kN}{m^2} = 6.895 \text{ psi}$$

$$1 \frac{g}{cm^3} = 0.016 \text{ pcf}$$

^d Friction angle = ϕ in degrees. ϕ is defined by the equation $\tau = c + \tau_n \tan \phi$ where τ = shear stress, c = cohesion, τ_n = normal stress on shear plane.

emissions decreased with time from the start of the increment. Figure 9 shows the results of these tests on three different soils, for which the following observations can be made:

- Both sands tested (soil Nos. 2 and 3) showed the same general response, in which the amplitude of the emissions increased with increasing stress levels up to failure. The average signal amplitudes are 100 times stronger at failure than in the initial stress range value. The response appears to substantiate the commonly observed phenomenon of "hearing" a granular soil sample when it approaches the failure state.
- The more angular concrete sand generally produced emissions of slightly higher amplitude than the rounded Ottawa sand.
- The clay response is markedly different in a number of respects. First, the signal levels from kaolinite clay (soil No. 6) are 1/2 to 1/400 those of granular soils at corresponding stress levels. Second, the general nature of the response is different. Initially, the signal level increases, as with sands; then it levels off and, finally, decreases as the maximum stress is approached. The explanation appears to involve particle reorientation. The initial random orientation of the particles is increasingly emissive up to 50% to 80% of the maximum stress. At this point, a plastic state is fully mobilized, and the particles become aligned with planes of maximum shear stress. As additional load is applied, the amplitude of the acoustic emissions begins to decrease until failure is reached. The slickensided surfaces of the failed specimens tend to substantiate this behavior. But the behavior described here is likely to apply to cohesive soils failing by shear plane development only, and not to those failing by bulging. (See Glossary.)

Frequency Distribution of Acoustic Emissions from Stressed Cohesive Soils

To select the proper pickup transducer for acoustic emission monitoring, a series of unconfined compression (see Glossary) tests were performed on kaolinite clay (soil No. 6) samples at different water contents. A typical response is shown in Figure 10, where the predominant frequencies are seen to be in the 2 to 3-kHz regions. Similar tests were conducted on confined kaolinite clay samples ranging in water content from 22% to 38%. The response was essentially the same. Note that these acoustic emission frequencies are the same as those resulting from unconfined tests on granular soils. However, when granular soils were tested in a confined state, an upward frequency shift to 8 kHz was observed. Such a shift did not occur in cohesive soils.

Though such information is of basic interest, its main practical importance is in the selection of the proper pickup transducer. Accelerometers that are responsive over the range of frequencies from 100 Hz to 8 kHz are judged to be well-suited to monitor all soil types. When

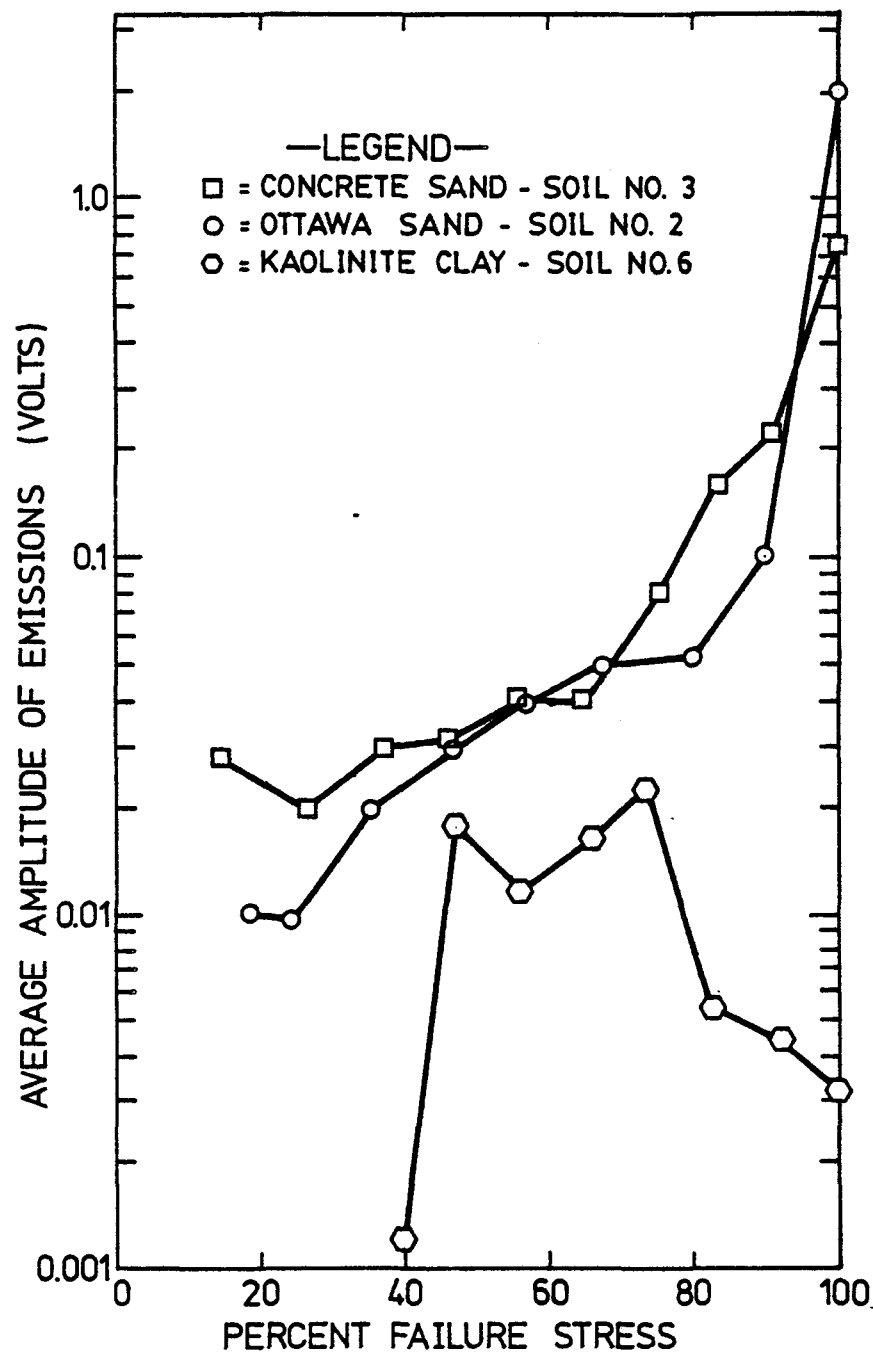


Figure 9. Average amplitude of acoustic emissions (measured as peak signal voltage output) for various soils as function of percentage failure stress in triaxial creep at 34 kN/m^2 (5 psi) confining pressure.

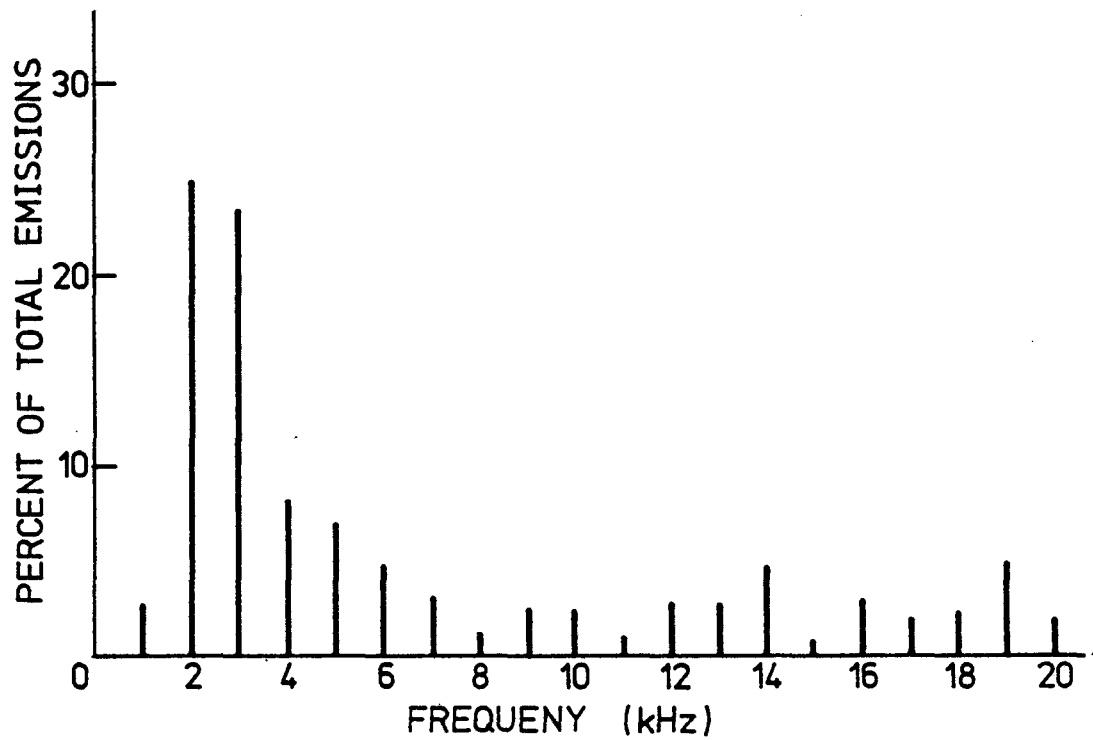


Figure 10. Frequency distribution of acoustic emissions from kaolinite clay (soil No. 6) tested in unconfined compression at 33% water content.

background noise at these monitoring frequencies is a problem, a high-pass filter of about 1 kHz can be used to eliminate some ambient noise at low frequencies.

Attenuation of Acoustic Emissions

The tendency of soils to attenuate various forms of elastic waves is well-known. In the preceding section on granular soils, attenuation was investigated, and its strong frequency dependence was quantified. Though such data are pertinent in this study, the relationship between water content and attenuation in cohesive soils should also be examined. Figure 11 shows how attenuation in clayey silt (soil No. 5) is affected as water content varies from 0% to 15%. The tests were conducted using a stress wave with a frequency of about 1 kHz. Details of the method were presented earlier. The attenuation decreases from its highest value of 1.9 dB/cm (57 dB/ft) in the dry state to a low, and perhaps asymptotic, value of about 1.0 dB/cm (30 dB/ft) at a water content of 15%.

Though these large attenuation values are not considered to be a dominant factor in laboratory monitoring of acoustic emissions (since the pickup accelerometer can be placed right at the source of the emissions within the sample), they do offer a severe challenge in field monitoring. For this reason, the use of long metal wave guides to bring the emissions to the ground surface is necessary in the field. The characteristics and features of these wave guides will be examined in Section 7 of this report, which describes field testing of the acoustic emission monitoring technique.

Macroscopic Behavior of Acoustic Emission in Cohesive Soils

Effect of Confining Pressure -- The effect of confining pressure on the acoustic emission behavior of cohesive soils was evaluated for two of the four soils listed in Table 3. The clayey silt (soil No. 5), with a total unit weight of 1.69 g/cc (105 lb/ft³) and a void ratio of 0.95, and Kaolinite clay (soil No. 6) with a total unit weight of 1.81 g/cc (113 lb/ft³) and a void ratio of 0.84, were each tested at confining pressures of 34, 69, and 138 kN/m² (5, 10, and 20 psi). As previously noted, the tests were consolidated-drained sustained load (creep) tests. The response curves are given in Figures 12 and 13. The close parallel in the behavior of stress/strain and stress/acoustic emission curves can be readily seen. Also, the fact that the overall acoustic emission count levels are slightly higher for the clayey silt with its silt-sized particle component than for the kaolinite clay is in agreement with the signal amplitude study previously cited (vide supra). The reader may wish to compare the level of acoustic emissions (counts) as a function of deviator stress and confining pressure for clayey silt (soil No. 5), kaolinite clay (soil No. 6), and the granular soils (Nos. 1 - 4, Fig. 8) to obtain a better appreciation of the relative "noisiness" of these various soils under different stress conditions.

This analogous behavior of strain and acoustic emission indicates that the two parameters are related and that either can be used in conjunction with stress to characterize and/or monitor a given soil.

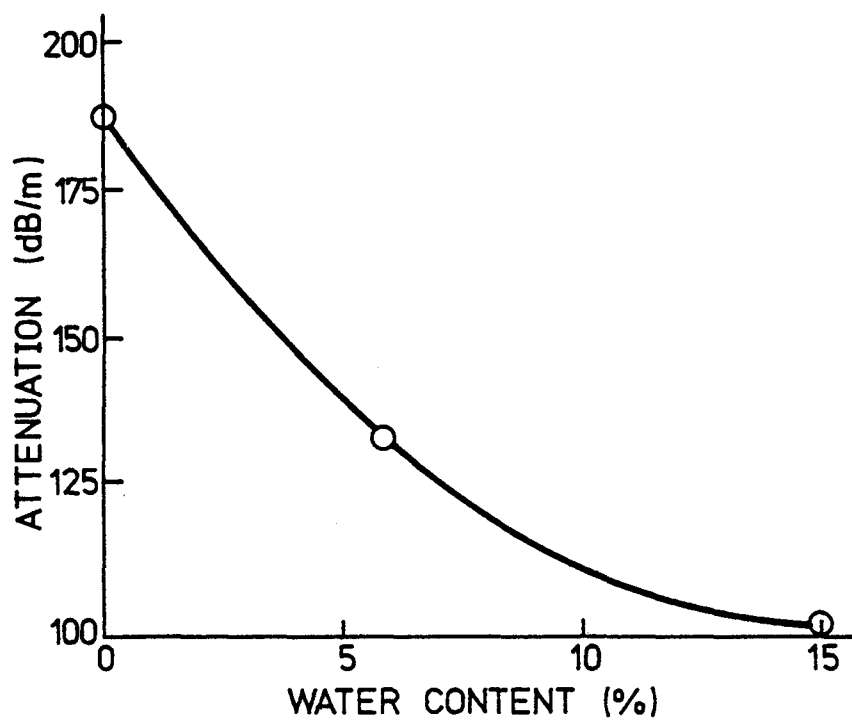


Figure 11. Attenuation of acoustic emissions in clayey silt (soil No. 5) at varying water contents at a frequency of about 1 kHz.

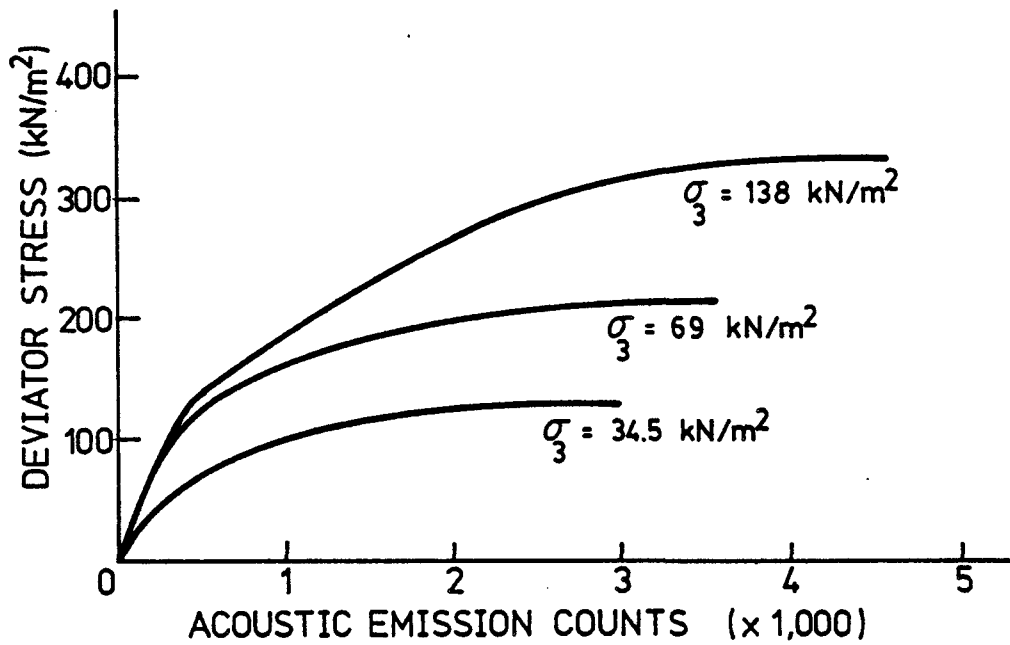
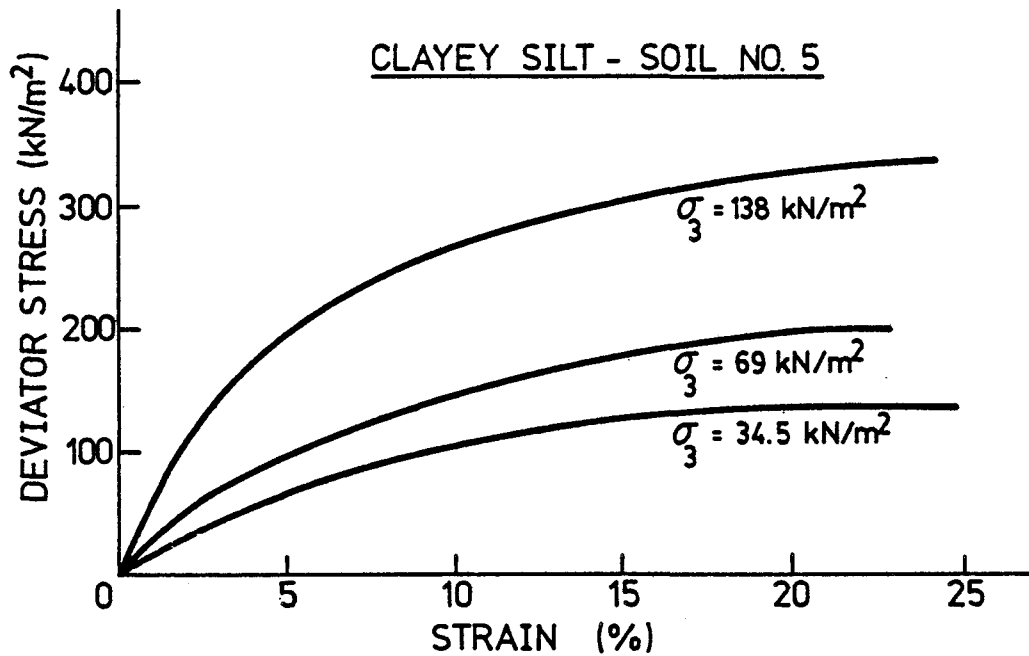


Figure 12. Triaxial creep response of clayey silt (soil No. 5) at varying confining pressures.

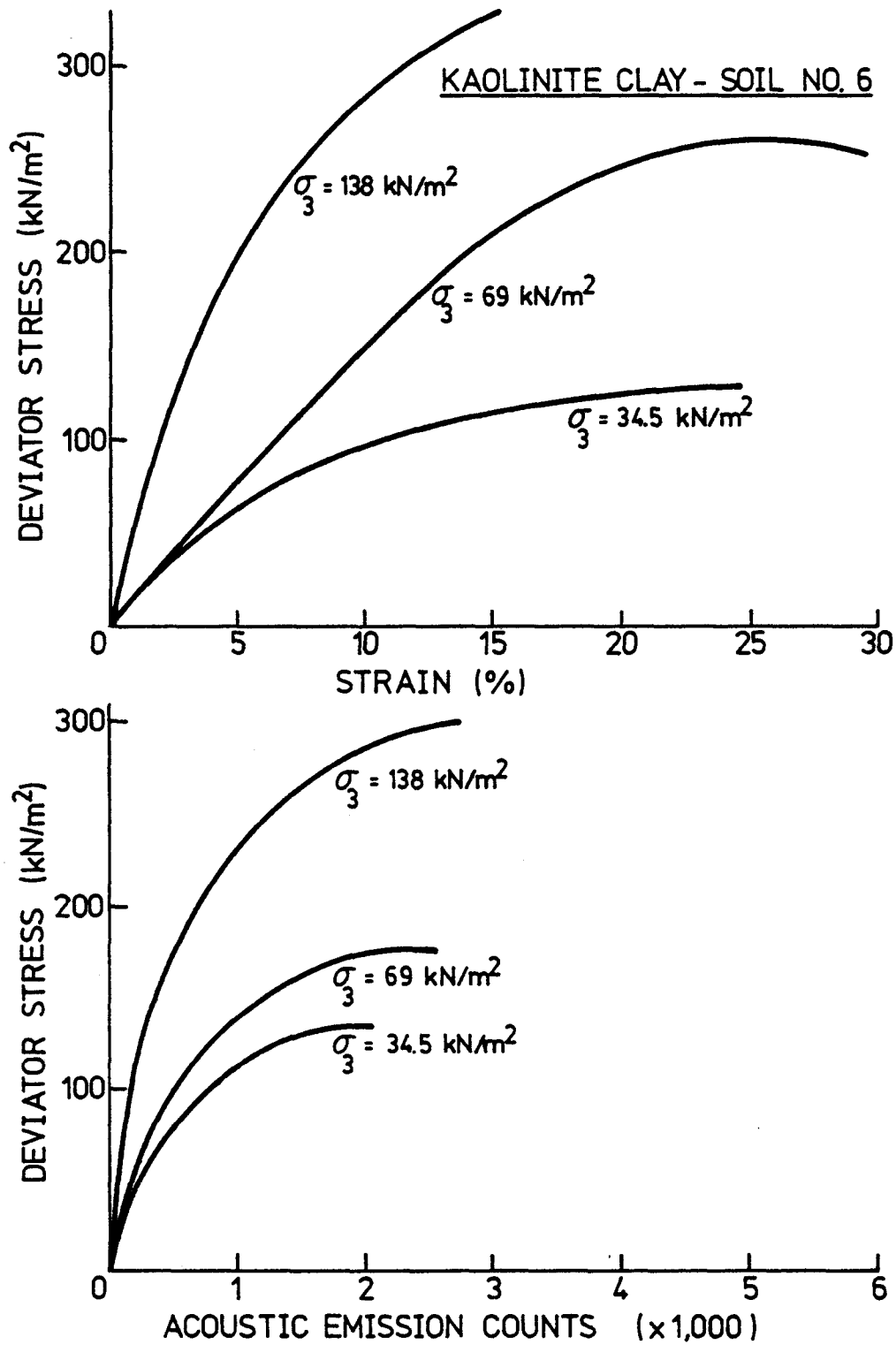


Figure 13. Triaxial creep response of kaolinite clay (soil No. 6) at varying confining pressures.

Effect of Water Content -- The initial series of acoustic emission tests reported in 1972 (2) were conducted on the clayey silt labeled soil No. 5 in this study. The samples were compacted at different water contents and tested in unconfined compression. Figure 14 shows the results, which indicate a decrease in strength and acoustic emissions with increasing water content. The extremely low number of emissions recorded at higher water contents in cohesive soils emphasizes the susceptibility of the technique to experimental error and noise interference as water content approaches the liquid limit when cohesive soils are being monitored. At the liquid limit, the soil changes from a plastic material that will deform, but not crack, to a viscous liquid or slurry that will fill and conform to the shape of a container. An earthen dam constructed of soil that attains the liquid limit will already be failing (visual observation).

Effect of Plasticity Index -- Table 3 indicates that the four cohesive soils tested in this study had plasticity indices (PI) of 10%, 19%, 19%, and 512%. Each soil was compacted to achieve a void ratio of 0.89 and tested in consolidated-drained triaxial creep at 34 kN/m^2 (5 psi) confining pressure. The results are presented in Figure 15. Cumulative acoustic emission counts are plotted versus percentage failure stress so that soils of different strengths can be directly compared. The most emissive soil is the clayey silt (soil No. 5), which has the lowest plasticity index and, correspondingly, the greatest amount of larger silt-sized particles. The least emissive soil is bentonite clay (soil No. 8), with an extremely high plasticity index and no silt-sized material. As shown in Figure 15, the kaolinite clay (soil No. 6) and silty clay (soil No. 7) have approximately the same emission response and plasticity index. Thus, a strong correspondence exists between acoustic emission response and plasticity of fine-grained soils.

Effect of Sample Structure -- All testing considered up to this point has been on remolded samples prepared in the laboratory under closely controlled and thus ideal conditions. Since one of the case histories to be examined later provided the opportunity of obtaining undisturbed samples, this soil (the silty clay labeled No. 7) was tested in the as-received condition. The significant properties were 1.97 g/cc (123 lb/ft^3) total unit weight, 1.14 void ratio, 56% water content, 100% saturation, and an average penetration resistance of 10 to 20 blows/m (3 to 6 blows/ft). The pickup accelerometer was embedded in the lower central portion of the sample by augering a 12-mm (0.5-in.) diameter, 25-mm (1.0-in.) deep hole in the soil sample and inserting the accelerometer. The sample was tested in unconfined compression in the creep mode. Results are shown in Figure 16. Note that the acoustic emission level is low, partly because of the cohesive character of the predominantly clay soil and its relatively high water content. However, the acoustic emission response closely resembles the stress/strain behavior shown in the upper part of the figure.

Effect of Stress History -- Well-established in acoustic emission literature (53) is the so-called Kaiser effect, in which acoustic emission levels are low until a material is stressed beyond that level which it has experienced in the past. Thus, many materials retain a record of their

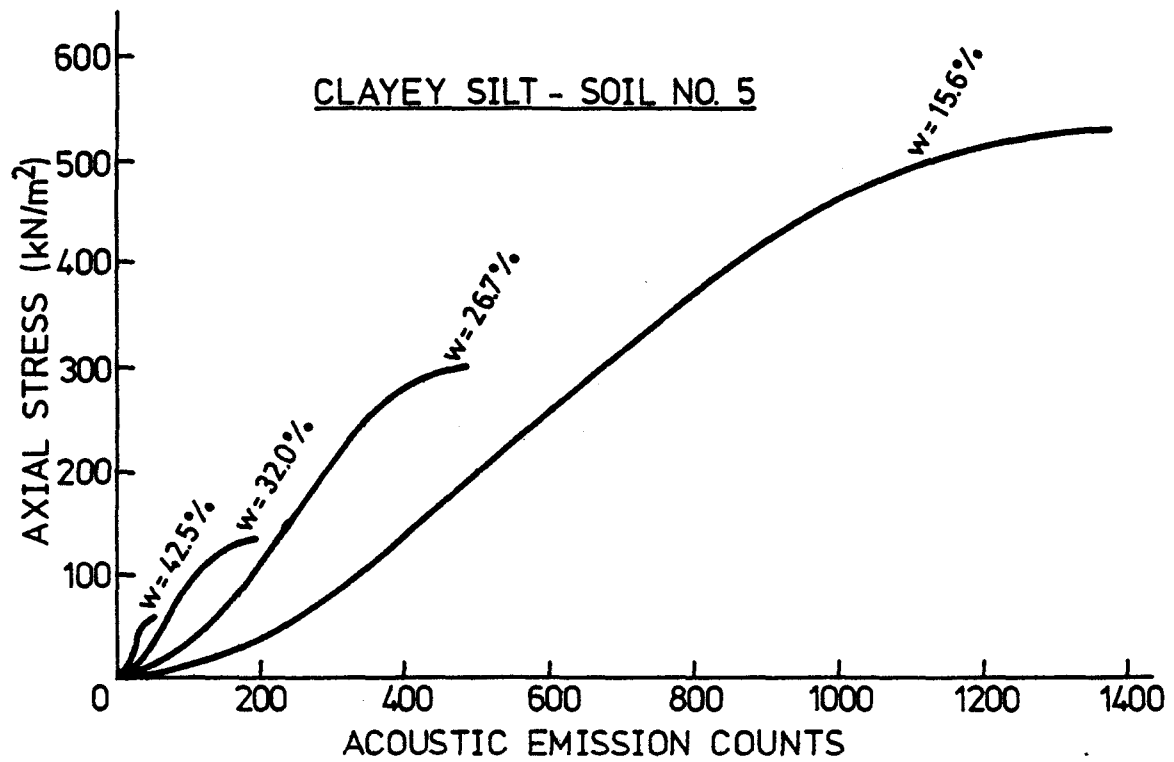


Figure 14. Stress/acoustic emission response of clayey silt (soil No.5) at varying water contents in unconfined compression.

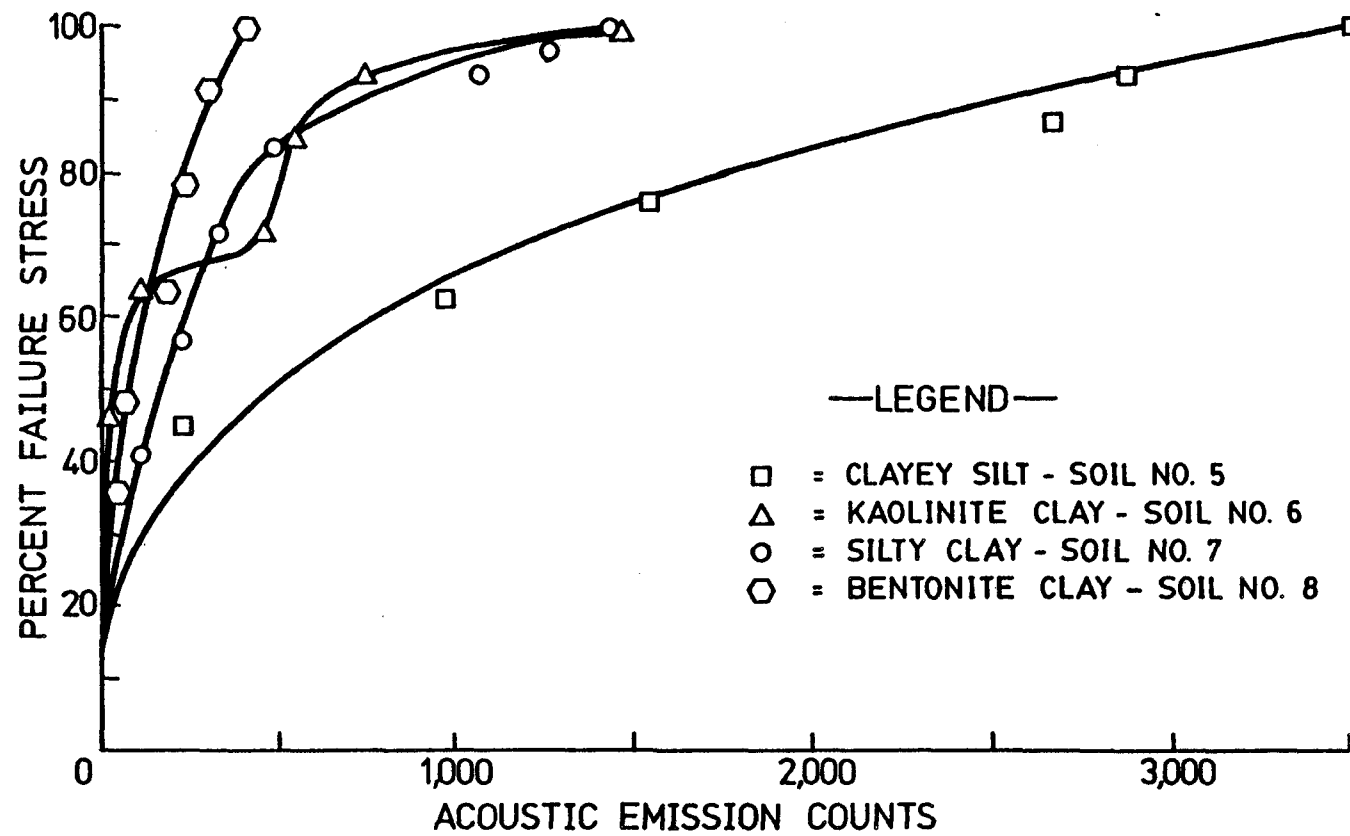


Figure 15. Stress/acoustic emission response of four cohesive soils in triaxial creep tests showing significance of plasticity index.

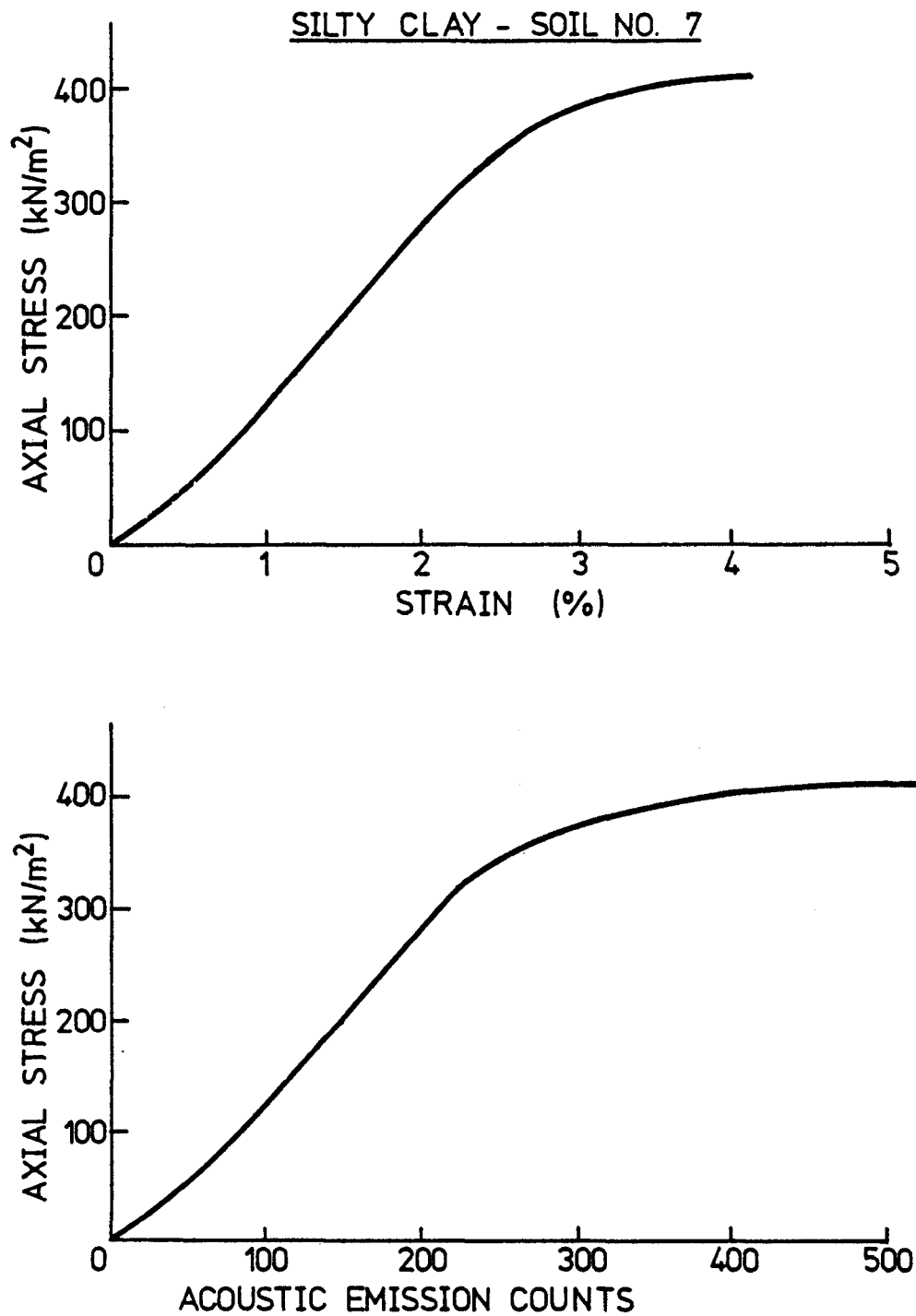


Figure 16. Unconfined compression test results for undisturbed sample of silty clay (soil No. 7) at 56% water content.

stress history. This concept has been recognized in geotechnical engineering through the identification of the preconsolidation pressure as determined in a standard consolidation test.

In this phase of the study, we have adapted such a stress history test for acoustic emission monitoring by fixing an accelerometer to the upper load platen of a consolidation oedometer. (A consolidation oedometer is a device for conducting confined compression tests as a function of time to determine the compression characteristics of soil.) Observation showed that the upper porous stone of the oedometer did not significantly attenuate the signals. Tests were conducted in a standard manner, which deflection/time and acoustic emission/time data sets generated for each pressure increment. The soil was a sandy silty clay known locally as a preconsolidated marl of low plasticity. It was used only for this test series and therefore is not listed in Table 3. The pertinent properties of this soil were 26% water content, 100% saturation, 1.59 g/cc (99 lb/ft³) dry unit weight, 2.65 specific gravity, 0.69 void ratio, a liquid limit of 30%, and a plastic limit of 27%. Figure 17 shows the typical response at a given pressure increment using a log-of-time fitting method. The standard deflection plot is roughly reflected in the curve of acoustic emission counts; that is, during periods of low deflection, acoustic emission count rates were low, and during periods of high deflection, rates were high. The fact that the time of transition from low to high rates of deformation does not completely coincide with the time of transition from low to high acoustic emission rates cannot presently be explained without further investigation. From a series of plots such as these, a pressure/strain curve was developed (see the upper portion of Figure 18), and a preconsolidation pressure of 408 kN/m² (53 lb/in² (psi) = 3.8 tons/ft² (tsf)) was determined by the Casagrande technique. Additionally, the time for 50% consolidation, t_{50} , of each pressure increment was used to obtain an acoustic emission count at 50% consolidation. The acoustic emission data were normalized by dividing the accumulated emission count at t_{50} for each pressure increment by the total emission count registered during all pressure increments. The results are given on the lower portion of Figure 18. The response consists of two nearly straight lines intersecting at about 858 kN/m² (8.0 tons/ft² = 111 psi. Though this value does not coincide with the preconsolidation pressure, it does coincide with the beginning of the straight line portion of the virgin compression curve. Most important, however, is that the acoustic emission levels are generally lower at stress levels below the preconsolidation pressure, P_c , than they are at stress levels that exceed P_c . Thus stress history seems to be identifiable using the acoustic emission monitoring technique.

COMPARISON OF ACOUSTIC EMISSIONS FROM GRANULAR AND COHESIVE SOILS

The following important observations were made:

Both for granular (sand) and for cohesive (clay and clayey silt) soils, stress vs. cumulative emissions curves corresponds closely to stress vs. strain curves. Thus, acoustic emissions are an indicator of deformation.

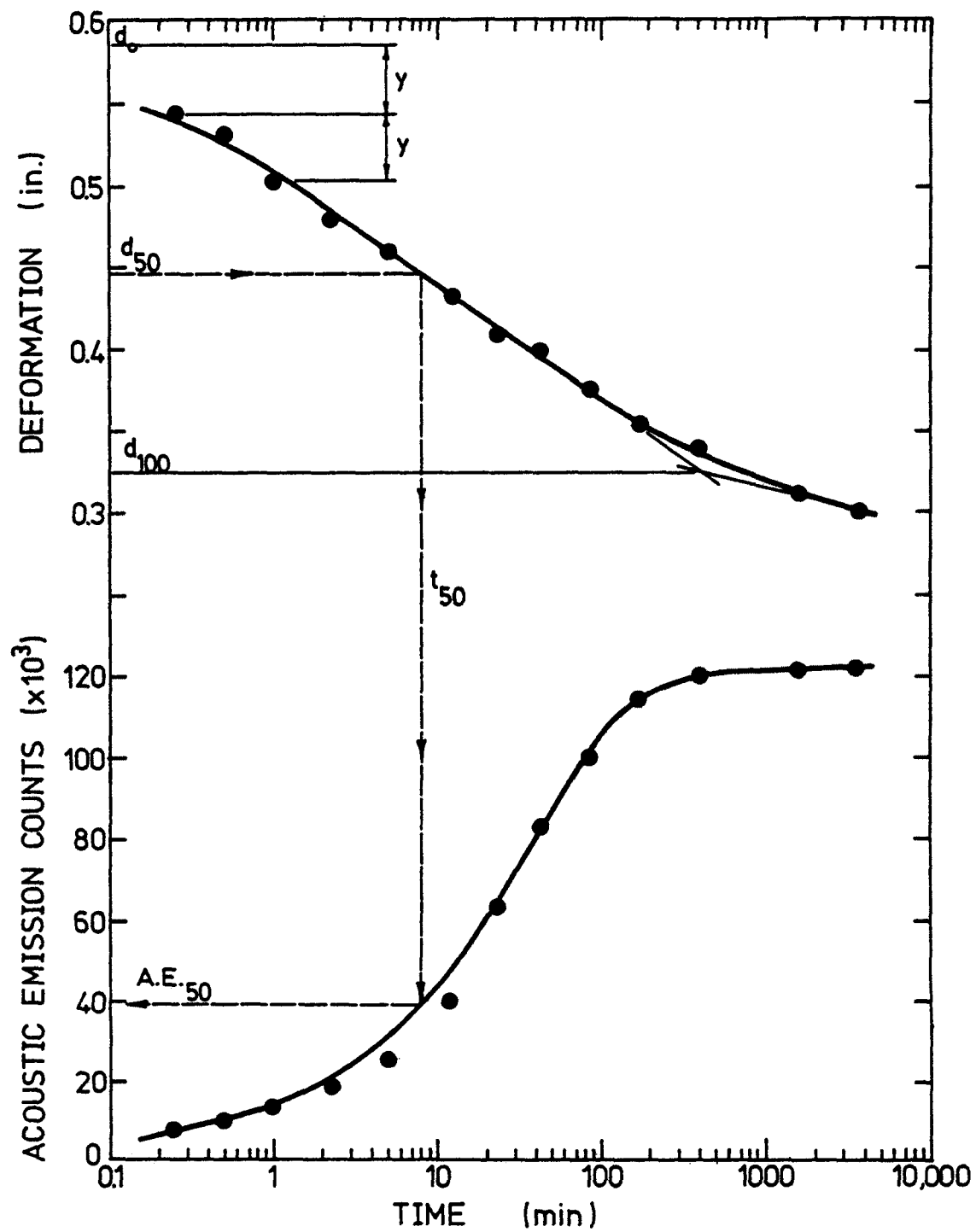


Figure 17. One-dimensional consolidation response of sandy silty clay at constant pressure on log-time scale.

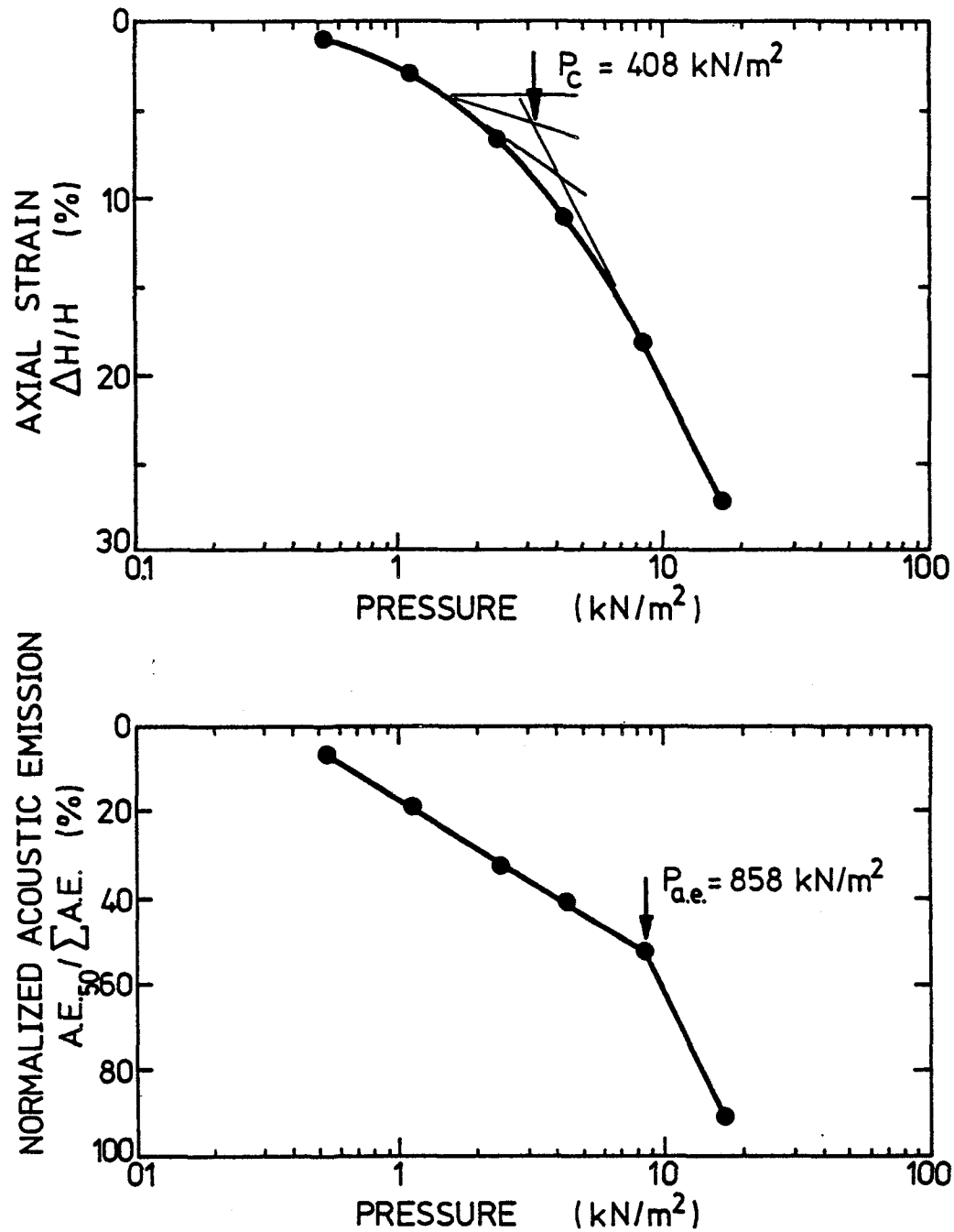


Figure 18. One-dimensional consolidation response of sandy silty clay over range of pressures showing strain and acoustic emission responses.

Most cohesive soils, and certainly all granular soils, can be monitored successfully using the acoustic emission technique. Possible exceptions are highly plastic clays with high water content (poor candidates for dam construction materials).

All granular soils (sands) tested showed the same general response. The behavior of cohesive soils is more dependent on water content and soil characteristics.

The amplitude of the emissions for the sands increased with stress up to failure, and the rate of increase was greatest as failure stress was approached.

The average signal amplitude for sands is 100 times greater near failure than at 20 percent of failure stress.

The cohesive soil (clay and silt) response is markedly different. Significant signals are not emitted from clay until a higher percent failure stress is reached than with granular soils.

Signal levels in clay are from 1/2 to 1/400 the level of signals from the sands at corresponding stress levels.

Initially, the signal level for the clay increases, as with sands; but then it levels off and decreases as the maximum stress is approached.

The decrease in signal level in clay as failure is approached is believed to result from reorientation of the platelike clay particles. At first they are randomly oriented, and emissions increase with increasing stress. But then the particles become aligned with the direction of maximum shear stress, and emissions decrease.

Emissions in cohesive soil decrease with increasing water content, and are reduced to very low levels as the liquid limit (water content beyond which a mass of soil cannot sustain a shear force) is approached.

A strong correspondence exists between acoustic emission response and plasticity (ability to be reshaped without developing surface cracks). Cohesive soils with the highest plasticity index give least response.

The frequency distributions of the acoustical emissions from granular and cohesive soils peak in the 2- to 3-kHz region at low stress. As confining pressure increases, the frequency shifts upward to 4 to 8 kHz for sands but remains nearly unchanged in cohesive soils.

There are marked differences in sound velocity, and attenuation coefficient, for granular and cohesive soils.

In sands, the acoustic emission increases monotonically with water content both because of lower attenuation and because of continuing contact between particles (at least until the sand liquifies and loses all shear strength).

In cohesive soils, the particles tend to move away from one another as water content increases, thus reducing the frictional interaction, which is a major cause of the emissions. Cohesion of particles is the major factor in the (shear) strength of clays, but release of cohesive energy does not provide as many emissions (acoustic energy) as does the overcoming of friction in sands (conversion of potential to various forms of kinetic energy). (The primary shear strength in sand arises from sliding and rolling friction and from structural resistance.)

ESTIMATED MAGNITUDE OF ACOUSTIC EMISSIONS IN SOIL

This section (54) presents a method to estimate the magnitude of the acoustic emissions at their source and at various distances from the source, e.g., at a transducer or wave guide pickup. It is based on very basic physical concepts and, as such, is intended to give a first order of approximation only. Furthermore, some of the values required for the numeric solution are rough estimates, which require a much more extended effort for a more exact value.

Theory

Consider a volume, V , of soil that is under stress and subsequently deforms elastically. From simple elastic theory, the elastic energy, U , stored in this volume is:

$$U = \frac{1}{2} M e^2 V \quad (1)$$

where M = elastic modulus and

e = elastic strain.

If this energy is released in a time interval, t , the average elastic power, P , released as waves during this interval is:

$$P = \frac{U}{\Delta t} R \quad (2)$$

where R is the radiation efficiency, i.e., the fraction of total energy released that is converted into elastic waves (acoustic emissions). If this energy spreads uniformly in three dimensions, the intensity, I , (i.e., the power per unit area) at a distance r from the source will be:

$$I(r) = \frac{P}{4\pi r^2} \quad (3)$$

where r is the distance from the source to the monitoring point. The simplified relationship between pressure, p , and intensity is (55):

$$I = \frac{p^2}{\rho c} \quad (4)$$

where ρ = density of the material

c = wave velocity.

It is easily shown (55) for sinusoidal waves that the maximum displacement is:

$$y_{\max} = \frac{p_{\max}}{\rho c^2 k}$$

where p_{\max} is the maximum pressure, k is the wave number ($2\pi/\lambda$), and λ is the wave length. Thus the monochromatic, spherical displacement wave spreads out as:

$$y = y_{\max} \sin(\omega t - kr) \quad (6a)$$

$$y = \frac{p_{\max}}{\rho c^2 k} \sin(\omega t - kr) \quad (6b)$$

where $\omega = 2\pi f$ is the angular frequency, and f is the frequency of the wave. Using Eq. (4) the above can be written as:

$$y = \frac{\sqrt{I \rho c}}{\rho c^2 k} \sin(\omega t - kr) \quad (7)$$

The particle acceleration is then:

$$\frac{d^2 y}{dt^2} = - \frac{\sqrt{I \rho c}}{\rho c^2 k} \omega^2 \sin(\omega t - kr) \quad (8)$$

and using $\omega = kc$ (55) one obtains for the maximum particle acceleration:

$$a_{\max} = \left(\frac{d^2 y}{dt^2} \right)_{\max} = \sqrt{\frac{I c k^2}{\rho}} \quad (9)$$

Using Equations (1) (2) and (3) substituted into Equation (9) along with the relationship $M = \rho c^2$, (55) the resulting maximum acceleration is:

$$a_{\max} = \sqrt{\frac{\pi f^2 e^2 V R c}{2 \Delta t r^2}} \quad (10)$$

Equation (10) thus represents the maximum acceleration of the acoustic wave produced by the source at some finite distance away.

Parametric Evaluation

To illustrate the significance of the developed theory, Equation (10) is solved using the following estimated values:

$$f = 500 \text{ Hz (from references 3 to 6)}$$

$$e = 0.002 \text{ (typical elastic strain in soils at the end of elastic range)}$$

$$V = 3.5 \times 10^6 \text{ cc, i.e., a 5 ft. cube (an estimated soil volume undergoing elastic deformation)}$$

$$R = 0.001 \text{ (seismology estimate from Cook (56))}$$

$$c = 18,300 \text{ cm/sec (600 ft/sec)}$$

$$\Delta t = 0.1 \text{ sec (a rough estimate)}$$

$$r = 760 \text{ cm (25 ft) (for waves to be isotropic, } r \text{ must be significantly larger than the soil volume under consideration)}$$

Use of the above data results in a maximum acceleration of 42 cm/sec², and using the acceleration of gravity, g , as 980 cm/sec², the maximum acceleration becomes 0.042 g . This value of acceleration appears to be compatible with the accelerations that have been measured in the field. However, due to the many variables involved (and the very real possibility of compensating errors), a parametric study of each variable is presented in Figures 19(a) to 19(g). In each figure, all the variables are kept constant (as per above) except the one being studied. (The figures should be read with a certain degree of caution, for in any real source modeling, there will certainly be interrelations between the above parameters. The most obvious is that as Δt decreases, f will increase. Also R will depend on f and c in some complicated manner.)

Acceleration at the Source

The previous theoretical development and numeric example were for the elastic spreading of the acoustic emissions as they propagate beyond the strained zone into the adjacent soil mass. The soil attenuation can now be superimposed onto the problem as follows: Consider a soil attenuation of 1.0 dB per foot, which corresponds to a dry granular sand at about 500 Hz. Over a distance of 762 cm (25 ft), this means that 25 dB of signal strength has been lost in traveling from its source to the monitoring station. Therefore, in the example problem stated previously, which resulted in a maximum acceleration of 0.042 g at 762 cm (25 ft) from the source, the source acceleration would have been:

$$(dB) = 20 \log (a_{\max} \text{ at source} / a_{\max} \text{ at station})$$

$$25 = 20 \log (a_{\max} \text{ at source} / 0.042g),$$

thus, $a_{\max} \text{ at source} = 0.75g$.

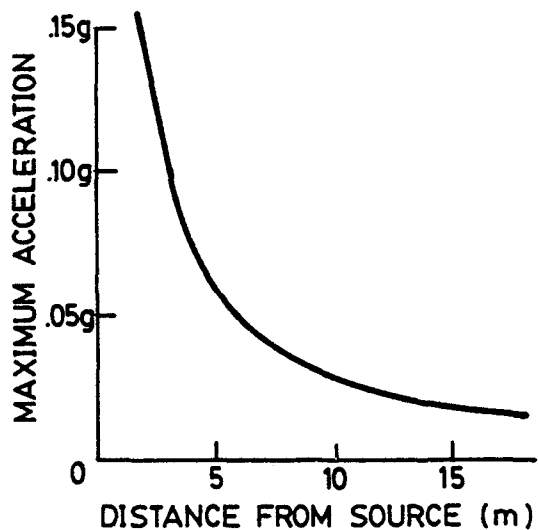


Figure 19(a). Variation of a_{\max} with distance from source in equation 10.

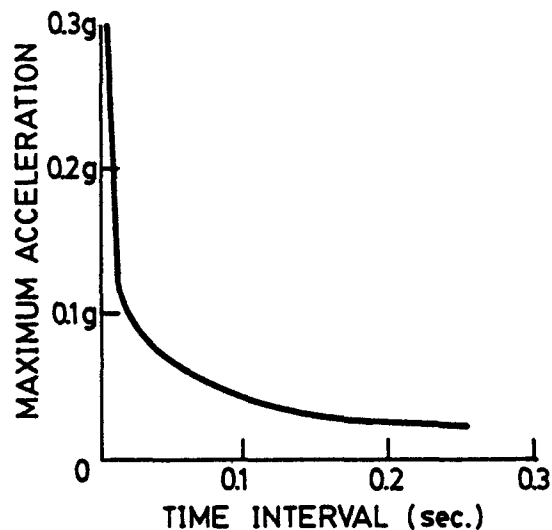


Figure 19(b). Variation of a_{\max} with time in equation 10.

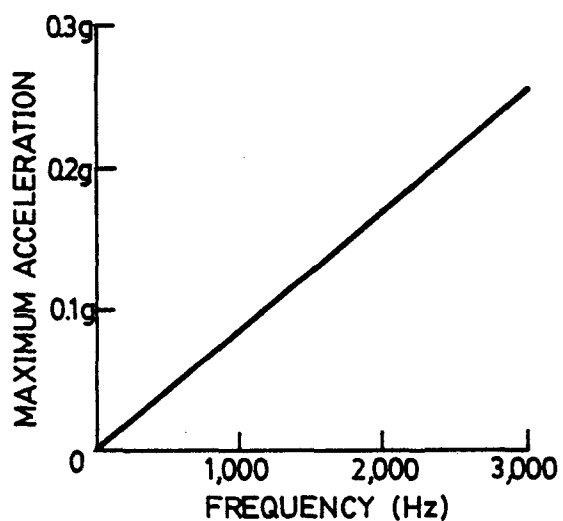


Figure 19(c). Variation of a_{\max} with frequency in equation 10.

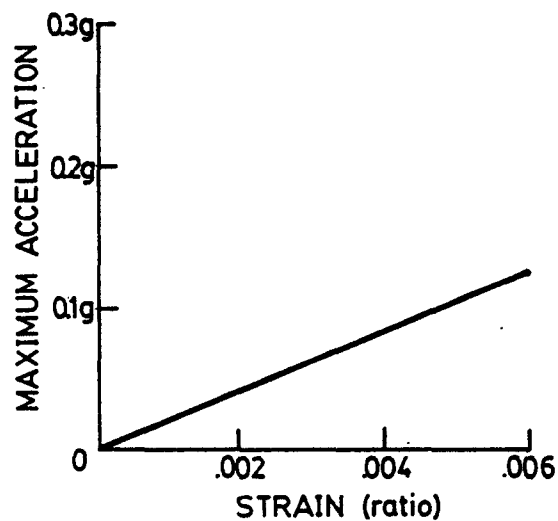


Figure 19(d). Variation of a_{\max} with strain in equation 10.

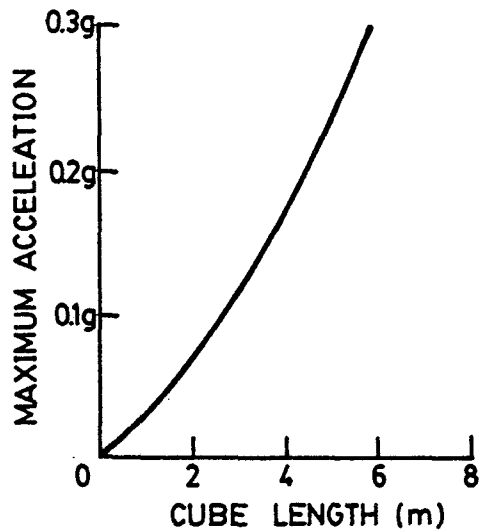


Figure 19(e). Variation of a_{\max} with volume via dimensions of one side of a cube in equation 10.

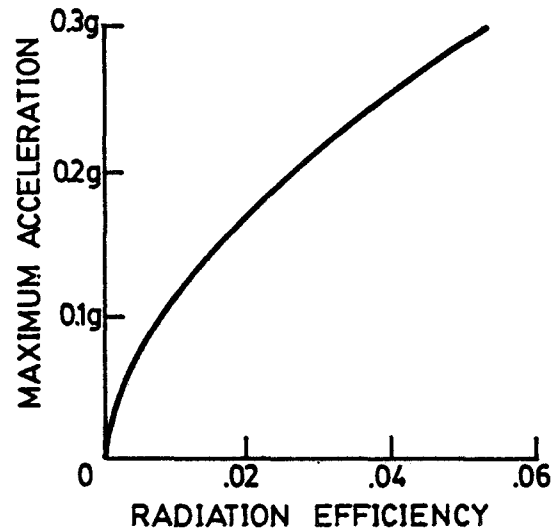


Figure 19(f). Variation of a_{\max} with radiation coefficient in equation 10.

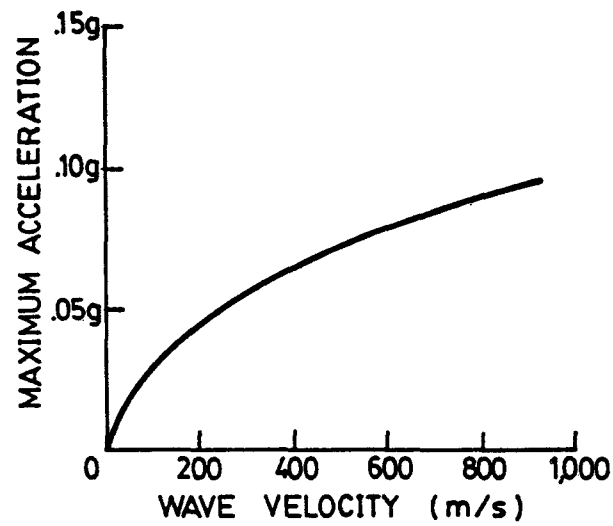


Figure 19(g). Variation of a_{\max} with wave speed in equation 10.

SECTION 7

APPLICATIONS OF ACOUSTIC EMISSIONS IN SOILS

In a soil mass, acoustic emissions are the self-generated noises that develop as a result of a deformation. The emissions are intimately related to the mobilization of shear strength components within the soil itself. Such components as sliding friction, rolling friction, degradation, dilatation, and probably cohesion all play a role in generating acoustic emissions. The resulting acoustic emissions are received by a metal rod wave guide, which is embedded in the soil and which transmits the emissions to an accelerometer (in this case a piezoelectric transducer with a relatively flat frequency response from 500 to 5,000 Hz) attached to the wave guide at the ground surface. The accelerometer then converts these mechanical waves into electrical pulses that are amplified and counted to obtain a numeric result. (See Figure 1 for a schematic of a typical acoustic emission monitoring system.) The use of electrical bandpass filters is optional and depends to a large degree on the level of background noise. A recorder is used if a hard copy of the results is required.

EQUIPMENT

For the field work described in this section, a monitoring system consisting of a Columbia 476-R accelerometer, Columbia VM-103 amplifier, and Hewlett-Packard 5300A counter was used. These components are all DC-operated and thus require no external power source--an important consideration for field work in remote areas. Other details concerning the instrumentation and relationships of acoustic emissions to basic soil properties were presented earlier. Photographs of the equipment are included in Section 8 and Appendix B.

Unlike some field structures (rock formations), soils require an extrinsic mechanism to bring the acoustic emissions from within the soil mass, where they are generated, to the ground surface, where they can be monitored. Such transmission element (called a wave guide) is necessary because of the high attenuation of elastic waves in soils. In most other non-soil structures, the pickup sensor can be mounted directly on the material being monitored and then retrieved upon completion of the work. The wave guides may simply be lengths of low-carbon-steel rod (e.g., bar or rod stock), reinforcing bar, bailing wire, instrument pipe, drain or outlet pipe, etc. that are driven into place when existing soil masses are to be monitored or, whenever possible, are placed in an earthen dam during construction. The wave guide must be placed in or near to a highly stressed zone in the soil being monitored. Choosing the best location is a difficult decision, not unlike the selection of instrumentation sites irrespective of the particular technique. The acoustic emissions generated

in the soil as it deforms will travel relatively unimpeded along the wave guide to the pickup accelerometer, which is threaded onto the wave guide at the ground surface. The following series of tests was performed to verify the conducting quality of the wave guide.

A steel wave guide was set up in the laboratory with a small minishaker attached to one end and a pickup accelerometer, amplifier, and readout oscilloscope to the other end. The shaker and pickup accelerometer were both mounted axially. Therefore this study is predominantly one of longitudinal wave propagation. Two different-size wave guides were used--3.2 mm (1/8 in.) and 12.7 mm (1/2 in.) in diameter--each with different lengths, surface conditions, and coupling mechanisms. Figure 20 shows the response obtained for wave guides up to 4.9 m (16 ft) long, the larger diameter being associated with the longer of the two sizes tested. Conclusions drawn from this portion of the study are as follows:

- Longer wave guides lower the frequency of the first resonance, making the system more sensitive in the 500 to 1,000 Hz range, where a large number of soil emissions actually occur (see Figures 2 and 10).
- Different diameter rods do not appear to influence the first resonant frequency of the system.
- Different surface conditions (threaded versus smooth) do not appear to affect the location of the first resonance.
- The method of connecting one rod to another does not appear to influence the resonances as long as such connections are solid and firm in their metal-to-metal contact.

These four conclusions are consistent with the fact that the first and higher resonances are caused by standing compressional elastic waves in the rod. From wave propagation theory, the values of the lowest rod resonances can be written simply as $f_0 = v/2L$, where f_0 is the resonant frequency, v is the velocity of sound in the rod, and L is the length of the rod. The velocity of sound in the rod was determined by measuring the time necessary for an elastic pulse to traverse the rod. The measured velocity of 4.5×10^5 cm/sec (1.5×10^4 ft/s) for a rod 4.9 m (16 ft) long gives a theoretical resonant frequency of 465 Hz, a value reasonably close to the measured value.

Still of concern regarding the resonant response of the wave guide/ accelerometer system was the influence of the soil medium around the wave guide. To study this effect, a sequence of tests was conducted on a 1.2-m (4-ft) long, 12.7-mm (1/2-in.) diameter rod surrounded by silty sand of various densities. The results (Table 4) indicate that the location of the first resonant frequency is only slightly varied by the influence of the surrounding medium. A slight peak is evident with the soil at 10% water content and at the highest density. This higher density condition has the effect of maximizing the particle contacts on the rod, which in turn lowers the amplitude of the first resonance. In general, it appears that the soil

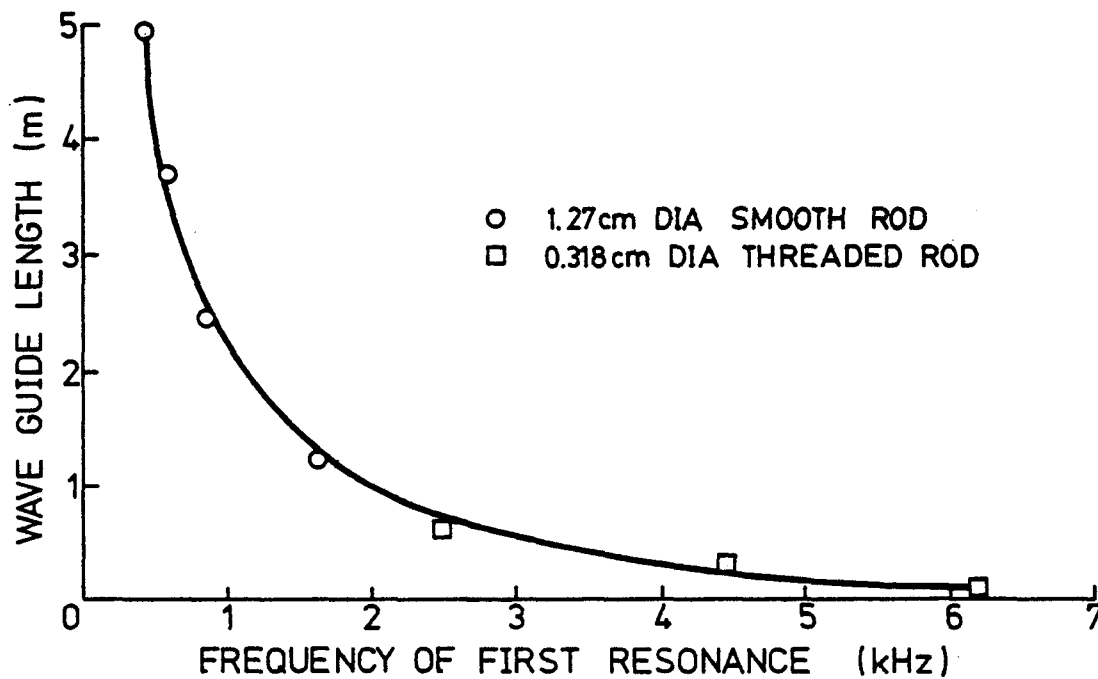
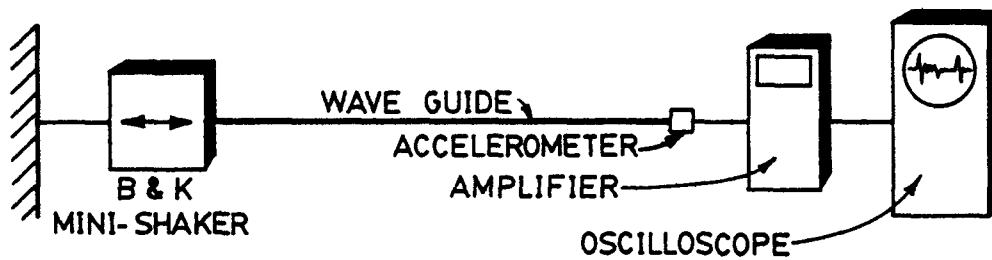


Figure 20. Experimental setup and location of wave guide/accelerometer's first resonance as a function of length considering different diameter and geometry of steel rods.

TABLE 4. INFLUENCE OF MEDIUM SURROUNDING WAVE GUIDE ON
FREQUENCY AND AMPLITUDE OF FIRST RESONANCE

Item	Loose dry soil	Dense dry soil	Soil at water content			Water	Air
			10%	20%	30%		
Wet density (gm/cm ³)	1.36	1.46	1.57	1.70	1.89	-	-
Dry density (gm/cm ³)	1.36	1.46	1.46	1.31	1.44	-	-
Resonant Frequency (Hz)	1,630	1,670	1,840	1,730	1,690	1,632	1,630
Amplitude (V.)	28	15	5	4	11	83	96

1 g/cm³ = 0.016 pcf (pounds per cubic foot)

V. = volts

mass around the wave guide has a negligible influence on the detector's frequency response, but does reduce the signal magnitude to a certain extent.

FIELD STUDIES

Nineteen field sites have been or are in the process of being monitored using the acoustic emission technique. A brief description of each and some comparative details are given in Table 5. Twelve are earth dams, two are surcharge fills, two are embankments, one is a gypsum dam, and two are seepage studies. Each site will be described briefly, along with the principal finding. The more important and informative sites will be examined in greater detail.

Site No. 1 is a 9.1-m (30-ft) high homogeneous earth dam near Doylestown, Pennsylvania. The 3.0-m (10-ft) deep foundation soil was instrumented for potential settlement by driving twenty 12.7-mm (1/2-in.) diameter steel rods to the underlying rock. During placement of the fill, no emissions were recorded, undoubtedly because the foundation soils were very dense ($130 \text{ lb/ft}^3 = 2.08 \text{ g/cc}$) and had very high strength (standard penetration resistance of approximately 164 blows/m (50 blows/ft)). When coupled with the fact that the dam is relatively small with reasonably flat side slopes, this lack of emission data seems justified.

Site No. 2 is a 20.1-m (66-ft)-high zoned earth dam near Doylestown, Pennsylvania. The dam is founded just above rock and was completed before its downstream slope was instrumented with twelve 12.7-mm (1/2-in.) diameter steel rod guides 3.0 to 4.6 m (10 to 15 ft) long. The purpose of this instrumentation was to monitor lateral embankment movement as the reservoir filled with water. For a number of reasons, the filling was very slow, so the embankment was subjected to relatively small increments of lateral pressure. This reservoir has taken 3 years to fill. At no time were emissions recorded, suggesting little or no deformation and a stable dam.

Site No. 3 is a 20-m (67-ft)-high homogeneous earth dam near McCook, Nebraska, and is shown in schematic form in Figure 21. This dam is founded on approximately 61 m (200 ft) of wind-blown silt generally known as loess. The dam was instrumented with 9.5-mm (3/8-in.) diameter reinforcing rods placed horizontally on the foundation soil at four stations, each consisting of a set of three rods of varying length. At one point during construction, it was found that, for two of these stations, the emissions shown in Table 6 occurred. The data appear to indicate that the longer rods on the far side of the crest of the dam give higher emission counts than the shorter rods, which terminate in the slope area. This response is logical because less loading, and hence less deformation, occurred in these regions. The fact that set No. 1 responded more than set No. 2 is not completely understood, since fills were slightly greater in the area of set No. 2.

However, emissions from the dam were very low overall (the data in Table 6 were the maxima recorded) during the entire course of construction, which lasted for 1-1/2 years. The soil's fine particle size, the prewetting of the construction site, the horizontal rod placement, and the short-term, random collection of data are all believed to have contributed to the low levels of emission.

TABLE 5. OVERVIEW OF SITES BEING MONITORED USING THE ACOUSTIC EMISSION METHOD

No.	Designation	Purpose	Height		Length		Relative Embankment Design and Const.	Relative Foundation Stability
			ft	m	ft	m		
1	Pa-616	Flood control	30	9	2600	800	Excellent	Excellent
2	Pa-617	Recreation	66	20	2500	760	Excellent	Excellent
3	Neb-200	Flood control	67	20	900	270	Excellent	Compressible
4	Md-BSC	Ore stockpile	40	12	300	90	Good	Very poor
5	Pa-PIA	Surcharge load	6	1	120	37	Good	Very poor
6	Neb-390B	Flood control	68	20	600	180	Excellent	Compressible
7	Can-LMM	Tailings dam	95	29	900	270	Good	Good
8	Del-GOC	Contain dredging spoil	15	4				
			40	12	6 mi	10 km	Poor	Very good
9	Pa-BOB	Water supply	120	36	600	180	Excellent	Excellent
10	NJ-RR	Contain chemical wastes	8	2				
			20	6	4 mi	7 km	Poor	Very poor
11	Va-KPN	Contain chemical wastes	4	1				
			15	4	500	150	Poor	Unknown
12	NY-OSW	Contain petroleum wastes	8	2				
			20	6	450	140	Poor	Unknown
13	Pa-DSP1	Stockpile for highway fill	15	4	20	6	Poor	Good
14	Pa-DSP2	Stockpile of highway fill	15	4	60	18	Poor	Good
15	Pa-LN	Seepage beneath earth dam	12	3	1200	370	Good	Poor
16	Tex-OC	Contain chem. waste	100	30	3 mi	5 km	Good	Satisfactory
17	Ky-WC	Waste water storage	28	9	3 mi	5 km	Good	Unknown
18	Del-CW	Water supply	18	6	200	60	Good	Good
19	NY-ASP	Recreation	60	20	1500	500	Good	Good

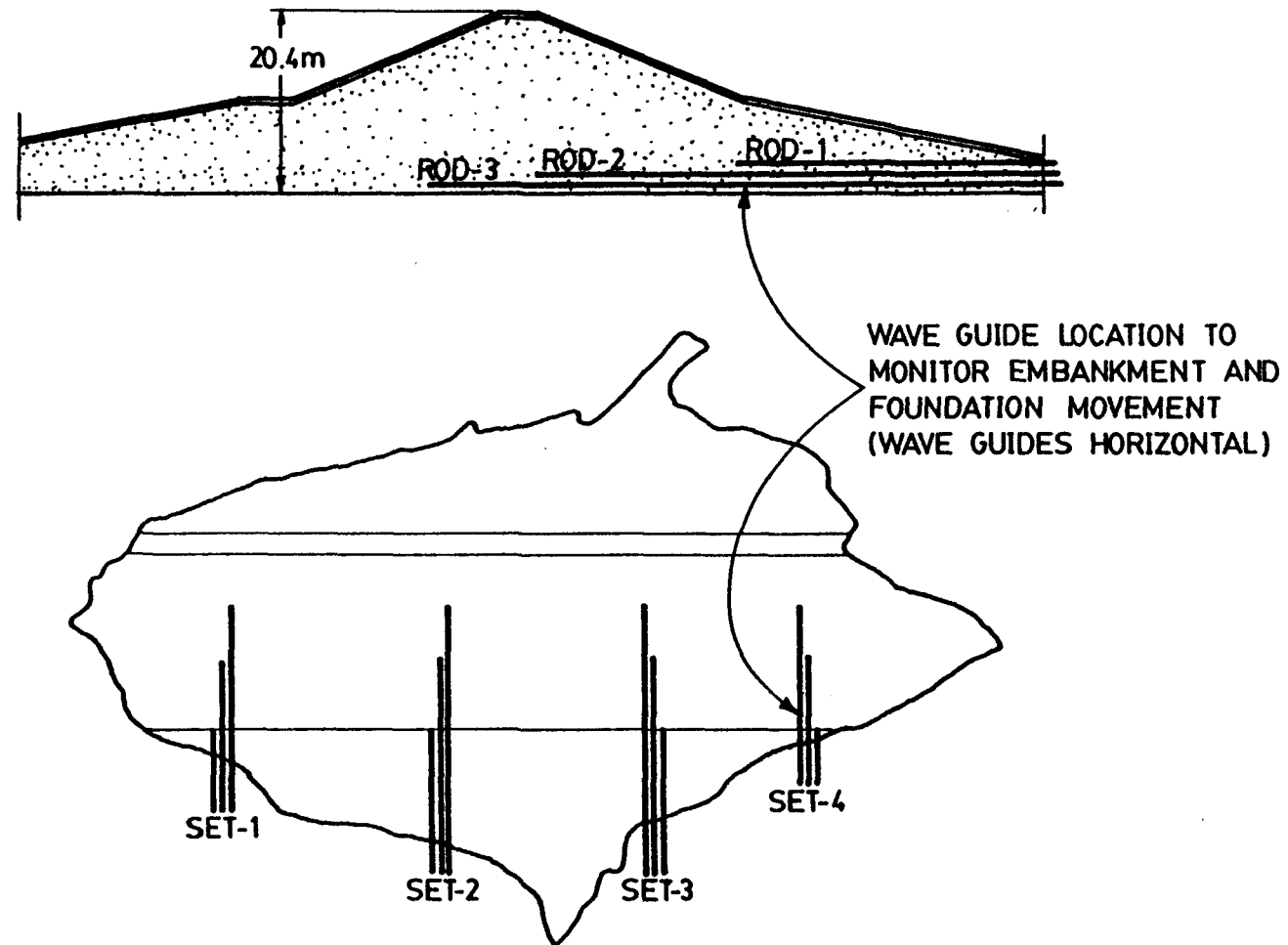


Figure 21. Elevation and plan views of site No. 3 near McCook, Nebraska, showing horizontal wave guide location scheme.

TABLE 6. ACOUSTIC EMISSIONS FROM NEB-200 DAM SITE

Set No.	Rod No.	Approx. length		Acoustic emission counts/min
		ft	m	
1	3	250	76	1958
1	2	210	64	639
1	1	140	63	80
2	3	270	82	16
2	2	230	70	7
2	1	160	49	0

Site No. 4 is a 12.2-m (40-ft) high stockpile of iron ore at Sparrow's Point, Maryland. It is adjacent to the location of a previous failure that resulted from overloading of the soft foundation soils by the ore. Four wave guides were placed: Two of them were horizontal beneath the fill, and two were vertical, beside the fill, penetrating deeply into the foundation soil. In addition to the standard type of instrumentation shown in Figure 1, an oscilloscope was included in the system monitoring the emissions. As fill was being placed, the emissions were noticeable on the oscilloscope but were not strong enough to trigger the counter. This lack of measurable emissions may be an indication that the Kaiser effect occurs in soils as it does in other materials. For cyclically loaded materials, the Kaiser effect predicts an absence of emissions during stress re-application until the highest previous stress level experience by the material has been attained. This particular site had been previously loaded with 12.2 to 21.3 m (40 to 70 ft) of iron ore many times in the past. Thus, the relatively low emission readings (and settlements for that matter) may be attributable to this preloading or stress history condition. Low emission levels at stresses less than the preconsolidation pressure were also observed in laboratory consolidation tests, as reported in Section 6.

Site No. 5 is a field study at the Philadelphia International Airport in Philadelphia, Pennsylvania, and is shown schematically in Figure 22. A surcharge fill has been placed around a previously installed, end-bearing pile to determine how much load will be added to the pile as a result of soil consolidation. This test constitutes a full-scale, negative skin friction or downdrag test. The test piles and settlement anchors were employed as acoustic emission wave guides to monitor the deformation of the settling soil. Figure 23 presents these results, where the similarity between the settlement/time and acoustic emission/time response curves should be noted. The fact that the acoustic emission response dissipated after 5 to 15 days actually agrees better with theoretical computations, using standard consolidation theory, than the 2 to 3 days for the settlement response. This significant case history illustrates the effectiveness of the acoustic emission monitoring techniques.

Site No. 6 is a 20.7-m (68-ft) high earth dam in the same watershed as site No. 3. Based on the experiences of that previous case history, vertical settlement plates were chosen for wave guides. These were 25.4-mm

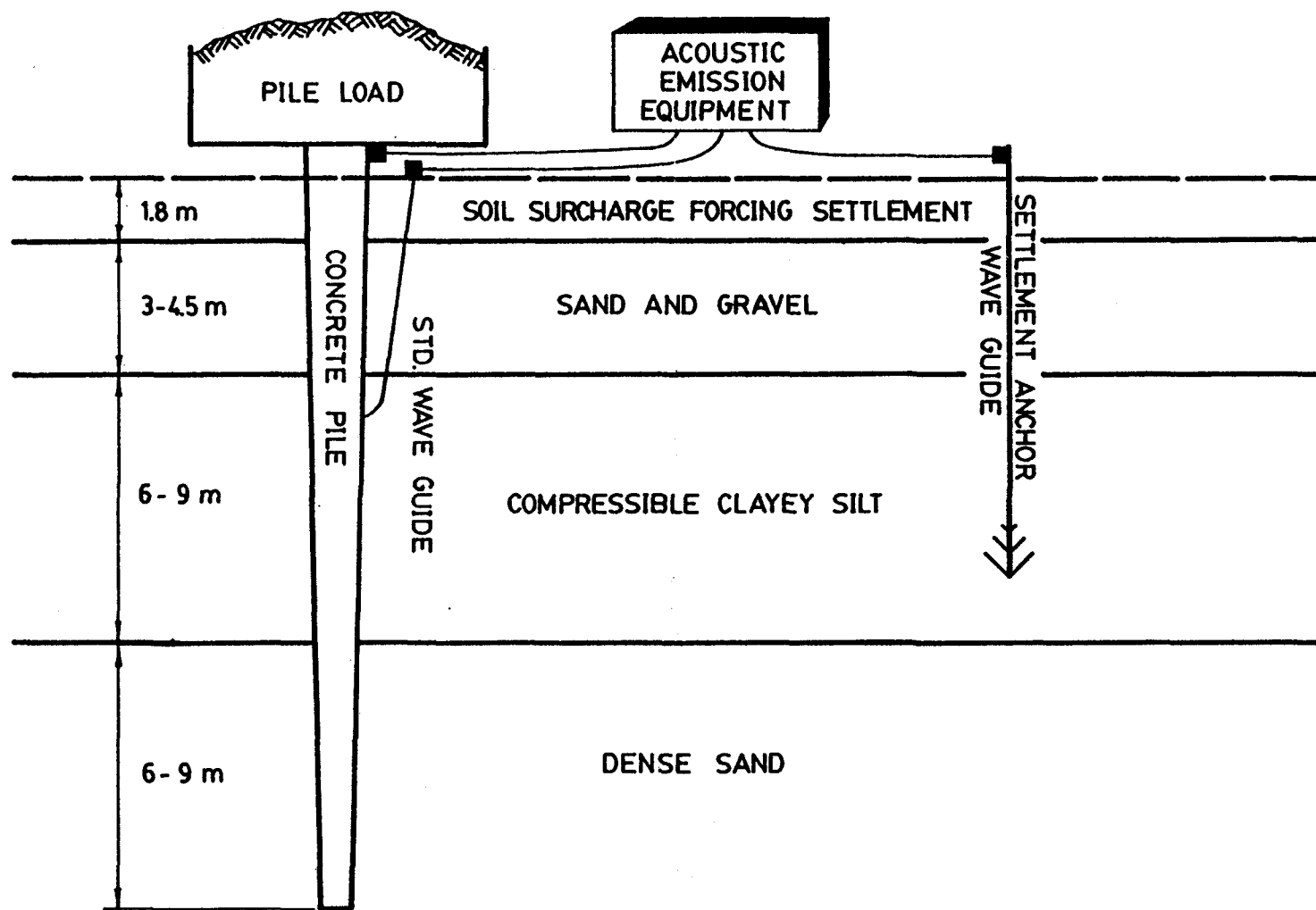


Figure 22. Elevation view of site No. 5 in Philadelphia, Pa., showing surcharge load and compressible soil along with different types of wave guides.

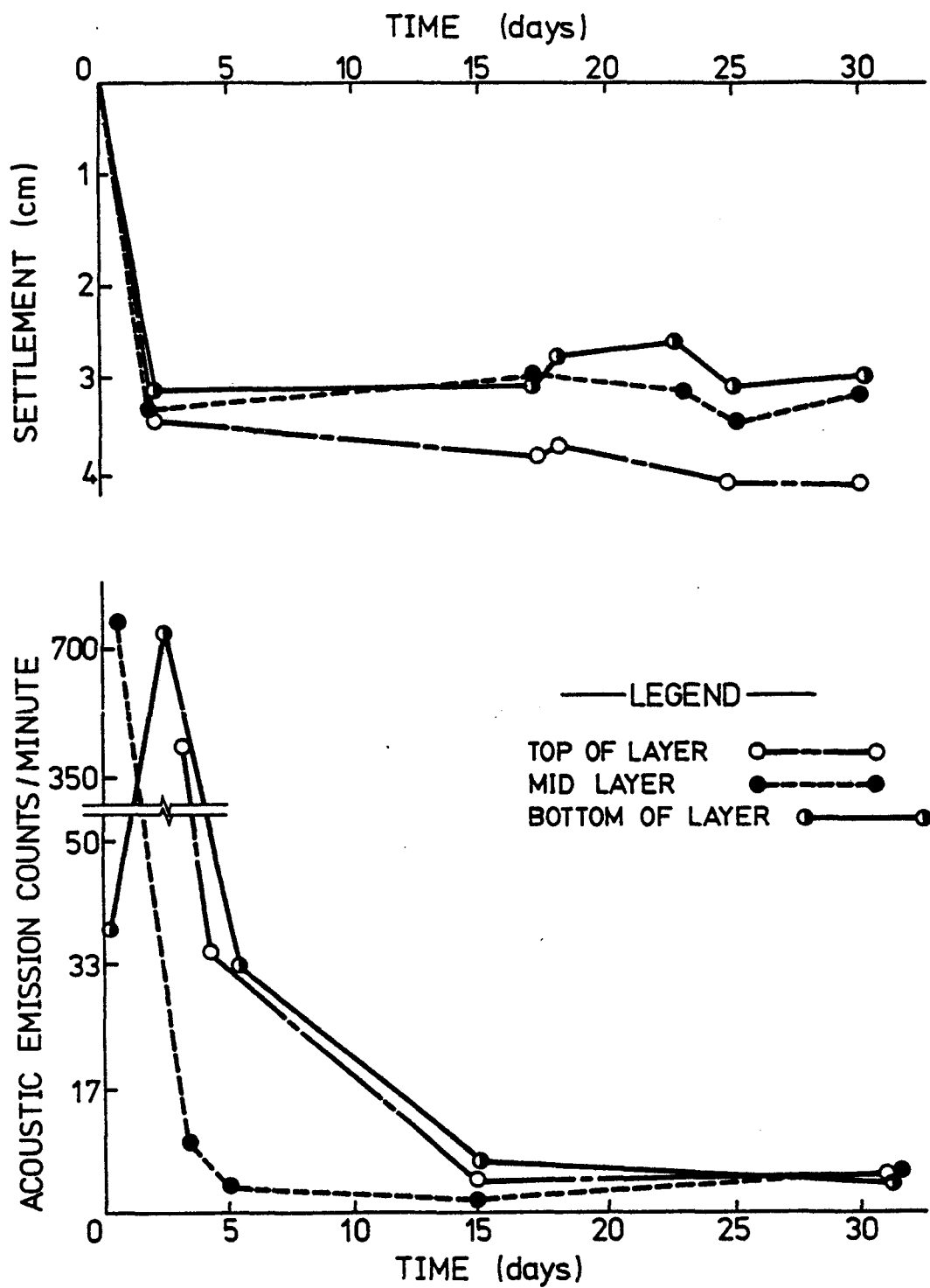


Figure 23. Time/settlement and time/acoustic emission response curves from site No. 5.

(1-in.) diameter rods within a 7.6-cm (3-in.) casing and would therefore serve both purposes. Though settlements were indeed recorded, acoustic emissions were not because of our inability to separate the actual signal from the banging of the rods within the casing. Thus no information was available from this site--a fact that illustrates the frequent problem of distinguishing signals from ambient noise.

Site No. 7 is an existing mine tailings dam in Quebec, Canada, that is being raised an additional 7 m (23 ft), making the total height 29 m (95 ft). Because a failure occurred at the site previously, greater than normal concern is being given to its stability. Both newly installed vertical wave guides and horizontal steel pipe drains are being used as wave guides. The site, however, is currently dormant because of mine inactivity.

Site No. 8 is a 4.6- to 12.2-m (15- to 40-ft) high homogeneous earth dam in Delaware City, Delaware, containing dredging spoils. Though the embankment itself appears stable, it is founded on a high-water content clayey silt of standard penetration resistance as low as 3 to 7 blows/m (1 to 2 blows/ft). The foundation soils are instrumented with 12.7-mm (1/2-in.) vertical rods, and acoustic emission counts vary from 0 to 10 counts/min. No noticeable long-term trends have been observed over the 18 months that this site has been monitored.

Site No. 9 is a 36.6-m (120-ft) high, zoned earth dam in Boyertown, Pennsylvania, constructed on rock containing an old inactive fault. The site is monitored with four sets of vertically placed, 12.7-mm (1/2-in.) diameter reinforcing rods. Each set has three bars of different lengths. The reservoir has recently been filled with no resulting acoustic emissions.

Site No. 10 is a system of holding ponds for various chemical waste liquids in New Jersey. The embankments vary in height from 2.4 to 6.1 m (8 to 20 ft), have steep side slopes (about 1 on 1), and are founded on extremely poor foundation soils. These foundation soils are silty clays and clayey silts of standard penetration resistance from 0 to 16 blows/m (0 to 5 blows/ft). A deep-seated base stability failure had occurred at the site before acoustic emission monitoring began. The site has since been monitored with twelve 12.7-mm (1/2-in.) diameter wave guides that were easily installed by pushing them, as 1/2-m (4-ft) sections, into the foundation soils to depths up to 6.1 m (20 ft). Acoustic emission activity is usually present, but count rates vary considerably. As an example, wave guide No. 7 (at the toe of the slope in the vicinity of the failure) has given the following response:

October 8, 1975	-	10 to 30 counts/min
November 5, 1975	-	0 to 5 counts/min
December 4, 1975	-	0 to 5 counts/min
February 25, 1976	-	20 to 40 counts/min
March 17, 1976	-	5 to 10 counts/min
June 3, 1976	-	10 to 15 counts/min
November 9, 1977	-	5 to 20 counts/min
June 7, 1978	-	10 to 30 counts/min

August 2, 1978	-	5 to 10 counts/min
October 6, 1978	-	0 to 20 counts/min
December 1, 1978	-	0 counts/min
March 27, 1979	-	10 to 40 counts/min

The site is an active one in which a permanent, on-line monitoring system has been recommended to the owners. Until such time as a continuous monitoring system is installed, periodic visits will be made.

Site No. 11 is the site of a small earth dam in Hopewell, Virginia, that bounds a lagoon containing an aqueous chemical Kepone in solution and as a sediment. Until such time that this extremely active substance can be "neutralized", the integrity of the impoundment, which is adjacent to the James River, must be assured. Four vertical wave guides (12.7-mm (1/2-in.) diameter steel rods) were placed through the embankment and into the foundation soil. Only one of these, at the location of obviously poor construction, gave any emission response (0-3 counts/min); maintenance work on the embankment was recommended to the owners to correct the situation.

Site No. 12 is almost identical to Site No. 11 except that the stored liquid consists of contaminated water, waste petroleum products, and sludges from various industries in and near Oswego, New York. There had been a failure of the dam, partly from erosion, and partly from overtopping as a result of inadequate freeboard. The break was repaired, and acoustic emission monitoring via four vertical wave guides was conducted. Significant acoustic emission activity was measured and corrective action was recommended. The contents of the lagoon were subsequently removed. Equilibrium of the earth dam was thus restored, and the acoustic emissions ceased.

Site No. 13 is a 4.6-m (15-ft) high stockpile of fill that was eventually used in the construction of an interstate highway in Philadelphia, Pennsylvania. Though it was not an engineered embankment, it did provide us with the opportunity of bringing a site to failure. A large front-end loader was used to excavate the toe of the slope for a length of about 6.1 m (20 ft) in a series of cuts, thereby incrementally decreasing the stability of the slope. One vertical wave guide about 3.0-m (10-ft) deep was installed at the top of the slope.

After each cut, the engine that powered the loader was shut off so that acoustic emission readings could be made without high background noise. Figure 24 gives the count rates for the four cuts made in bringing the slope to failure. For the first two cuts, the acoustic emission count rates--recorded as soon as the loader engine was stopped--attained their maximum values and rapidly decreased thereafter. No data were obtained during the third cut because of wind noise effects on the accelerometer at the relatively unsheltered site. The accelerometer was subsequently wrapped in a foam blanket. The fourth cut resulted in the same trend as the earlier ones until 20 minutes after the cut was made, when the count rate increased rapidly. The increased count rate was accompanied by the detachment of a large mass of soil from the top of the slope, an event that could easily be classified as a failure. Though this set of data is far

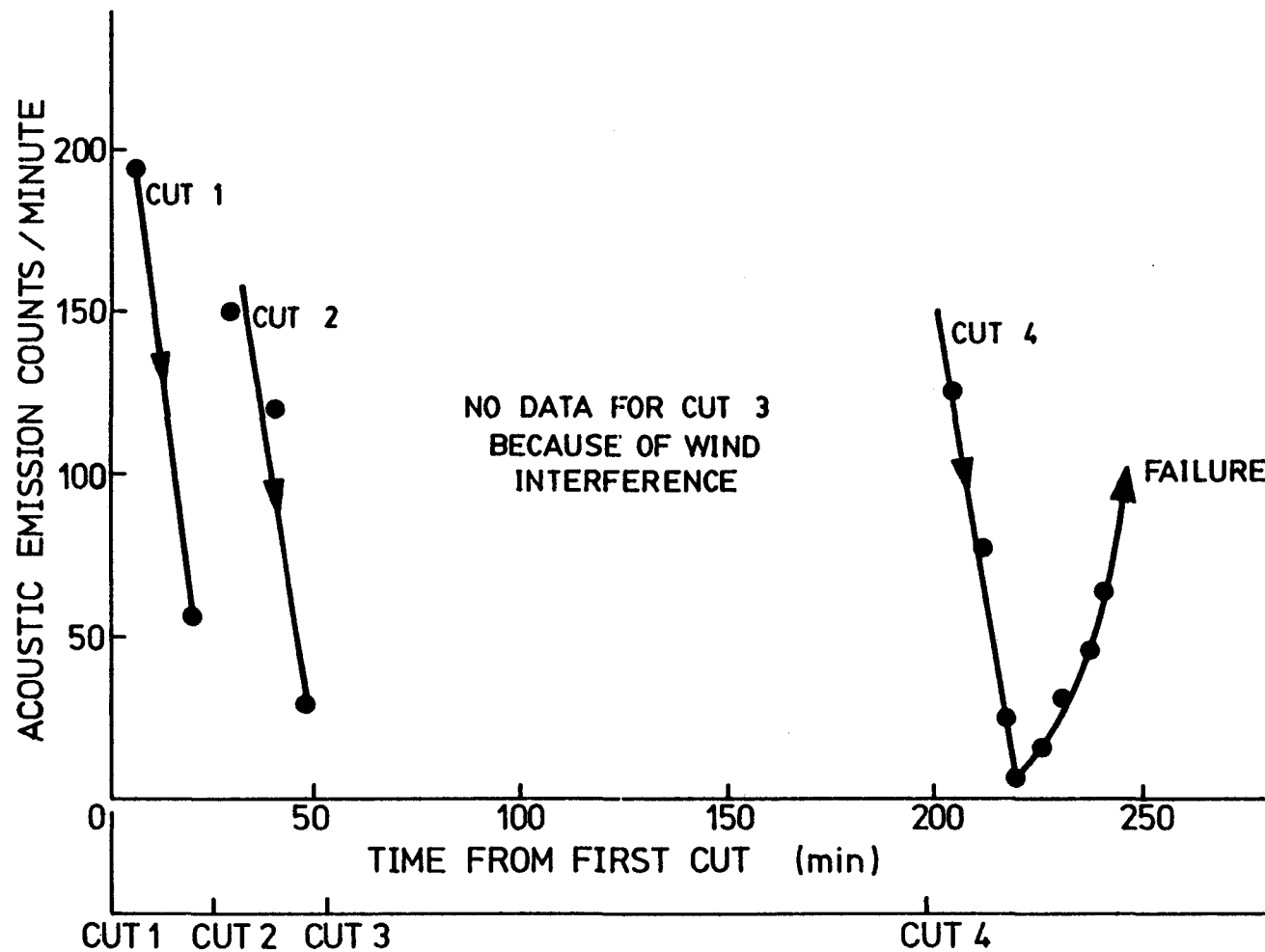


Figure 24. Acoustic emission count rate versus time of cut for site No. 13 showing failure after fourth cut.

from complete or clean, it gave us the encouragement needed to proceed to the more detailed and carefully controlled case history that follows.

Site No. 14 was a 4.6-m (15-ft) high stockpile of earth that was being stored for future highway construction near the Philadelphia International Airport. The soil was sampled, tested, and subsequently found to be a well-graded, silty sand with some clay (approximately 17%). The in-situ water content was approximately 12%, and the average unit weight was 2.00 g/cc (125 lb/ft³). Consolidated-drained triaxial shear tests resulted in an angle of shearing resistance of 16° and a cohesion of 11.0 kN/m² (1.6 lb/in² (psi)).

The site had a slope of approximately 1:1. A relatively uniform 18-m (60-ft) long section was selected for excavation. The excavation was made using a large front-end loader, which made successive cuts from the toe of the slope (Figure 25). Before excavation, the site was instrumented with the following systems:

- A grid of surface stakes was installed to be monitored using standard surveying methods.
- Soil strain gages were embedded in the slope and at the top of the slope to measure deformation and thus obtain soil strain.
- Slope inclinometers were installed to measure horizontal movements along a line at the top of the slope.
- Steel-rod wave guides were installed vertically at the top of the slope for acoustic emission monitoring.

The excavations were made as shown schematically in Figure 24, where the first cut of 17 m³ (22 yd³) produced little in the way of visual movement of the slope. The second cut of 55 m³ (67 yd³) was made 4 days later. A small tension crack was noted slightly above the cut and extended for a length of approximately 10.7 m (35 ft). The third cut of 72 m³ (94 yd³) was made 3 days later, and tension cracks were again noted one meter or so above the top of the cut. While this cut was open, a relatively heavy rain occurred. The fourth cut of 98 m³ (128 yd³) was made 8 days later, and tension cracks were very evident extending up to and beyond the top of the slope for the entire length of the slope. Rain again fell during the time period when this cut was open. The fifth and last cut of 110 m³ (144 yd³) was made 6 days later. Thirty-seven minutes after the cut was made, a large wedge of soil separated from the main embankment and collapsed into the area where the previous cuts had been made. This event was considered to be an actual earthen bank failure; monitoring was discontinued shortly thereafter.

Throughout this excavation process, monitoring was continued for as long as possible using the techniques described. Relevant comments regarding the results follow:

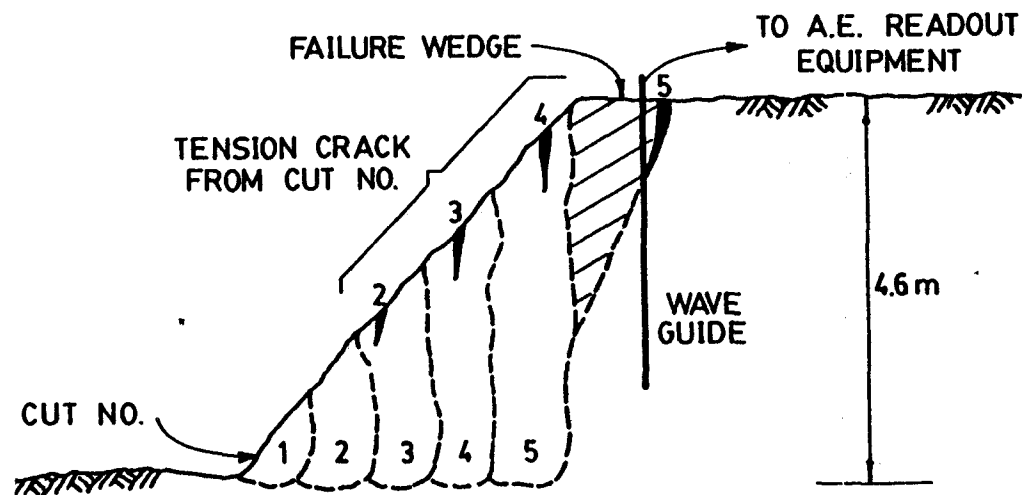


Figure 25. Schematic diagram of site No. 14 showing approximate boundaries of five cuts made and photographs after cuts Nos. 1 and 4.

1. The horizontal movement of the surface stakes indicated a gradually increasing movement away from the slope during the first three cuts. The movement immediately after the third cut averaged about 0.51 cm (0.20 in.). As noted earlier, both the second and the third cuts resulted in tension cracks that caused a loosening of the wooden stakes in the slope area above the cut to the point where readings were no longer reliable. The slope stake readings were discontinued at this point.
2. Soil strain gage readings were also interrupted by the tension cracks, since the coils used in this technique were hand-placed near the surface of the slope. They were judged to be reasonably accurate, however, until shortly after the fourth cut was made. At that time, the soil strain gages indicated an average strain of approximately 0.4%. The readings were not uniform, however, and they initially showed a slight compression before indicating tension. The sensors were easy to install and to calibrate initially, and they probably gave a reasonable assessment of the strain conditions up to the point of large-scale cracking of the embankment.
3. The slope inclinometers responded after the first cut was made, showing a movement of 0.76 to 1.02 cm (0.3 to 0.4 in.) ranging from zero at the top of the slope and zero at the bottom. After the first cut, and for most of the cuts thereafter, little additional movement was detected. Apparently, the deeper soil beneath the near surface did not deform enough to be accurately measured by this method. All three inclinometers gave essentially the same information.
4. The acoustic emission response curves for each of the five cuts are shown in Figures 26 through 30. From these curves, the following observations can be made:
 - a. Each response from the first four cuts indicates a high acoustic emission response initially, then an approximately exponential decay with time until stability of the particular cut is reached.
 - b. The fifth and last cut follows this general trend, but 30 minutes after the cut was made, the acoustic emission rate began to increase rapidly. When the count rate reached its maximum, about 7700 counts/min, a large section of soil pulled away from the intact mass and slid down the remaining slope. Thereafter, the count rate began to subside and eventually came to equilibrium. The post-failure count curve rate appears to rejoin the original curve (shown as the dashed line in Figure 30).
 - c. Not indicated on these figures is the effect of rain on the acoustic emission count rate. Approximately 8,200 min (5.7 days) after the third cut was made, a heavy rainfall caused

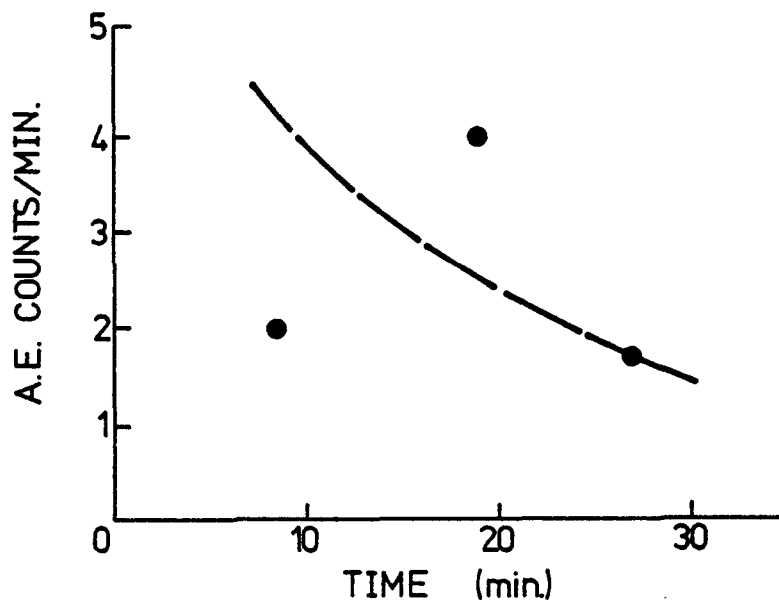


Figure 26. Acoustic emission response after cut No. 1.

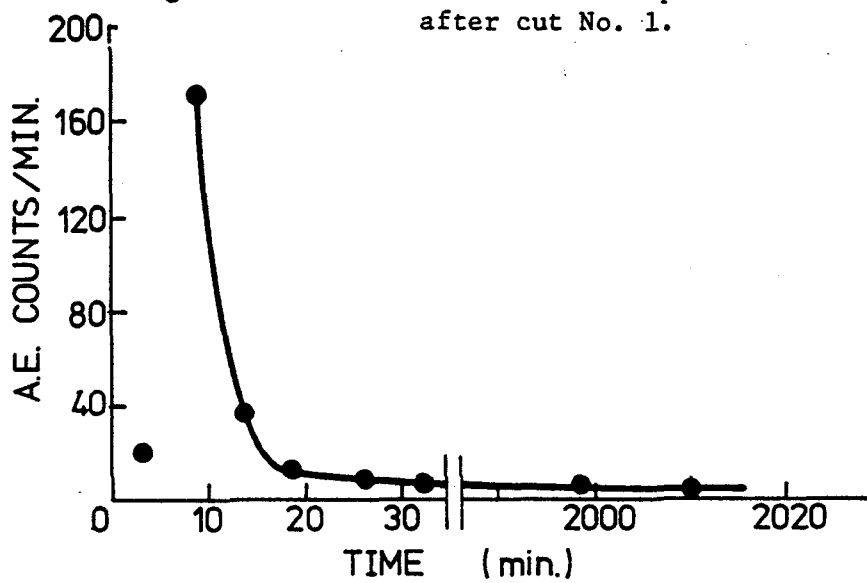


Figure 27. Acoustic emission response after cut No. 2.

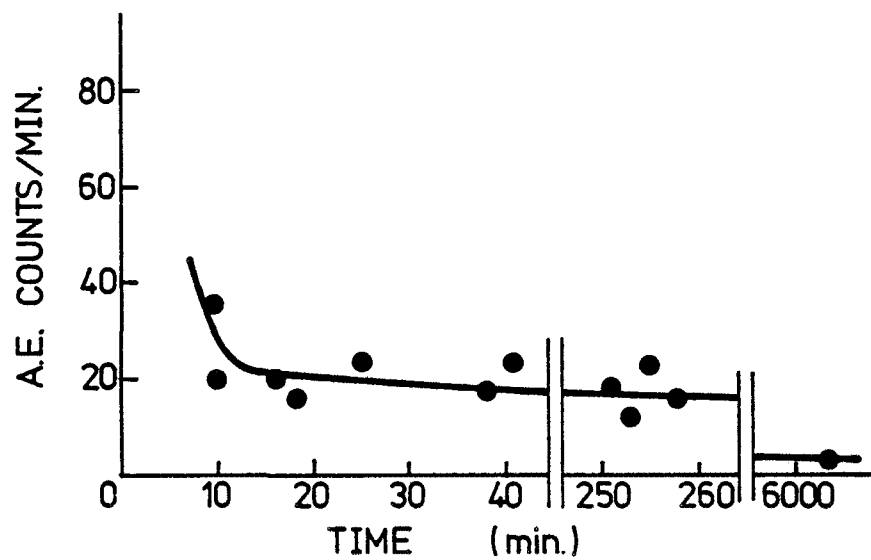


Figure 28. Acoustic emission response after cut No. 3.

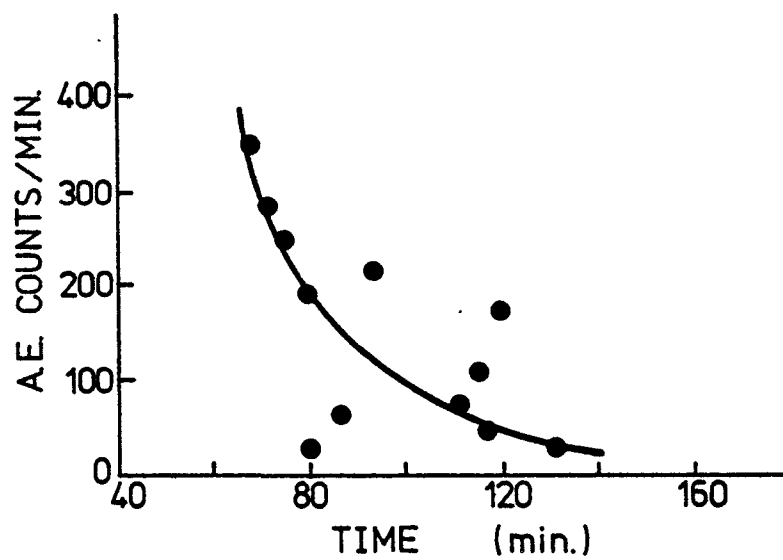


Figure 29. Acoustic emission response after cut No. 4.

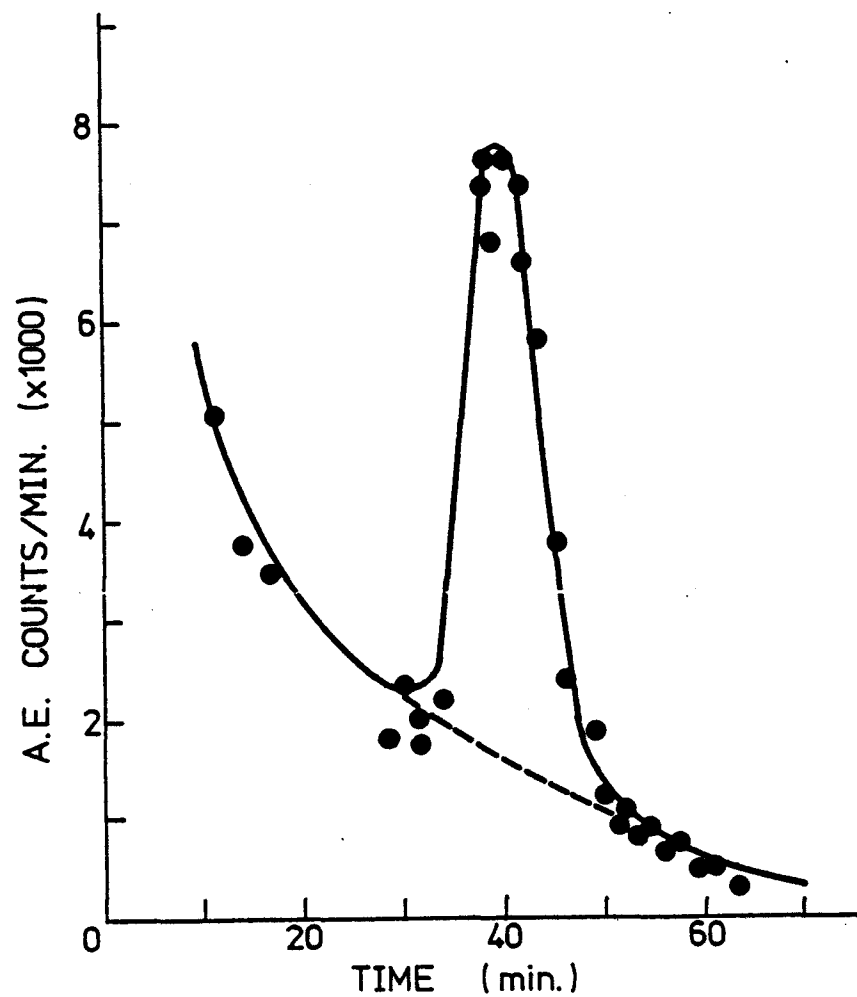


Figure 30. Acoustic emission response
after cut No. 5.

the count rate to rapidly increase to 200 counts/min. After 1,300 minutes (0.9 day), the count rate was back to its former level of 2 to 5 counts/min. Rain again interrupted the testing program after the fourth cut was made. Approximately 3,000 min (2.1 days) after the cut was made, rainfall occurred and the count rate increased to 350 counts/min. After an additional 2,500 min (1.7 days), the count rate decreased to zero. Thus it took a longer period for the slope to readjust to equilibrium when the rainfall ceased after cut No. 4, a fact that may be due to the gradual decrease in the slope's factor of safety. Regardless of the relative magnitudes involved, it can be concluded that the two rainfalls did have at least a temporary effect on the slope's stability.

Additional data can be obtained from this particular site by plotting the acoustic emission count rate of each cut (Figure 31). Here are presented curves for both the maximum count rate and the average count rate during the 1-hour period after monitoring began. The response curves are plotted for the first four cuts, and thereafter the count rates increase rapidly, as indicated. This type of behavior that loss of stability in slopes is not a linear process, but rather one in which instability occurs at a rapidly increasing rate as failure is approached.

Site No. 15 is an acoustic emission study of seepage beneath a 3.6-m (12-ft) high earth dam in northeastern Pennsylvania. Since this application of the technique is slightly different, it will be described separately in Appendix C of this report.

Site No. 16 involves the stability monitoring of piles of waste gypsum material, some of which was used to form a dike containing waste liquid. The site is near Houston, Texas, adjacent to the Houston Ship Channel. Acoustic emission wave guides have been installed at numerous locations around the area (which is actually in the form of three separate piles) and data are being collected by the owner. Acoustic emission monitoring equipment has also been purchased by the owner who, after a number of field visits, is monitoring the site with his own personnel. This particular site is of additional importance since the data are being compared to other geotechnical monitoring systems, i.e., piezometers. We are in regular correspondence with the owner's representatives on this particular site.

Site No. 17 is a waste water storage facility including sludge lagoons, aeration ponds, and stabilization lagoons in Kentucky near the Mississippi River. Embankment heights vary from 4 to 9 m (13 to 28 ft) with some relatively steep slopes of up to 40° from horizontal. Erosion of the slopes is easily observable.

Eight wave guides were installed to depths ranging from 1 to 4 m (4 to 12 ft). The highest acoustic emission count rate recorded was 2 counts/min with most locations registering 1.4 counts/min or less. We feel that no deformation at the site is presently occurring and, with proper

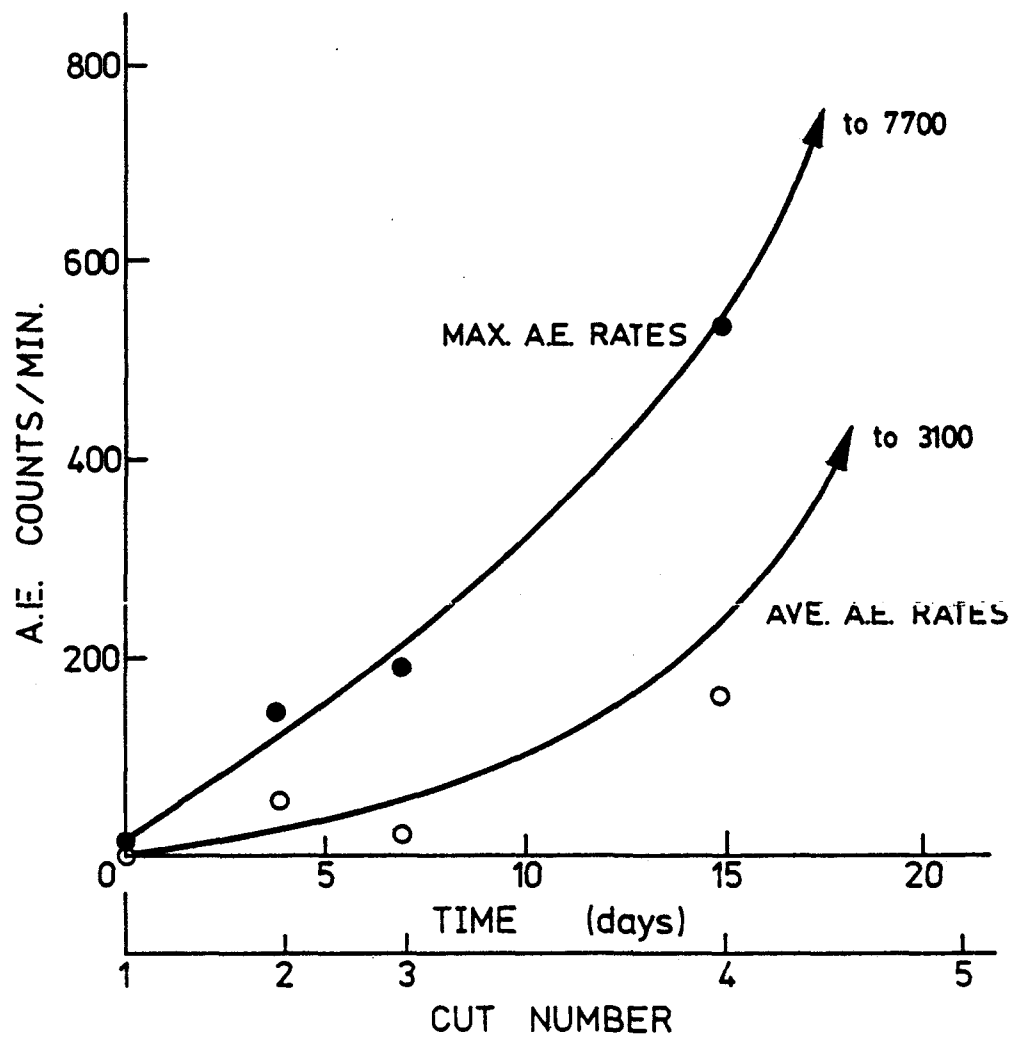


Figure 31. Summary of acoustic emission rates after each cut.

embankment maintenance, a stability failure is not likely to occur.

Site No. 18 is a water reservoir in Delaware, which was drained for inspection of the bottom. Subsequent to drawdown, a localized section of the sloped innerside slid into the empty reservoir. After this initial movement had occurred, we were asked to monitor the slope to see whether instability was a continuing problem and to assess remedial measures. As the data of Figure 32 indicate, settlements were still continuing and did so up to 127 cm (50 in.) of settlement. Acoustic emission monitoring wave guides were installed immediately and indicated initially high count rates (from February 3 to 10, 1978), followed by a periodic decreasing count rate until no emissions were detected after March 2, 1978. This latter stage corresponded to the lack of recorded settlement. The relatively high acoustic emission behavior between February 21 to 28 was a result of localized sloughing of the soil in the failure wedge's falling against the wave guides and resulting in high emission count rates. This behavior was not due to instability of the main failure wedge itself. This case history illustrates the need for continuous monitoring in many natural situations. During and after remedial work to the failed slope, no acoustic emission counts were recorded.

Site No. 19 is an earth dam in western New York that bounds a reservoir used for recreation purposes. It was inspected and found to be leaking at and beyond its downstream toe in a number of locations. Ten acoustic emission wave guides were installed to measure whether soil deformation was accompanying the seepage and to detect exactly where the seepage paths were located. At this time, it appears that the dam is stable but requires additional monitoring for actual seepage detection. Appendix C will further elaborate on the application of acoustic emission monitoring to seepage problems.

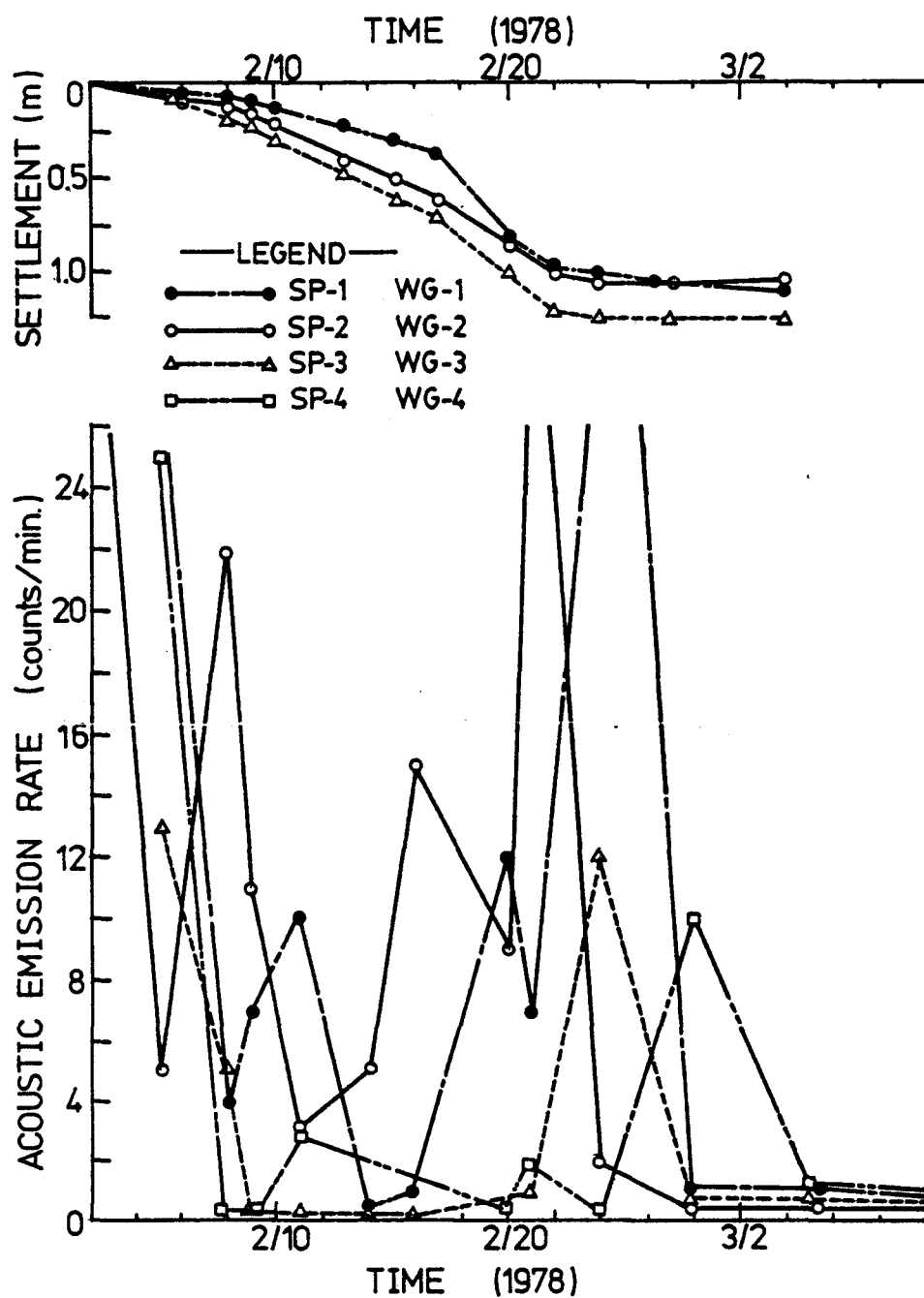


Figure 32. Settlement and acoustic emission response curves from site No. 18, showing response at various locations along slide area.

SECTION 8

SPILL ALERT DEVICE DETAILS

A series of photographs of the acoustic emission system used for field and laboratory monitoring is given in Figures 33 through 37. The field (basic) system (Figures 33 and 34) consists of an accelerometer, amplifier and counter. (A list of equipment suppliers with approximate prices as of December, 1978 is given in Table 7.) For the operation of this basic system, a user's manual has been prepared and is included as Appendix B of this report.

The laboratory (modified) system (Figures 35, 36, and 37) is intended for laboratory work where power is available and portability is not a critical factor. This modified system has, in addition to the basic system, two alternative high pass filters--one at 500 Hz and the other at 1,500 Hz. These filters eliminate some of the background noise that often accompanies work in crowded areas. Also provided for in this modified system is a chart recorder for a permanent record of the emission levels. Any one of a number of commercial recorders can be used.

The possibility of signature analysis (from either basic or modified systems) from a taped emission or entire test sequence is also possible using advanced computer techniques common to the acoustic emission industry in aerospace and nuclear applications. The literature abounds with such methods, but their application was judged to be beyond the scope of this research and development program because of high costs. The emphasis in this program has been to obtain an approximate, qualitative assessment of earth dam stability. Any count rate readout and recording (beyond visually observing a meter reading and recording the data in a notebook) raises the system's cost considerably; the cost of such improvements can, certainly, be justified in industrial and commercial applications.



Figure 33. Photograph of acoustic emission field system, showing (right to left) steel wave guide rod with coupling and attached accelerometer (note that, for purposes of illustration, the components have not been fully screwed together), thin coaxial cable of moderate length, amplifier (center, reading full scale) with coaxial cable connection to battery-powered electronic counting system (left, reading 000969).



Figure 34. Photograph of acoustic emission system in actual field use, showing (right to left) waveguide, coupling, and accelerometer (an unused wooden stake is also shown), coaxial cable connecting the accelerometer to the amplifier (center, lying on the ground), and battery-powered electronic counting unit with coaxial cable connection to amplifier. The carrying case for all the equipment is shown to the right of the amplifier.

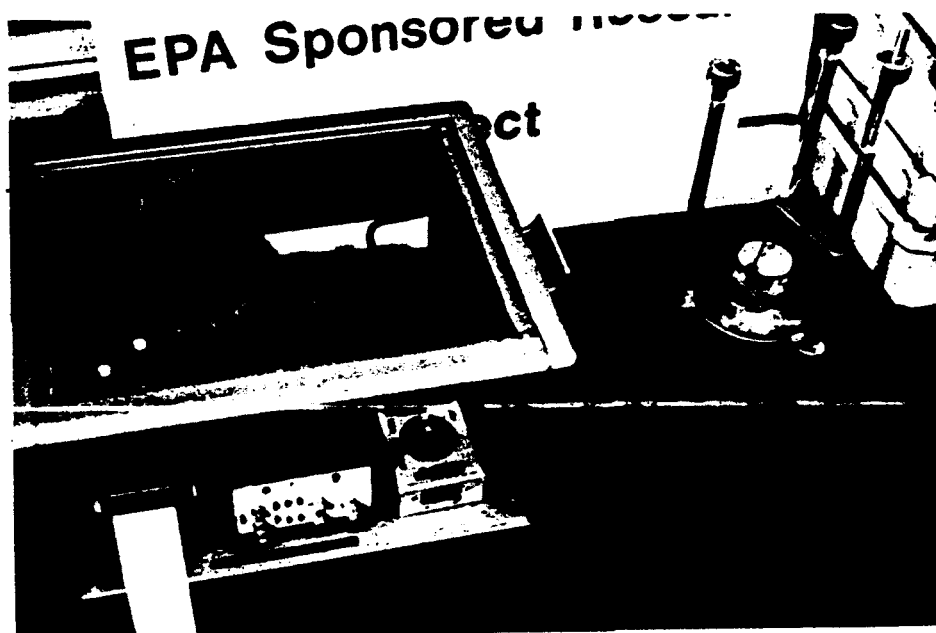


Figure 35. Photograph of laboratory version of acoustic emission system, showing (right to left) disassembled triaxial cell test unit where accelerometer and short waveguide can be seen supported by rubber band assembly, cable, and instrument chassis that contains amplifier, counting unit, and strip-chart recorder.



Figure 36. Photograph of front view of laboratory-use acoustic emission system, showing (left to right) strip-chart recorder, counting unit (displaying a count of 000120), and amplifier. Not visible (rear, behind counter) are band-pass filters.



Figure 37. Photograph of side and front of laboratory-use acoustic emission system, showing (left to right) side panel controls (for power, band-pass filters, etc.), strip-chart recorder, counting unit (without battery power component, but with count selector), and amplifier.

TABLE 7. COMMERCIALLY AVAILABLE ACOUSTIC EMISSION EQUIPMENT

Equipment	Price as of December 1978
Accelerometer:	
Columbia; Model No. 476	\$175 (less than 6)
nominal resonance = 7.5 KHz	\$155 (6 to 10)
Amplifier:	
Columbia; Vibration Meter	
model VM-103	\$395
Electronic counting system:	
Hewlett-Packard;	
5300 A Measuring System	\$500
5304 A Timer/Counter	\$385
5310 Battery Pack	\$275
Cable Connectors:	
B & K Instruments;	
Coaxial microdot cable,	
item A0-0037	\$2/ft
Microdot to Microdot	
JP-0012 connectors	\$3

Addresses of vendors cited: -

B & K Instruments, Inc.
 5111 W. 164th Street
 Cleveland, Ohio 44142 (216)267-4800

Columbia Research Laboratories, Inc.
 McDade Blvd. & Bullens Lane
 Woodlyn, Pa. 19094 (215)872-0381

Hewlett-Packard Co.
 King of Prussia Industrial Park
 King of Prussia, Pa. 19406 (215)265-7000

REFERENCES

1. Sowers, G. F., "The Use and Misuse of Earth Dams," Consulting Engr., July 1962. See also: Sowers, G. B., and Sowers, G. F., Introductory Soil Mechanics and Foundations, 3rd Edition, Macmillan, New York, 1970.
2. Koerner, R. M. and Lord, A. E., Jr., "Acoustic Emissions in a Medium Plasticity Clayey Silt," Jour. of Soil Mechanics and Foundations Div., ASCE, Tech. Note, Vol. 98, No. SM1, January 1972. pp. 161-165.
3. Lord, A. E., Jr., "Acoustic Emission - A Review," in Physical Acoustics, Vol. 11, W. P. Mason and N. Thurston, Eds., Academic Press, 1975. pp. 289-353.
4. Koerner, R. M., Lord, A. E., Jr., McCabe, W. M. and Curran, J. W., "Acoustic Emission Behavior of Granular Soils," Journal of the Geotechnical Engineering Division, ASCE, Vol. 102, No. GT7, July 1976. pp. 761-773.
5. Koerner, R. M., Lord, A. E., Jr., and McCabe, W. M., "Acoustic Emission Behavior of Cohesive Soils," Journal of the Geotechnical Engineering Division, ASCE, Vol. 103, No. GT8, August 1977. pp. 837-850.
6. Koerner, R. M., Lord, A. E., Jr., and McCabe, W. M., "Acoustic Emission (Microseismic) Monitoring of Earth Dams," Proceedings of Engr. Fdtn. Conf. on the Evaluation of Dam Safety, Calif., November 1976.
7. Koerner, R. M., Lord, A. E. Jr., and McCabe, W. M., "Acoustic Emission Monitoring of Soil Stability," Journal of the Geotechnical Engineering Division, ASCE, Vol. 104, No. GT5, May 1978. pp. 571-582.
8. Obert, L., "Use of Subaudible Noises for Prediction of Rockburst," RI-3555, United States Bureau of Mines, 1941.
9. Obert, L., and Duval, W. I., "Microseismic Method of Predicting Rock Failure in Underground Mining: Part I and Part II," RI-3797 and 3803, United States Bureau of Mines, 1946.
10. Hodgson, E. A., Bulletin of the Seismological Society of America, Vol. 32, 1942. p. 249.
11. Hodgson, E. A., Transaction of the Canadian Institute of Mining and Metallurgy, Toronto, Ontario, Canada, Vol. 46, 1943. p. 313.

12. Blake, W., Leighton, F., and Duvall, W. I., "Microseismic Techniques for Monitoring the Behavior of Rock Structures," Bulletin 665, United States Department of the Interior, Bureau of Mines, 1974.
13. Hardy, H. R., Jr., "Evaluating the Stability of Geologic Structures Using Acoustic Emission," ASTM-STP-571, American Society for Testing and Materials, Philadelphia, Pa., 1975.
14. Mearns, R., and Hoover, T., "Subaudible Rock Noise (SARN) as a Measure of Slope Stability," Final Report CA-DOT-TI-2537-1-73-24, United States Department of Transportation, Federal Highway Administration, August 1973.
15. Kaiser, J., "Untersuchungen uber das auftreten Gerauschen Beim Zugversuch," Thesis presented to Technische Hochschule at Munich, Germany, 1950.
16. Kaiser, Jr., "Erkenntnisse und Folgerungen aus der Messung von Gerauschen bezugbeanspruchung von Metallischen Werkstoffen," Arkiv. fur das Eisenhüttenwesen, Vol. 25, 43, 1953.
17. Tatro, C.A., and Liptai, R. G., "Acoustic Emission from Crystalline Substances," Proceedings of the Symposium on the Physics of Nondestructive Testing, Southwest Research Institute, San Antonio, Texas, 1962. pp. 145-174.
18. Tatro, C. A., and Liptai, R. G., Proceedings of the 4th Symposium on Nondestructive Testing of Aircraft and Missile Components, Southwest Research Institute, San Antonio, Texas, 1963. pp. 287-346.
19. Green, A. T., "Detection of Incipient Failure in Pressure Vessels by Stress-Wave Emissions," Nuclear Safety, Vol. 10, 1969. pp. 4-18.
20. Nakamura, Y., "Acoustic Emission Monitoring System for the Detection of Cracks in a Complex Structure," Materials Evaluation, January 1971. pp. 8-12.
21. Liptai, R. G., "Acoustic Emission Techniques in Materials Research," International Journal of Nondestructive Testing, Vol. 3, 1971.
22. Dunegan, H. L., and Tatro, C. A., "Acoustic Emission Effects During Mechanical Deformation," in Techniques of Metal Research, Vol. 5, R. F. Bunshah, Ed., Interscience, New York, 1971.
23. Knill, J. L., Franklin, J. A., and Malone, A. W., "A Study of Acoustic Emission from Stressed Rock," International Journal of Rock Mechanics and Mining Sciences, Vol. 5, 87, 1968.
24. Drouillard, T. F., "Acoustic Emission: A Bibliography of 1970-1971-1972," ASTM-STP-571, American Society for Testing and Materials, 1975.

25. Goodman, R. E., and Blake, W., "Rock Noise in Landslides and Slope Failures," Highway Research Board, Vol. 119, 1966. pp. 50-60.
26. Cadman, J. D., and Goodman, R. E., "Landslide Noise," Science, Vol. 15, December 1, 1967. pp. 1182-1184.
27. Pollock, A. A., "From Metals to Rocks: Physics and Technology in Common and in Contrast," Proceedings of the Conference on Microseismic Activity in Geologic Materials, Pennsylvania State University, University Park, Pa., June 9-11, 1975, Academic Press, Inc., New York, 1976.
28. Van Vlack, L. G., "Elements of Materials Science and Engineering," 3rd ed., Addison-Wesley, New York, 1975.
29. Clark, D. S., and Varney, W. R., Physical Metallurgy for Engineers, 2nd ed., Van Nostrand, New York, 1962.
30. Engle, R. B., "Acoustic Emission and Related Displacements in Lithium Fluoride Single Crystals," Thesis presented to Michigan State University, Ann Arbor, Mich., 1966, (available through University Microfilms 48160-6707535, Ann Arbor, Mich.).
31. Sedgwick, R. T., "Acoustic Emission from Single Crystals of LiF and KCl," Journal of Applied Physics, Vol. 39, No. 3, 1968. pp. 1728-1740.
32. Scholz, C. H., "Mechanism of Creep in Brittle Rock," Journal of Geophysical Research, Vol. 73, 1968. pp. 3295-3302.
33. Chugh, Y. P., Hardy, H. R., Jr., and Stefanko, R., "Investigation of the Frequency Spectra of Microseismic Activity in Rock Under Tension," Proceedings of the Tenth Rock Mechanics Symposium, Austin, Texas, May 1968.
34. Koerner, R. M., "Behavior of Single Mineral Soils in Triaxial Shear," Journal of the Soil Mechanics and Foundations Division, ASCE, Vol. 96, No. SM4, Proc. Paper 7432, July 1970. pp. 1373-1390.
35. Lee, K. L., and Seed, H. B., "Drained Strength Characteristics of Sand," Journal of the Soil Mechanics and Foundation Division, ASCE, Vol. 93, No. SM6, Proc. Paper 5561, November 1967. pp. 117-141.
36. Horn, H. M., and Deere, D. U., "Frictional Characteristics of Minerals," Geotechnique, London, England, Vol. 12, 1962. pp. 319-335.
37. Hardy, H. R., Jr., "Application of Acoustic Emission Techniques to Rock Mechanics Research," STP-505, ASTM, Philadelphia, 1972. pp. 41-83.
38. Hardy, H. R., Jr., and Khair, A. E., "Applications of Acoustic Emission in the Evaluation of Underground Gas Storage Reservoir Stability," Proc. 9th Can. Rock Mech. Symp., Montreal, December 1973. pp. 77-111.

39. Wisecarver, D. W., Merrill, R. and Stateham, R. M., "The Microseismic Technique Applied to Slope Stability," Soc. of Mining Engineers, Trans. A.I.M.E., Vol. 224, 1969. pp. 378-385.
40. Liptai, R. G., "Acoustic Emission from Composite Materials," Report URCL-72657, Lawrence Radiation Lab., Livermore, Calif., 1971.
41. Hutton, P. H., "Acoustic Emission Applied Outside of the Laboratory," STP-505, ASTM, Philadelphia, 1972. pp. 114-128.
42. Galambos, C. F., and McGogney, C. A., "Opportunities for NDT of Highway Structures," Materials Evaluation, ASTM, Vol. 33, No. 7, July 1975. pp. 169-175.
43. Williams, D. R., Jr., "Five Decades of Progress in Pipelining," Jour. of Const. Div., ASCE, Vol. CO4, December 1975. pp. 751-767.
44. Koerner, R. M., Lord, A. E., Jr., and Deisher, J. N., "Acoustic Emission Leak and Stress Monitoring to Prevent Spills from Buried Pipelines," Proc. of 1976 Natl. Conf. on Control of Hazardous Matls. Spills, New Orleans. pp. 8-15.
45. Parry, D. L., "Industrial Applications of Acoustic Emission Analysis Technology," STP-571, ASTM, Philadelphia, 1975. pp. 150-183.
46. van Reimsdijk, A. J., and Bosselaere, H., "On Stream Detection of Small Leaks in Crude Oil Pipelines," Proc. 7th World Petroleum Conf., Vol. 6, Mexico, 1967. pp. 239-250.
47. Laura, P. A., Vanderveldt, H., and Gaffney, P., "Acoustic Detection of Structural Failure of Mechanical Cables," Jour. Acoust. Soc. of Amer., Vol. 45, No. 3, 1969. pp. 791-793.
48. Laura, P. A., Vanderveldt, H. H., and Gaffney, P. G., "Mechanical Behavior of Stranded Wire Rope and Feasibility of Detection of Cable Failure," Marine Technology Society Jour., Vol. 4, No. 3, 1970. pp. 19-32.
49. Harris, D. O., and Dunegan, H. L., "Acoustic Emission Testing of Wire Rope," Tech. Report DE-72-3A, Dunegan/Endevco, Livermore, Calif., October 1972.
50. Hardin, B. O., "The Nature of Damping in Sands," Journal of the Soil Mechanics and Foundations Division, ASCE, Vol. 91, No. SM1, Proc. Paper 4206, January 1965. pp. 63-97.
51. Hardin, B. O., "Elastic Wave Velocities in Granular Soils," Journal of the Soil Mechanics and Foundations Division, ASCE, Vol. 89, No. SM1, Proc. Paper 3407, January 1963. pp. 33-65.

52. Nyborg, W. L., Rudnick, I., and Shilling, H. K., "Experiments on Acoustic Absorption in Sand and Soil," J. Acous. Soc. Amer., Vol. 22, No. 4, July 1950. pp. 422-425.
53. Kaiser, J., "Erkenntnisse und Folgerungen aus der Messung von Gerauschen bei Zugbeanspruchung von metallischen Werkstoffen," Arkiv fur das Eisenhüttenwesen, Vol. 1/2, January/February 1953. pp. 43-45.
54. Lord, A. E., and Koerner, R. M., "Estimated Magnitude of Acoustic Emissions in Soil," Tech. Note, Journal of the Geotechnical Engineering Div., ASCE, 1979.
55. Halliday, D., and Resnick, R., Physics, Wiley, New York, 1966.
56. Cook, N. G. W., "Seismicity Associated With Mining," Engineering Geology, 10, 1976. pp. 99-122.
57. U.S. Environmental Protection Agency Proposal Solicitation, "Petroleum Pipeline Leak Detection Study," RFP No. C1-76-0145.
58. Proc. First Intl. Conf. on the Internal and External Protection of Pipes, Univ. of Durham, England, (BHRA Fluid Engr., Publ.), September 9-11, 1976.
59. Koerner, R. M., Lord, A. E., Jr., and Deisher, J. N., "Acoustic Emission Stress and Leak Monitoring to Prevent Spills from Buried Pipelines," Proc. 1976 Natl. Conf. on Control of Hazardous Materials Spills, New Orleans, La., April 25-28, 1976. pp. 761-773.
60. Lord, A. E., Jr., Deisher, J. N., and Koerner, R. M., "Attenuation of Elastic Waves in Pipelines as Applied to Acoustic Emission Leak Detection," Materials Evaluation, ASTM, Vol. 35, No. 11, November 1977. pp. 49-60.
61. McCabe, W. M., Koerner, R. M., and Lord, A. E., Jr., "Acoustic Emission Behavior of Concrete Laboratory Specimens," ACI Journal, July 1976. pp. 367-371.

APPENDIX A

PUBLISHED AND/OR SUBMITTED TECHNICAL PAPERS ON ACOUSTIC EMISSION MONITORING

1. Koerner, R. M., and Lord, A. E., Jr., "Acoustic Emissions in a Medium Plasticity Clayey Silt," Tech. Note, ASCE, Journal of Soil Mechanics and Foundations Div., Vol. 98, January 1972. pp. 161-165.
2. Lord, A. E., Jr., and Koerner, R. M., "Acoustic Emission Response of Dry Soils," Jour. of Testing and Evaluation, ASTM, Vol. 100, No. 3, May 1974. pp. 159-162.
3. Koerner, R. M., and Lord, A. E., Jr., "Earth Dam Warning System to Prevent Hazardous Material Spills," AIChE/EPA Conference on Control of Hazardous Material Spills, San Francisco, Calif., August 1974.
4. Koerner, R. M., and Lord, A. E., Jr., "Acoustic Emission in Stressed Soil Samples," J. Acoust. Soc. Am., Vol. 56, No. 6, December 1974. pp. 1924-1927.
5. Lord, A. E., Jr., and Koerner, R. M., "Acoustic Emissions in Soils and Their Use in Assessing Earth Dam Stability," Jour. Acoust. Soc. Am., Vol. 57, No. 2, February 1975. pp. 416-419.
6. Lord, A. E., Jr., and Koerner, R. M., "Application of Acoustic Emission Techniques to Materials Studies - Soils," Amer. Soc. for Nondest. Testing Handbook, R. C. McMaster, Ed., to be published.
7. Koerner, R. M., and Lord, A. E., Jr., "Application of Acoustic Emission Monitoring to Earth Dam and Foundation Stability," Amer. Soc. for Nondest. Testing Handbook, R. C. McMaster, Ed., to be published.
8. Lord, A. E., Jr., and Koerner, R. M., Fundamental Studies of Acoustic Emissions in Soil and Laboratory Specimens, First Conf. on Acoustic Emission in Geologic Structures and Materials, Pennsylvania State Univ., Vol. 2, No. 3, Trans. Tech. Publ., Switz., June 9-11, 1975.
9. Koerner, R. M., and Lord, A. E., Jr., Applied Studies of Acoustic Emissions in Soil Masses at Field Sites, First Conf. on Acoustic Emission in Geologic Structures and Materials, Pennsylvania State University, Vol. 2, No. 3, Trans. Tech. Publ., Switz., June 9-11, 1975.

10. Koerner, R. M., Lord, A. E., Jr., and McCabe, W. M., "Acoustic Emission Monitoring in Concrete and Foundation Soils," Conf. Proc. of Analysis and Design of Foundations for Tall Buildings, Lehigh Univ., Aug. 4-8, 1975. pp. 637-653.
11. Koerner, R. M., and Lord, A. E., Jr., "Acoustic Emission Monitoring of Earth Dam Stability," Water Power and Dam Construction, Vol. 28, No. 4, London., April, 1976. pp. 45-49.
12. Lord, A. E., Jr., Koerner, R. M., and McCabe, W. M., "Acoustic Emission Behavior of Sand as Used in Foundation Bearing Capacity," ASTM, Materials Evaluation, May 1976. pp. 103-108.
13. McCabe, W. M., Koerner, R. M., and Lord, A. E., Jr., "Acoustic Emission Behavior of Concrete Laboratory Specimens," American Concrete Institute, ACI Jour., July 1976. pp. 367-371.
14. Koerner, R. M., Lord, A. E., and Deisher, J. N., "Acoustic Emission Stress and Leak Monitoring to Prevent Spills from Buried Pipelines," Proc. 1976, Natl. Conf. in Control of Hazardous Material Spills, New Orleans, La., April 25-28, 1976. pp. 8-15.
15. Koerner, R. M., Lord, A. E., Jr., McCabe, W. M., and Curran, J. W., "Acoustic Emission Behavior of Granular Soils," Jour. of Geotechnical Div., ASCE, Vol. 102, No. GT7, July 1976. pp. 761-773.
16. Koerner, R. M., Lord, A. E., Jr., and McCabe, W. M., "Acoustic Emission Behavior of Cohesive Soils," Jour. of Geotechnical Engr. Div., ASCE, Vol. 103, No. GT8, August 1977. pp. 837-850.
17. Koerner, R. M., Lord, A. E., Jr., and McCabe, W. M., "Acoustic Emission Monitoring of Soil Stability," Jour. of Geotechnical Engr. Div., ASCE, Vol. 104, No. GT5, May 1978. pp. 571-582.
18. Lord, A. E., Jr., Curran, J. W., and Koerner, R. M., "A New Transducer System for Determining Dynamic Mechanical Properties and Attenuation in Soils," J. Acous. Soc. of Amer., Vol. 60, No. 2, August 1976. pp. 517-520.
19. Lord, A. E., Jr., Diesher, J. N., and Koerner, R. M., "Attenuation of Elastic Waves in Pipelines as Applied to Acoustic Emission Leak Detection," ASNT, Materials Evaluation, Vol. 35, No. 11, November 1977. pp. 49-54 and Proc. of 1977 ASNT Conf. in Phoenix, Arizona.
20. Koerner, R. M., Lord, A. E., Jr., and McCabe, W. M., "Acoustic Emission (Microseismic) Monitoring of Earth Dams," Conf. Proc. of the Evaluation of Dam Safety, Engr. Fdtn. Conf., Pacific Grove, Calif., December 1976. pp. 274-291.
21. Koerner, R. M., Lord, A. E., and Deisher, J. N., "Acoustic Emission Detection of Underground Gasoline Storage Tank Leaks," Proc. ASNT Conf. in Phoenix, Arizona, March 28-30, 1977.

22. Koerner, R. M., and Lord, A. E., Jr., "Acoustic Emission Response of Coal and Charcoal Briquettes," 15th Biennial Conf. of the Inst. for Briquetting and Agglomeration, Vol. 15, August 1977.
23. Koerner, R. M., McCabe, W. M., and Lord, A. E., Jr., "Advances in Acoustic Emission Monitoring," Vol. 30, No. 10, Water Power and Dam Construction, London, October 1978. pp. 38-41.
24. Lord, A. E., Jr., and Koerner, R. M., "Acoustic Emission Generation in Soil Masses," invited paper for Acoustic Societies of America and Japan Conference in Hawaii, November 1978 (in Conference Proceedings).
25. Koerner, R. M., and Lord, A. E., Jr., "Predicting Dam Failure," Research Direction, Vol. 1, No. 1, Winter 1978, Drexel University. pp. 1-4.
26. Koerner, R. M., Lord, A. E., Jr., and McCabe, W. M., "The Challenge of Field Monitoring of Soil Structures Using A. E. Methods," Second Conf. on Acoustic Emission/Microseismic Activity in Geologic Structures and Materials, The Pennsylvania State University, November 13-15, 1978 (in Conference Proceedings). pp. 275-290.
27. McCabe, W. M., "Acoustic Emission in Coal: A Laboratory Study," Second Conf. on Acoustic Emission/Microseismic Activity in Geologic Structures and Materials, The Pennsylvania State University, November 13-15, 1978 (in Conference Proceedings). pp. 35-54.
28. Koerner, R. M., "Overview of A. E. Monitoring of Rock Structures," 5th Proceedings of Philadelphia Section, ASCE Geotechnical Group, 1979.
29. Lord, A. E., Jr., and Koerner, R. M., "On the Magnitude of Acoustic Emissions in Soil and/or Rock," Geotechnical Engineering Division, ASCE, August 1979. pp. 1249-1253.
30. McCabe, W. M., and Koerner, R. M., "Acoustic Emission (Microseismic) Monitoring for Ground Control in Tunnels," Presented at Rapid Excavation and Tunneling Conference, June 18-21, 1979, Atlanta, Georgia (in Conference Proceedings).

APPENDIX B

SPILL ALERT DEVICE USERS MANUAL*

Theory of Operation

The system described in the following pages and shown in Figure B-1 is designed to sense very small vibrations that occur within the soil mass and that are propagated along the steel rod (wave guide) to the ground surface. The accelerometer is attached to the wave guide, where it converts the vibrations into electrical impulses that are amplified by the Columbia model VM-103 vibration meter and then counted by the Hewlett-Packard 5300 series counter/timer. The preparation and actual use of this equipment during the monitoring process are outlined below.

Equipment Preparation

The accelerometer must be connected to the wave guide through a small brass fitting called a coupler (Figure B-2). The coupler has male threads at each end, the larger end (5/16-NC thread) of which must be screwed into the end of the wave guide protruding from the ground. This connection should be made tightly with pipe wrenches for best results. The accelerometer is then threaded just barely hand-tight onto the smaller end (10/32-NF thread). Caution: over-tightening the accelerometer may cause damage.

Use thin coaxial cables with "Microdot" connectors on each end to join the accelerometer to the top of the VM-103. To connect the VM-103 amplifier to the Hewlett-Packard counter, insert the banana-plug end of the special coaxial cable into the VM-103 and attach the BNC connector end to INPUT A (lower connector) on the counter panel. The initial setting on these instruments should be as follows:

* Prepared by W. Martin McCabe and Robert M. Koerner, Department of Civil Engineering, Drexel University.



Hewlett-Packard counter



VM-103 amplifier

Figure B-1. Photographs of spill alert device components.

VM-103

Turn range dial fully counter clockwise (0.01g).

Push in ACC button.

After turning on, push BAT TEST switch up. If red light below switch goes on, batteries are good. If not, remove back of VM-103 and replace the two 9-volt batteries. These batteries can be obtained at any radio or electronics supply shop.

HEWLETT-PACKARD COUNTER

Turn battery pack switch to BATTERY when operating in field, and to CHARGE when recharging batteries.

Turn COM-SEP-CHK switch to SEP.

Turn ATTEN switches to x1.

Turn AC/DC switches to AC.

Turn SLOPE switches to +/-.

Turn LEVEL dials to PSET.

Turn inner mode control dial to OPEN/CLOSE A and outer DELAY dial fully counterclockwise.

Turn on by turning OFF-SAMPLE RATE-HOLD dial just far enough clockwise to produce a click.

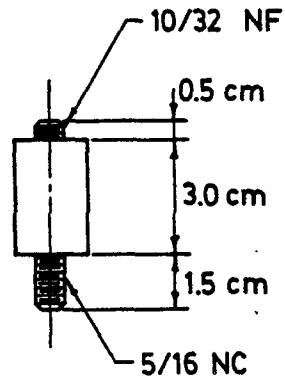
Push OPEN/CLOSE button to activate counting operation (small red c will appear to right of the display). Push this same button once more to deactivate the counting operation (c will disappear).

Monitoring Operation

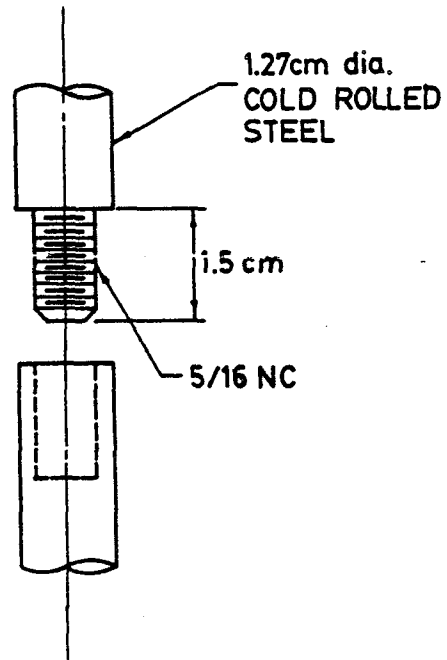
Once all the connections have been made at the desired monitoring location, place the instruments firmly on the ground and do not touch unless to re-zero the display or change the sensitivity settings. If the wind is blowing moderately, place a bucket or box over the top of the wave guide and accelerometer (or wrap the components in flexible polyurethane foam sheet padding) to prevent wind-induced noise from being counted. Turn all instruments on, activate counting, and wait 2 to 3 min for warm-up. The instruments at this point are on the most sensitive settings. If counts are registering continuously after warm-up, the sensitivity must be reduced. This step is accomplished by turning the RANGE dial on the VM-103 one click clockwise (from .01g to .03g). If continuous counting is still observed, turn the RANGE dial to its original setting (.01g) and push the ATTEN switch on the counter to X10. If continuous counting still occurs, recheck all the connections or wait for a quieter period of the day.

When a sensitivity setting is found that produces only intermittent counts or no counting at all for 1/2 min, zero the display, activate the

COUPLER
FOR CONNECTING ACCELEROMETER
TO WAVE GUIDE



WAVE GUIDE
SEGMENT
CONNECTION



STEEL WAVE GUIDE

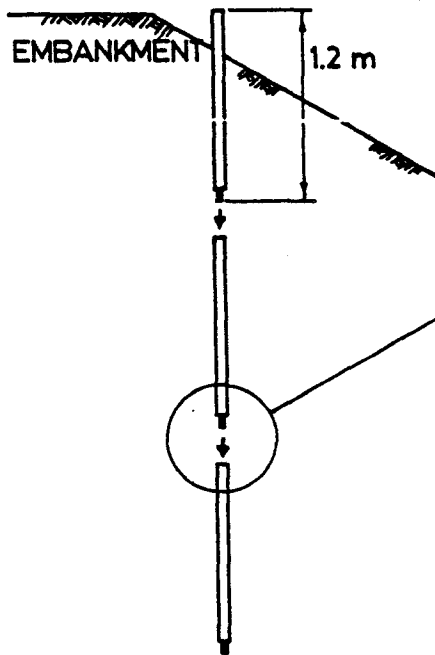


Figure B-2. Details of wave guides used in acoustic emission monitoring. Wave guide is driven in 4 ft segments and extended with threaded connections to the desired depth or refusal. (1 ft = 0.3048m)

counting, and record the number of counts at 1-min intervals for 5 to 15 min. With little or no wind and otherwise quiet environmental conditions, the most sensitive initial settings should be satisfactory. Such conditions are usually achieved early in the morning. Remain as motionless as possible during the monitoring period. This sequence should be repeated at each monitoring location.

All instrument settings and counting data should be entered on the monitoring sheets provided, one for each location. Any reading believed to have been caused or affected by environmental conditions (gust of wind, low flying airplane, movement of yourself or nearby bird or animal, etc.) should be so marked on the monitoring sheet in the COMMENTS column. This observation is very important and should be strictly attended to. A sample monitoring sheet is shown in Figure B-3.

Please note that when fully charged, the battery pack in the Hewlett-Packard counter will provide approximately 5 hr of continuous field use. When the batteries have fully discharged, the LOW BATTERY light will come on and the pack must be recharged for a full 18 to 24 hr. CAUTION: do not exceed 24 hr of charge. To charge, attach AC power cord to back of counter chassis, plug into 110-volt outlet, switch battery pack to CHARGE, and leave counter OFF. A battery-use tag is attached to the battery pack and should be marked after each use to determine when recharge is necessary.

ACOUSTIC EMISSIONS MONITORING POINT

Location:

Depth:

[illegible]

Figure B-3. Sample monitoring sheet.

APPENDIX C

APPLICATION OF ACOUSTIC EMISSION MONITORING IN SEEPAGE

Sowers (1) suggests the 40% of all earth dam failures are caused by seepage in whole or in part. Seepage can be of the controlled variety, as analyzed in flow net studies by use of Laplace's Equation, or can lead progressively to high-velocity flow, then piping, collapse of soil arches, and subsequent seepage failure. Seepage flows also occur around outlet pipes placed beneath the dam for control of the upstream reservoir level or through holes initiated by burrowing animals. Whatever the source, the fact remains that water does indeed flow through soil voids and that this flow may be an emissive phenomenon. The first potential application of acoustic emission monitoring of seepage was site No. 15, which is cited in Table 5 of the text. The problem was brought to our attention by a site developer who was losing water from a lake created by a small earth dam. The dam had a maximum height of 3.6 m (12 ft) and was approximately 370 m (1,200 ft) long. While grouting was the obvious solution to the problem, the cost involved in grouting the entire length off the dam was prohibitive. Thus a series of borings was made along the axis of the dam, and seepage tests were conducted with the results shown in Figure C-1. The results indicated that the 62-m (200-ft) section between borings B-3 and B-4 seemed most likely to be the major contributor to the loss of water.

Since open borings were available, acoustic emission monitoring was also attempted. However, the plastic casing of the boring could not conduct emissions and was not therefore suitable as a wave guide. Instead, a heavy steel wire was inserted down to the bottom of the borehole where the seepage was presumably occurring. Acoustic emission count rates were recorded, and the AE counts per minute were also plotted (Figure C-1). The general agreement between seepage and acoustic emission activity in the zone from B-3 to B-4 should be noted. The actual mechanism causing the emissions is not known (perhaps it was the turbulent flow of the seepage against and around the casing), but the use of the acoustic emission technique in monitoring for seepage seems to hold great promise.

Current efforts in evaluating acoustic emissions emanating from seepage flow are being directed at laboratory studies for the following reasons: to understand the basic phenomena involved; to help determine whether an acoustic emission detected in an embankment or earth dam is due to soil movement alone or to some combination of soil movement and seepage; and to determine the location and extent of subsurface leaks from reservoirs, lagoons, deep-well pumping, pipeline leakage, etc.

A seepage apparatus was constructed to systematically vary soil types and seepage velocity and to examine the tendency to cause emission. The apparatus (Figure C-2) is a plastic cylinder 20 cm (8 in.) in diameter into which 46 cm (18 in.) of soil is placed. Water is introduced at the bottom of the column of soil through a perforated base plate and flows upward where it is collected and measured at the top. The velocity of fluid flow is controlled by regulating the pressure under which the fluid is introduced. Forcing the flow upward ensures complete saturation and a more uniform velocity profile. The wave guide is a shortened version of the actual 12-mm (0.5-in.) steel wave guides used in the field and has been cut into two segments. The first segment extends from the exterior through the plastic wall and terminates just inside the column. This short segment is threaded to receive an accelerometer on the exterior end, and an 18-cm (7-in.) extension on the interior end. The longer segment is embedded in the soil column and serves as the primary receiver for acoustic emission signals.

Each test must be run at least twice. During the first run, only the short wave guide segment is in place. The resulting acoustic emission rate (counts/sec) represents boundary effects and extraneous noise. The soil is then removed, the wave guide extension is inserted, the soil is replaced at the same density as before, and the test is repeated at the same flow velocity. The difference in acoustic emission rates registered for the two tests is that rate transmitted by the longer extension alone, exclusive of any boundary noises.

The soil being tested is Ottawa sand with an in-place density of 1.70 g/cm^3 (106 lb/ft^3) and a corresponding void ratio of 0.55. The acoustic emission count rate as a function of the velocity of water flowing through the voids is given in Figure C-3. There is a general tendency of increasing emission rate (of both noise and seepage) with increasing water flow velocity, but considerable scatter exists. Action of these seepage tests is under way using acoustic emission filters and different pickup transducers sensitive to higher frequencies than those used in tests described. Additional information will be published.

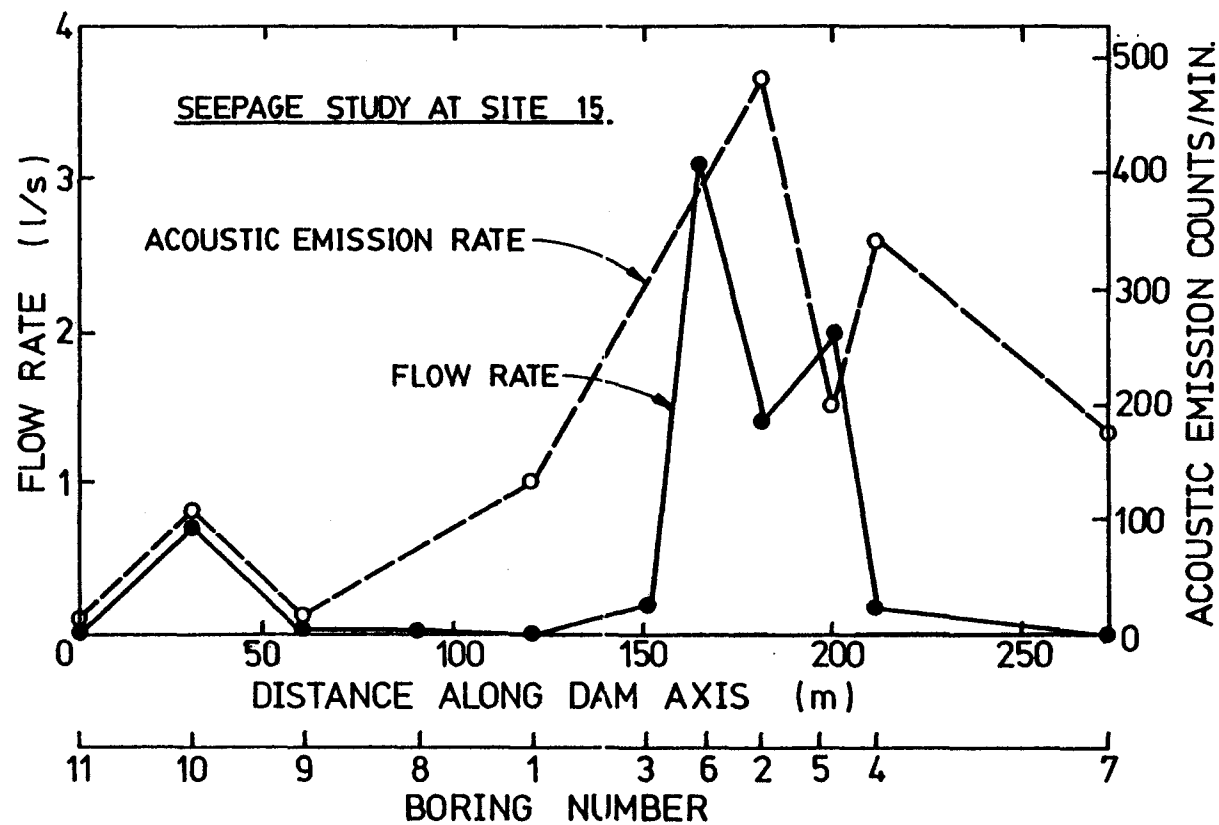


Figure C-1. Flow rates and acoustic emission rates compared for seepage study at site No. 15.

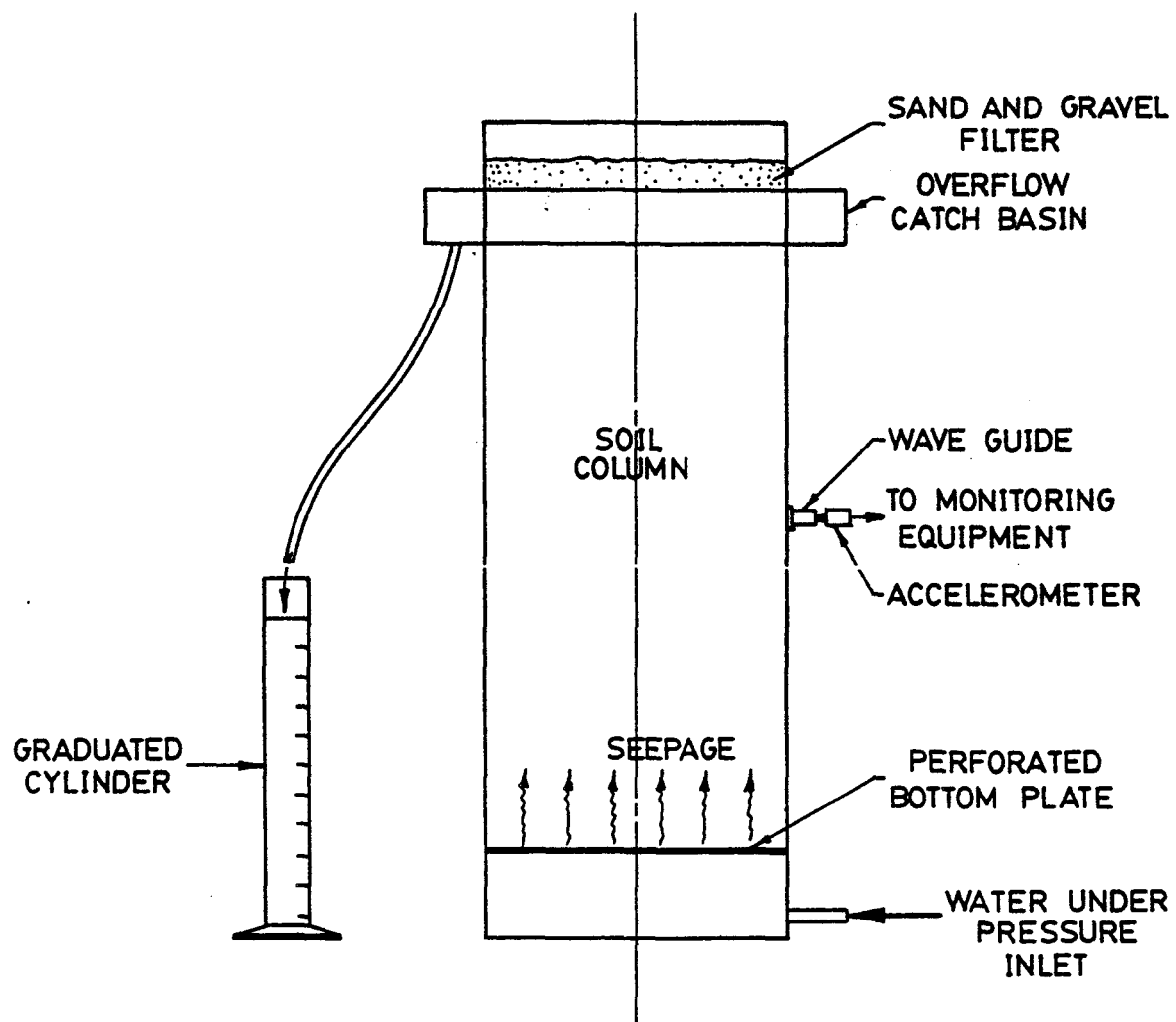


Figure C-2. Experimental setup for study of acoustic emission results from soil void seepage.

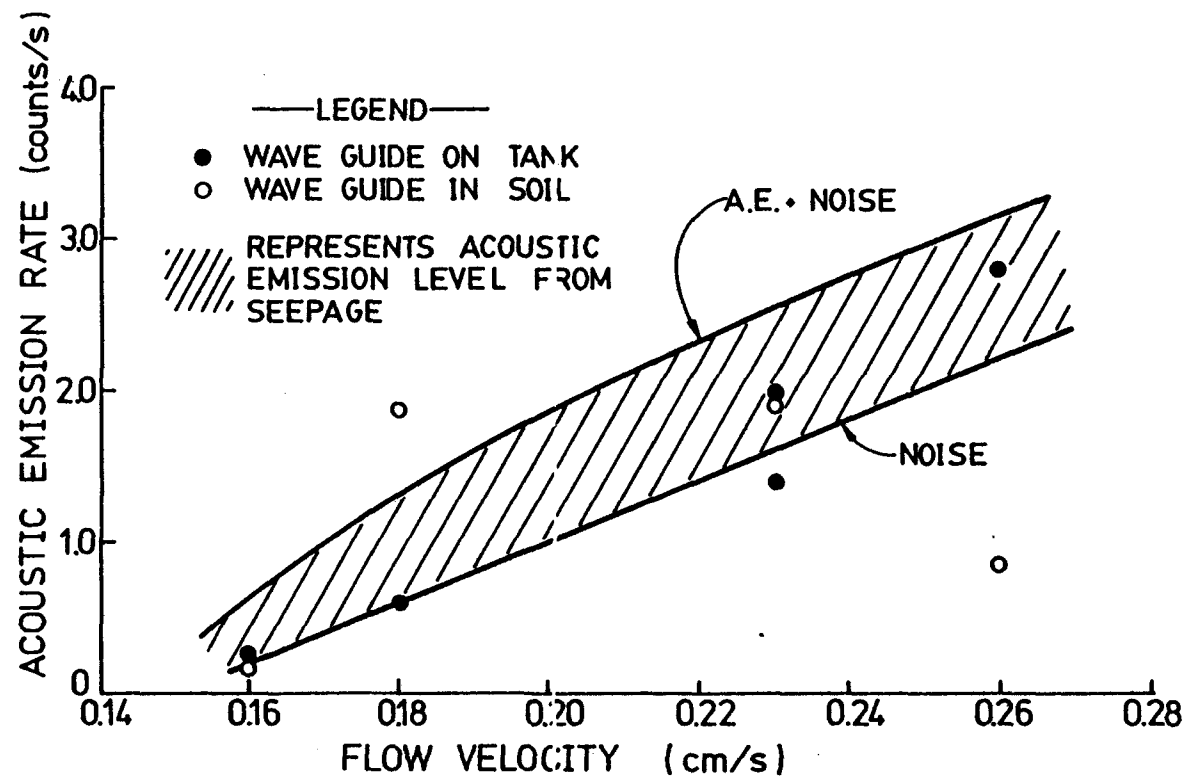


Figure C-3. Acoustic emission rates for flow of water through a column of Ottawa sand.

APPENDIX D

APPLICATION OF ACOUSTIC EMISSION MONITORING IN PIPELINES

A critical feature of the acoustic emission technique in monitoring earth dams is a method of transmitting the emissions from their source within the soil mass to the ground surface where they can be monitored. This transmission is being accomplished by means of steel rods that in some instances are 76 m (250 ft) long. The similarity of long steel rods to pipelines is obvious, and thus an extension of the acoustic emission monitoring into pipeline leak detection seems natural. Pipeline leakage is indeed a serious concern, for in 1974 there were 557 oil pipeline spill incidents reported by the U.S. Coast Guard (57). These breaks resulted in an economic loss of 24 million liters (6.3 million gal) of oil, along with the attendant environmental consequences. The trend toward installing more pipelines of larger diameter only increases the need for leak detection systems. An equally important area for the application of pipeline leak detection methods is the rapidly growing number of chemical pipelines, which are mainly found in internal plant systems. Actual data on flow rate and volume of material transported are not so well quantified as with interstate petroleum systems but are significant to this study, for stress corrosion problems are abundant in this type of pipeline (58).

Various commercially available leak detectors and monitoring systems are designed to detect leaks immediately after they occur or to detect pipeline cracks that would eventually lead to leaks. These systems can be categorized as follows: flow monitoring (quantity, rate); pressure monitoring (drop, wave); acoustic methods (passive, impact); mobile systems (active, magnetic flux); eddy current methods (inertia, probolog); and radioactive methods.

Clearly, no one system will serve all situations, and thus it is necessary to characterize each technique for its range of applicability. This appendix concentrates entirely on acoustic methods and on the acoustic emission technique (a passive method) in particular. In this technique, the propagation of elastic waves along the pipeline is the basis of the method. Just what type (mode) of elastic wave is generated in the pipeline is rarely discussed by those using the technique. Furthermore, the attenuation (damping) and velocity of the elastic wave as it traverses the pipeline is usually not mentioned explicitly and is left for on-site experimentation (which is both expensive and time consuming). For more details, the reader is directed to references 59 and 60. The object of the first phase of the study was to monitor leaks from small pipe sections in the laboratory, and that of the second phase was to field-monitor leaks and to investigate the possibility of leak location by the acoustic emission signals.

Though it is recognized that any type of leak in a pressurized pipeline is undesirable and serious, many of these leaks do occur and often persist for considerable periods of time. Such leaks range from small (hence, nuisance type) to sufficiently large to warrant concern that crack propagation and pipeline rupture will eventually occur.

To evaluate the possibility of leak detection using acoustic emission techniques, a 1.27-cm (1/2-in.) diameter hole was drilled near the center of a 1.2-m (4-ft) long, closed-end, 15.2-cm (6-in.) diameter steel pipe. Into this hole was placed a plug containing a small hole carefully drilled to a known diameter. Several such plugs were fabricated, with hole diameters ranging from 0.33 to 1.98 mm (0.013 to 0.078 in.). The holes were temporarily capped, and the pipeline was pressurized using air, water, and light machine oil separately as the internal pipe media. The acoustic emission monitoring scheme was essentially the same as that shown in Figure 1 (text), except that the pickup accelerometer used for this set of tests had a flat frequency response from a few Hz to 10 kHz. Using this system, it was possible to detect accelerations as low as 0.01g.

When sufficient pressure was reached, usually 1380 kN/m² (200 psi), the temporary cap was removed from the leak, and pressure and acoustic emission data were recorded as the material escaped. Figures D-1, D-2, and D-3 show these results for air, water, and oil as the escaping medium. A number of tests were run using a variety of hole sizes. For the air response (Figure D-1), an acoustic emission rate was monitored (i.e., counts/sec), but as a result of the rapid loss of pressure in the water and oil tests (Figures D-2 and D-3), a cumulative acoustic emission count was recorded. From these response curves, a series of observations can be made:

1. Greater internal pipe pressures cause greater acoustic emissions to occur.
2. In all cases, the acoustic emission response is approximately linear (each curve is the average of about five tests).
3. At a given internal pressure, the larger the hole size the greater is the acoustic emission response.
4. From these data, it appears that air is more emissive than water, which in turn is more emissive than oil. This conclusion is reasonable because the acoustic emissions are in reality noise created by the escaping medium within the pipeline. Because this is a friction phenomenon, it seems reasonable for the liquids to act as lubricants (the oil more than the water), which has the effect of diminishing the emission levels.

The first field study was made on an insulated 7.6-cm (3-in.) steam line that had a constant source leak in the packing of a valve stem. The detection system consisted of an accelerometer attached to a 6.3-mm (1/4-in.) diameter, 30-cm (12-in.) long steel rod wave guide that was pushed through the insulation making firm contact with the pipe being monitored. The response of the pickup transducer was resonant at 5 kHz and was attached to an amplifier and then to an electronic counter.

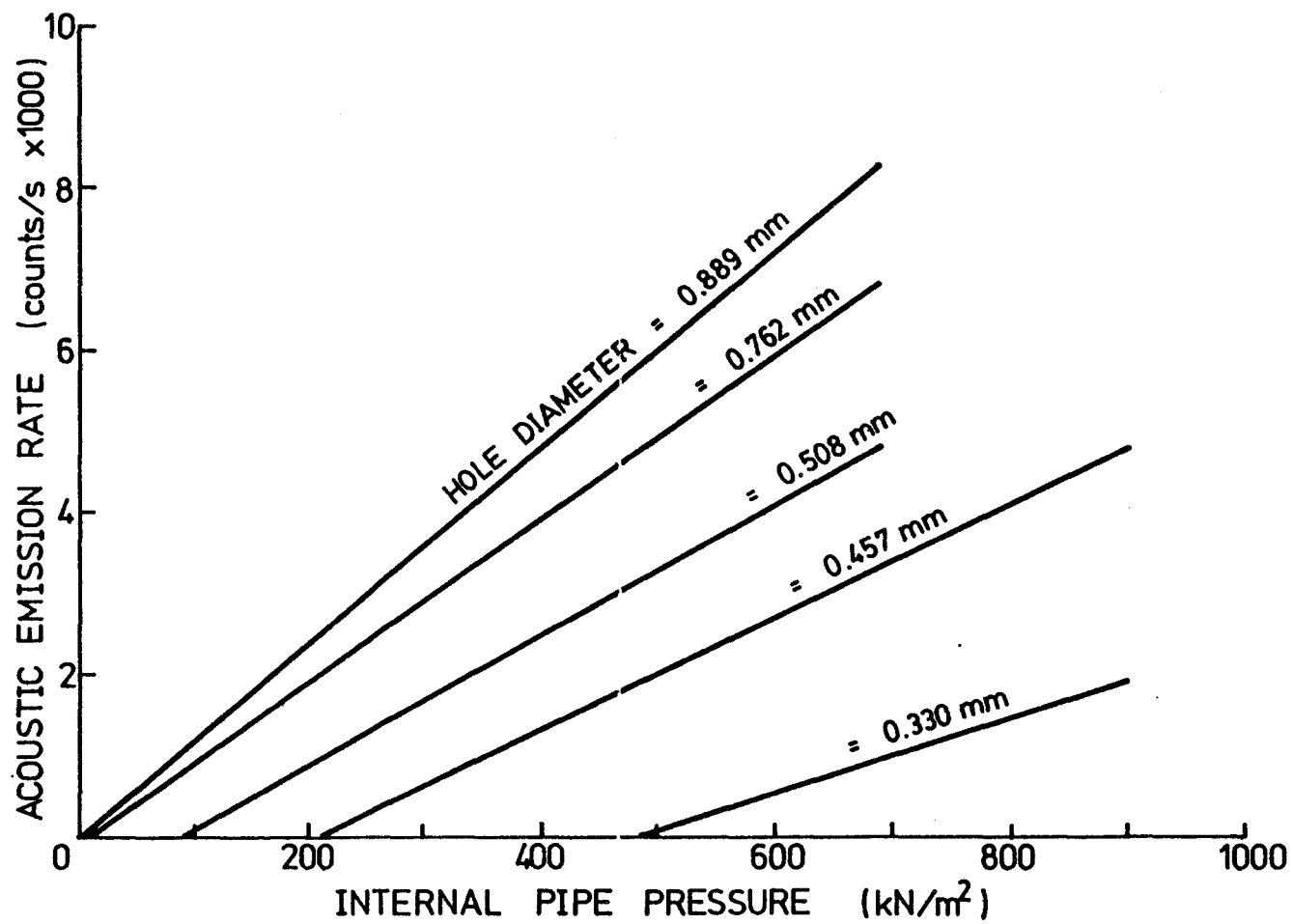


Figure D-1. Acoustic emission count rate versus internal pipe pressure for air leaking from 15.2 cm (6-in) diameter pipe.

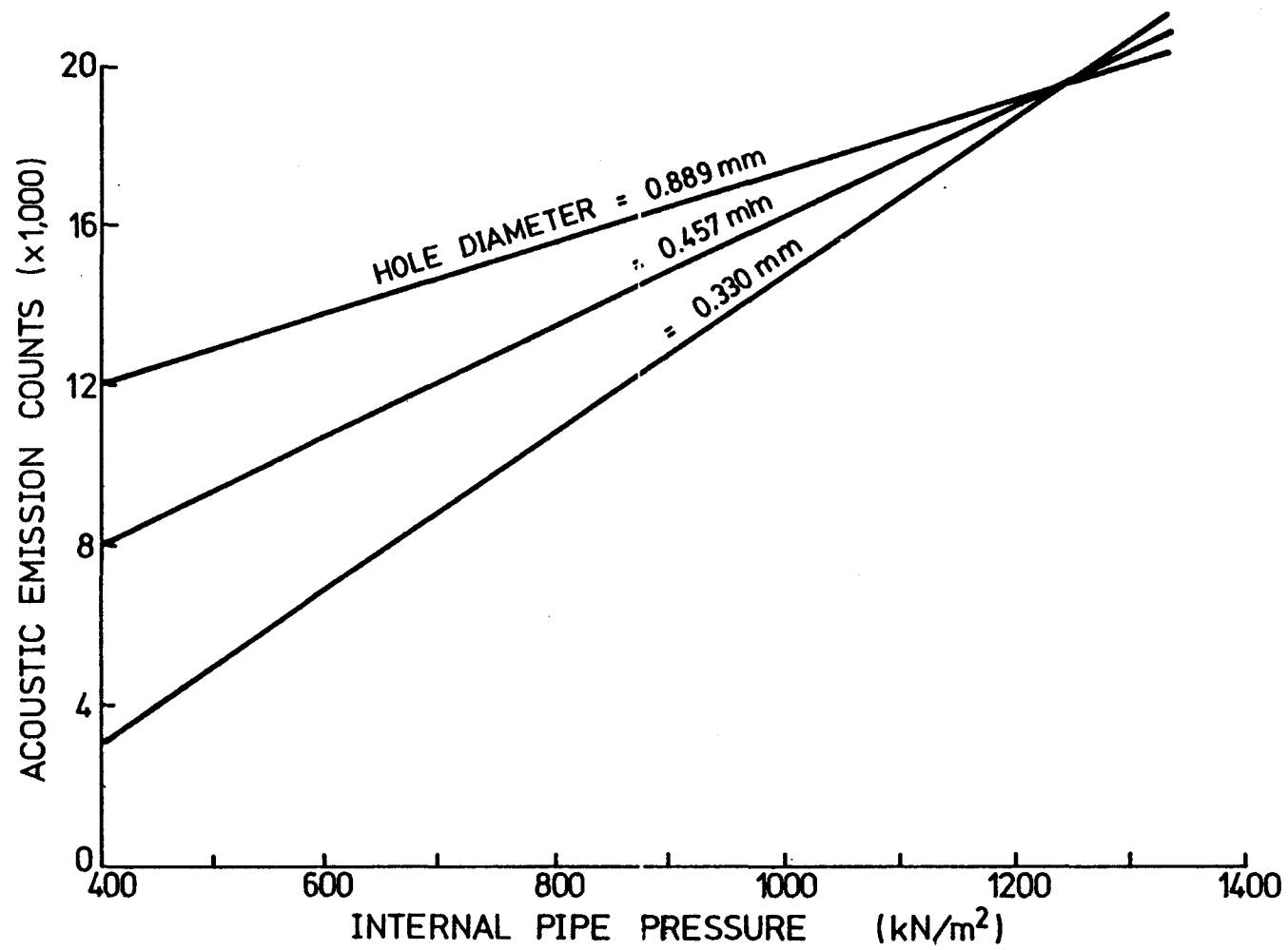


Figure D-2 Acoustic emission counts versus internal pipe pressure for water leaking from 15.2 cm (6-in) diameter pipe.

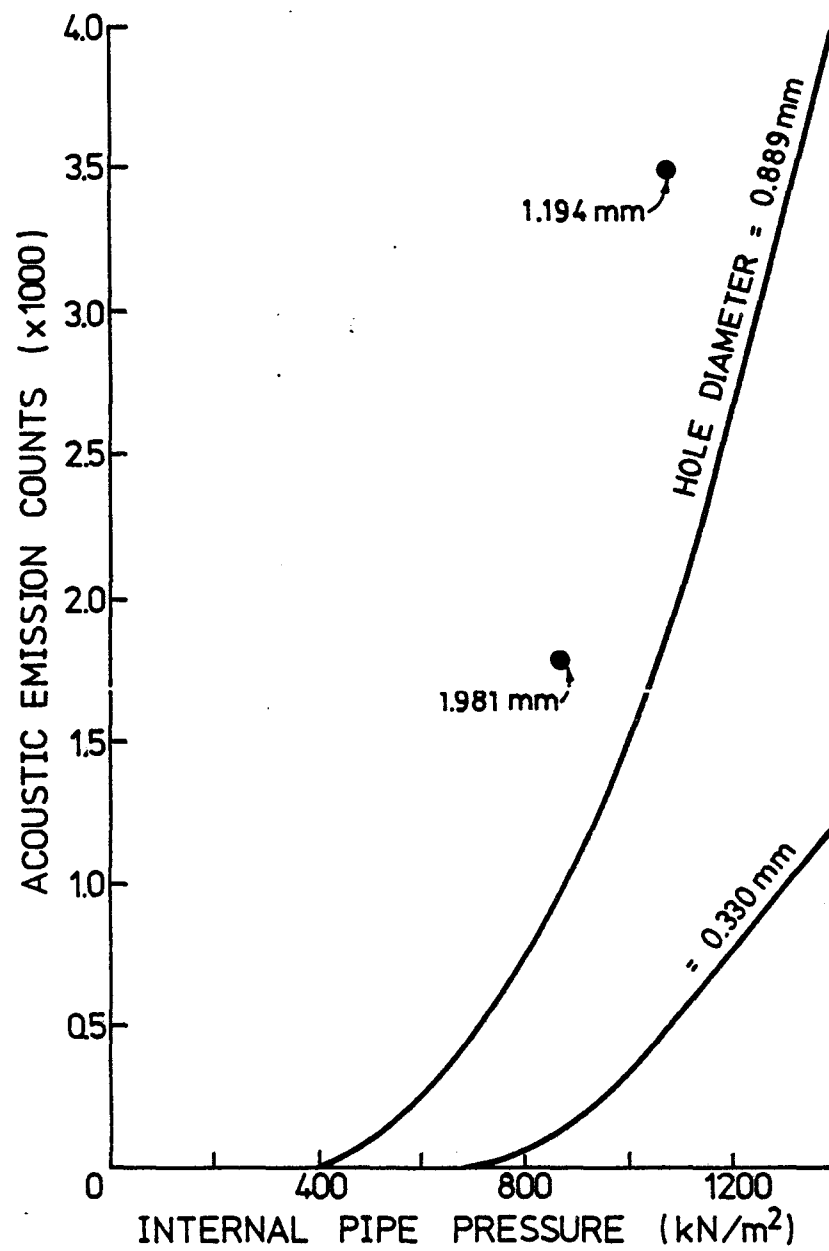


Figure D-3. Acoustic emission counts versus internal pipe pressure for oil leaking from 15.2 cm (6-in) diameter pipe.

A series of readings was taken at successive distances from the leak. These readings were obtained from the amplifier (for signal level in acceleration units, i.e., "g's"), and from the counter (for acoustic emission data in counts per second). Figure D-4 shows these results, where the amplitude response is seen to be approximately linear and the acoustic emission response is exponential. It is significant that the leak signal becomes indistinguishable from the background noise at this particular site beyond approximately 30 m (100 ft).

The second field study was conducted at the same site on a similar steam pipe that functioned as a pulsating bleeder line. The pulse was set at 15-sec intervals, and the leak lasted for a 5-sec duration. Instrumentation was the same as with the first field study. Data were taken on both sides of the leak. Although signal amplitude levels were obtained, they were not so sensitive as the acoustic emission rate readings taken from the counter. These latter data are plotted in Figure D-5, where the response on each side of the leak is seen to agree and is approximately exponential. The signal exists in a relatively strong state for 30 m (100 ft), becomes weaker in the next 15 m (50 ft). The background noise at this site was approximately 50 to 55 dB as registered on a sound level meter. It should also be mentioned that the pulsing leak was located between straight pipe on the north side and pipe with a series of five bends on the south side. Thus, the significance of pipe bends seems to be nominal as far as signal attenuation is concerned.

Use of Equation 1 allows a graphical determination of the location of the actual leak source. The attenuation coefficient can be computed from the following formula:

$$a = \frac{8.68}{x} \ln \frac{A_0}{A_1} \quad (1)$$

where a = attenuation coefficient in dB/distance, x = distance between measured wave peaks, A_0 = initial wave amplitude, and A_1 = subsequent wave amplitude.

The computation is done by plotting the $\log (A_0/A_1)$ response against distance from some arbitrary field location data (see Figure D-6). The points fall in two straight lines that intersect at the approximate location of the leak. Furthermore, the slope of the lines gives an average attenuation coefficient of 0.98 dB/m (0.30 dB/ft), which agrees with published laboratory test data (57).

Throughout the field monitoring phase of the project, the significance of background noise (i.e., background vibration levels) cannot be overstated. When such ambient noise levels are great with respect to the signal levels being monitored, the technique is quite limited in its application. For the site described here, sound level readings of 50 to 55 dB (A-scale) were measured to give a general idea of background noise. At a more remote site, where there would be less background noise, greater equipment sensitivity could be used, thereby increasing the distances over which this type of monitoring could be utilized.

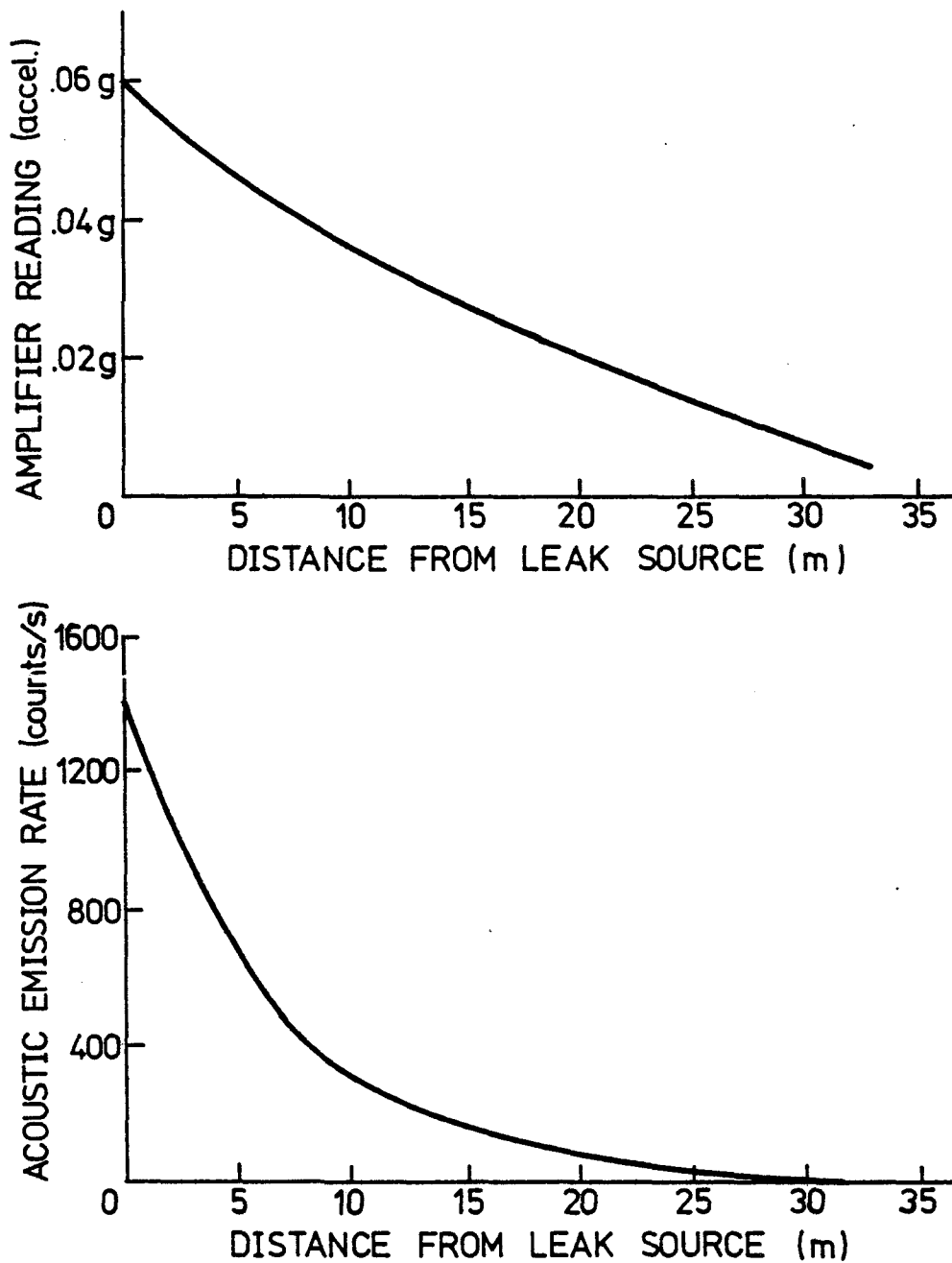


Figure D-4. Field results of signal amplitude and acoustic emission count rate for a constant-source leak in a 7.6 cm (3-in) diameter pipeline as a function of distance from the leak.

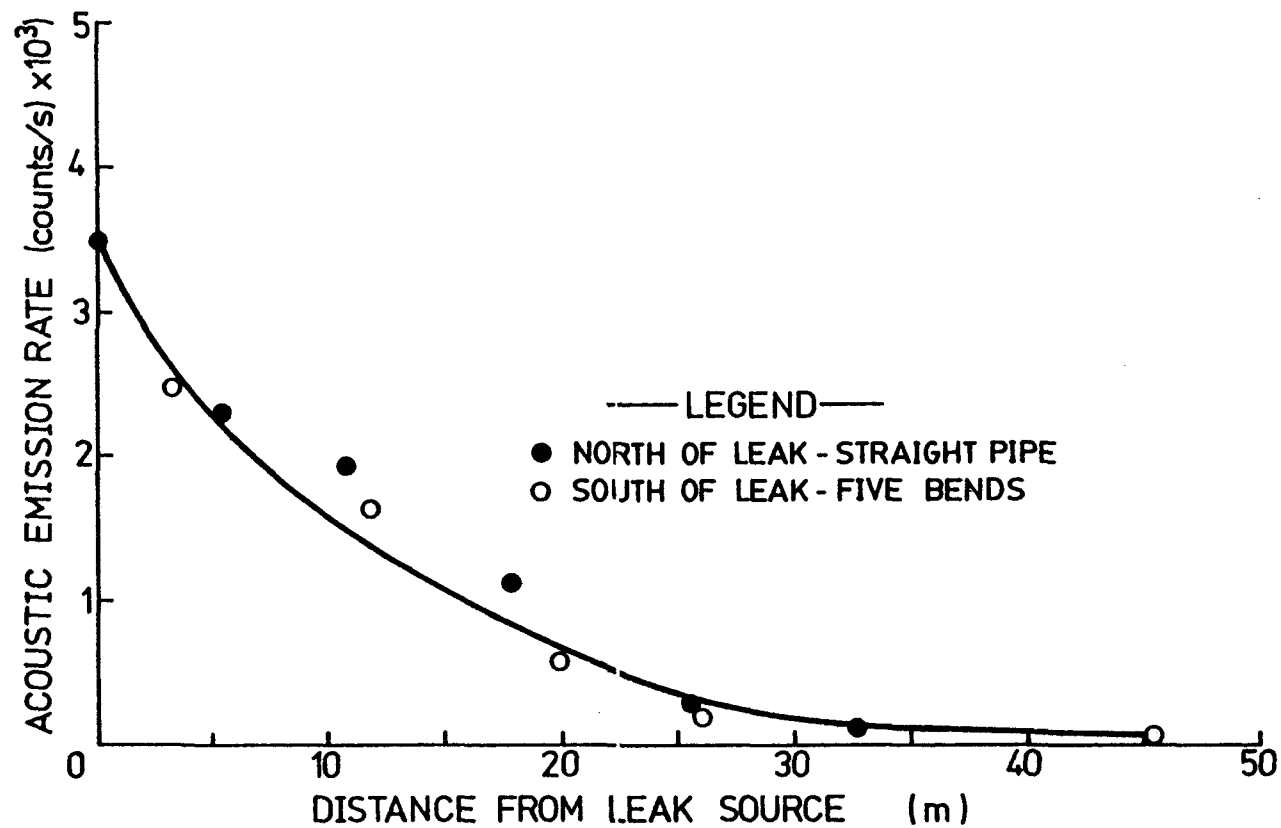


Figure D-5. Field results of acoustic emission count rate for a pulsating leak in a 7.6 cm (3-in) diameter pipeline as a function of distance from the leak and on both sides of the leak.

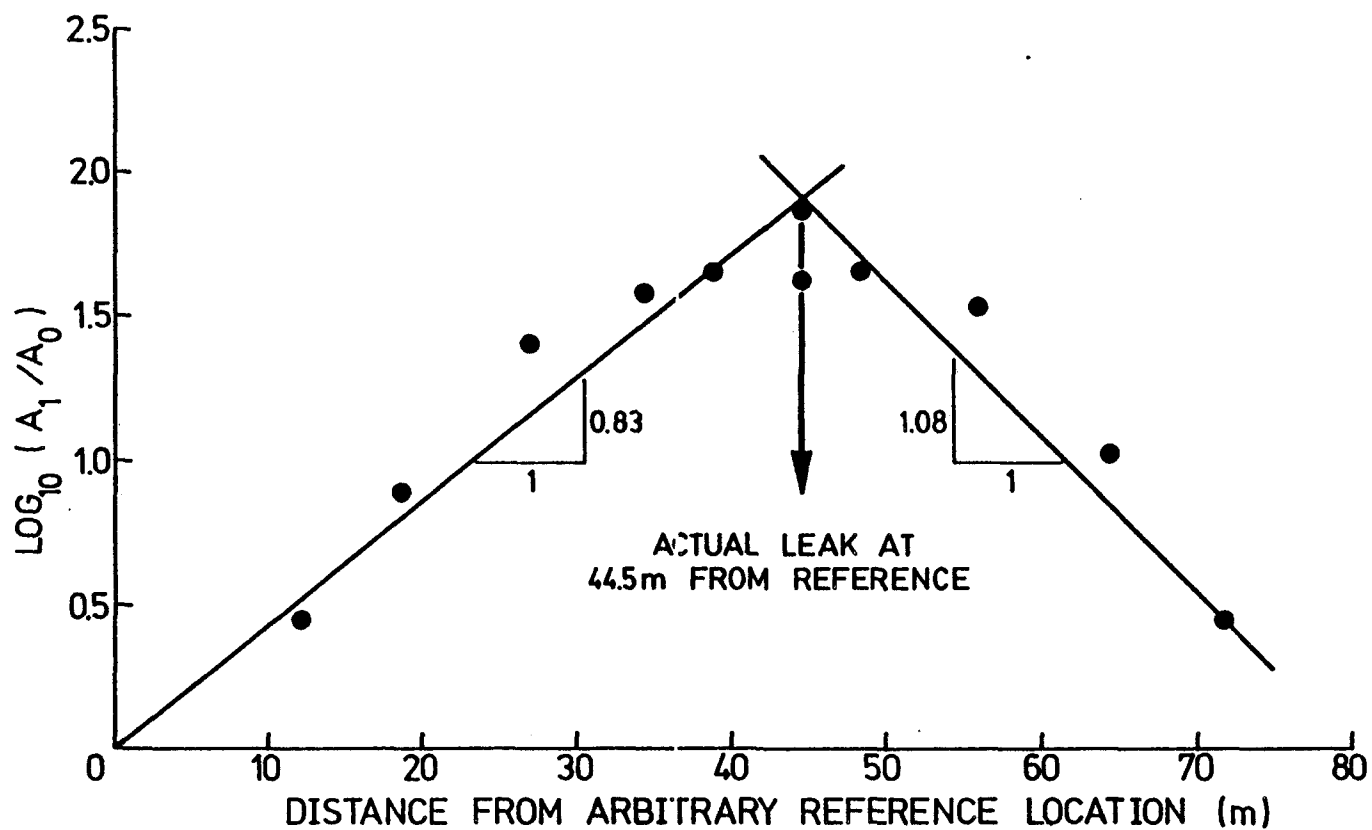


Figure D-6. Data from Figure D-5 replotted to illustrate the method of leak source location using the acoustic emission monitoring technique.

APPENDIX E

APPLICATION OF ACOUSTIC EMISSION MONITORING IN CONCRETE

When one considers a material that owes part of its strength to a noise-emitting, frictional-based composite and a natural, in-place, wave-carrying steel rod system, and one can readily visualize that reinforced concrete is an appropriate candidate for the acoustic emission monitoring technique. By attaching pickup sensors to the reinforcing bars (which are embedded only a few inches inside the concrete), a large zone of concrete can be monitored at a single pickup station. Insofar as the emissive nature of concrete itself is concerned, many mechanisms could interact. Possible acoustic emission mechanisms in plain concrete as a function of stress state are as follows:

Pure compression:

- crushing of matrix
- crushing of aggregate

Pure tension:

- bond breaking in matrix
- bond breaking between matrix and aggregate

Shear or torsion:

- sliding friction
- rolling friction
- crushing of matrix
- crushing of aggregate
- bond breaking in matrix
- bond breaking between matrix and aggregate

Prior acoustic emission work in this area of concrete monitoring (61) gives an overview of the past work, and we have attempted to supplement these efforts. Of particular interest is that the Kaiser effect ("memory" effect) seems applicable to concrete (Figure E-1), that aging of concrete can be monitored (Figure E-2), and that sustained load sequences can be analyzed (Figure E-3). In Figure E-3, the cumulative acoustic emissions increased rapidly as the load came closer to the ultimate failure load. Figure E-4 presents additional information from the same test sequence, but now the rate of emissions is plotted against time on a log-log scale. The figure shows that acoustic emissions are still being generated at a rate of about 100 counts/min after 80 hr of loading. This fact is significant, since field testing of concrete structures (as in geologic and metal structures) will require use of acoustic emission rates as opposed to cumulative acoustic emission counts to assess structural stability. The linear response of these creep tests on a log-log scale is of great fundamental

interest. The three curves have nearly identical slopes of approximately -1.0. Whether or not this behavior is a property of the concrete and its respective load state remains a subject for future research. Note that this sequence of tests (and the following series) was made using a transducer resonant at 175 kHz, a filter band width from 125 to 250 kHz, and a total gain of approximately 80 dB.

The next series of tests was performed on 10.2 x 15.2 x 76.2-cm (4 x 6 x 30-in.) beams in a flexure mode (third point loading). Figure E-5 shows the results with the transducer mounted on the compression face (single test) and on the tension face (average of three tests). In comparison, the curves are related to the total failure load. Tension, however, was observed to be the governing failure mode in the unreinforced beams. Note that the acoustic emissions detected at the tension face were considerably more numerous than those detected at the compression face at all stress levels up to tensile failure. Furthermore, above 85 percent of fracture load (tension), the acoustic emissions begin to increase rapidly. This increase is significant because it indicates that the technique may be valuable as a good precursive indicator of failure in a field monitoring scheme.

The previous experimental work dealt with plain concrete, which was seen to be emissive while in a deforming state. Future work will be directed at reinforced concrete, which is more typical of actual field structures. Initial tests will be with laboratory-sized beams in flexure, and subsequent work will be conducted on large-scale members and actual field structures.

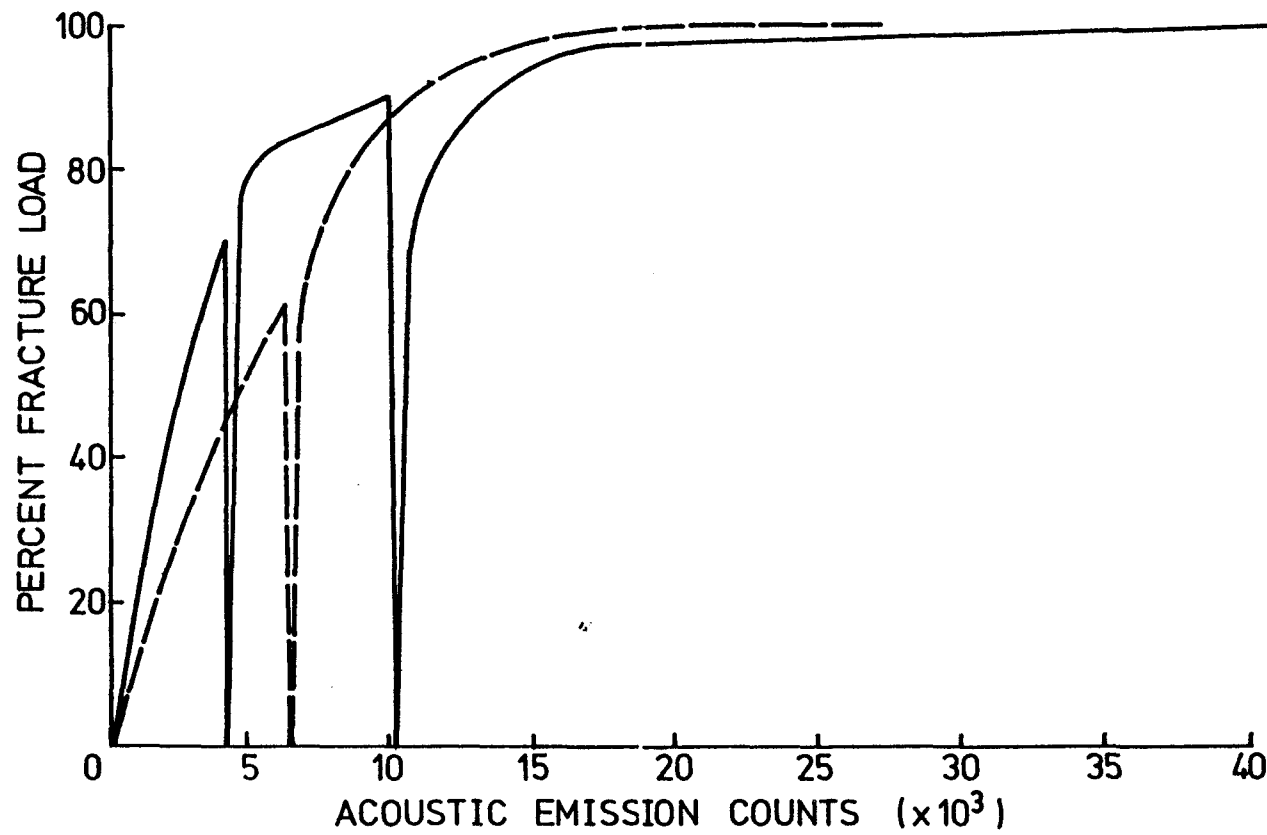


Figure E-1. Load versus acoustic emission response of 3-day-old concrete specimens showing effect of load cycling on acoustic emissions.

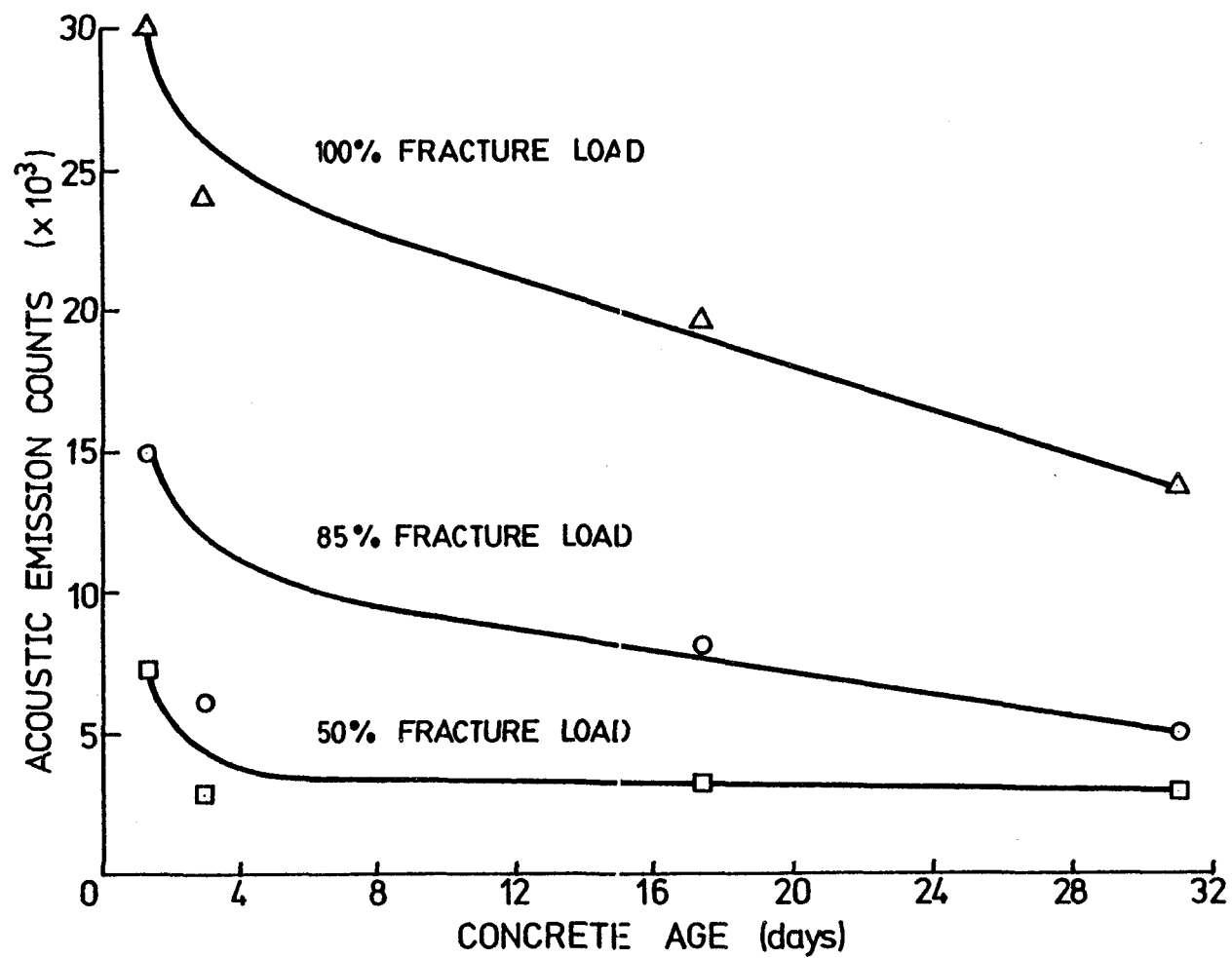


Figure E-2. Acoustic emission response of concrete cylinders as a function of age (curing time) at various percentages of ultimate fracture load.

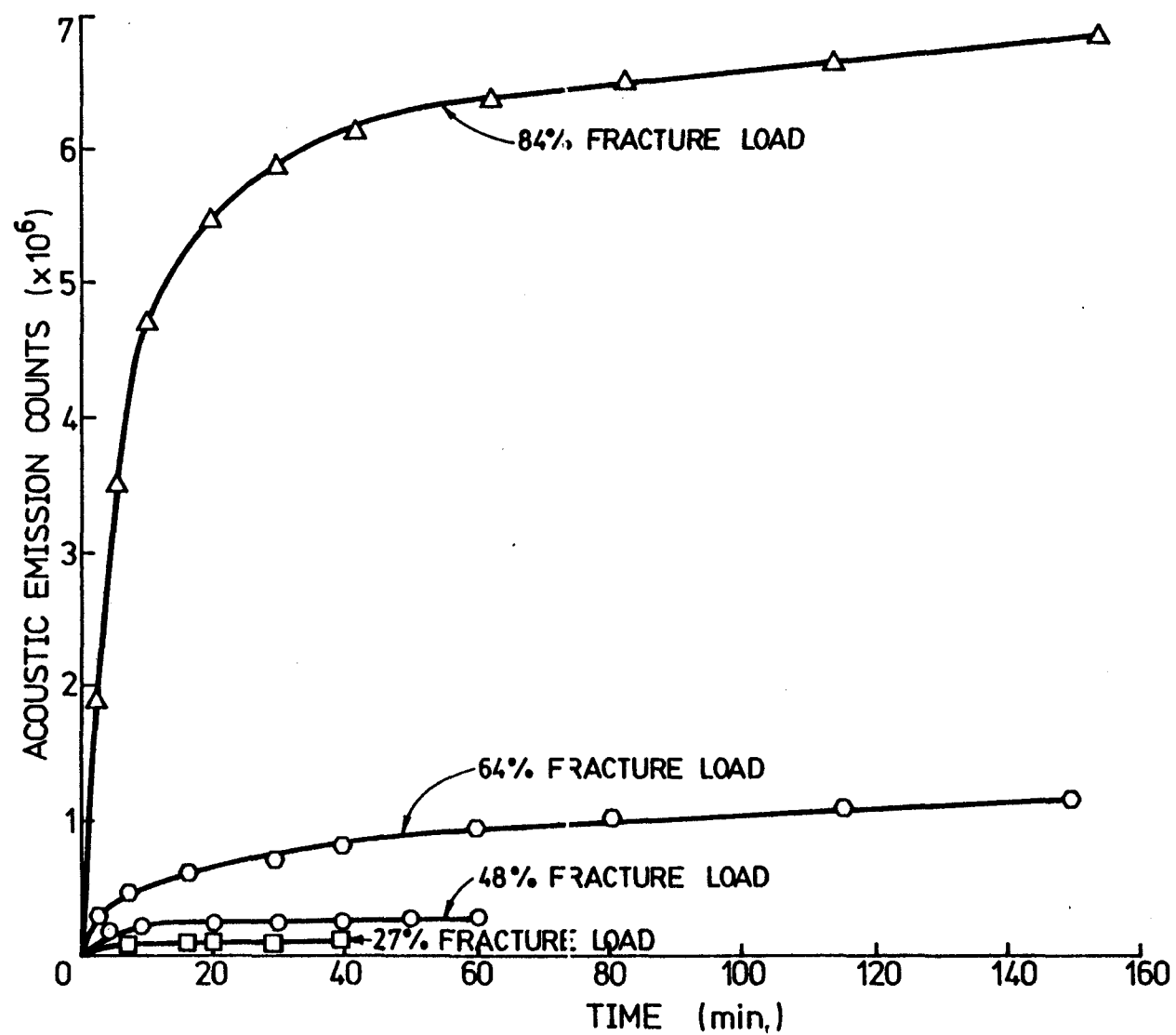


Figure E-3. Acoustic emission versus time response for creep tests (sustained-load tests) at various percentages of ultimate failure load.

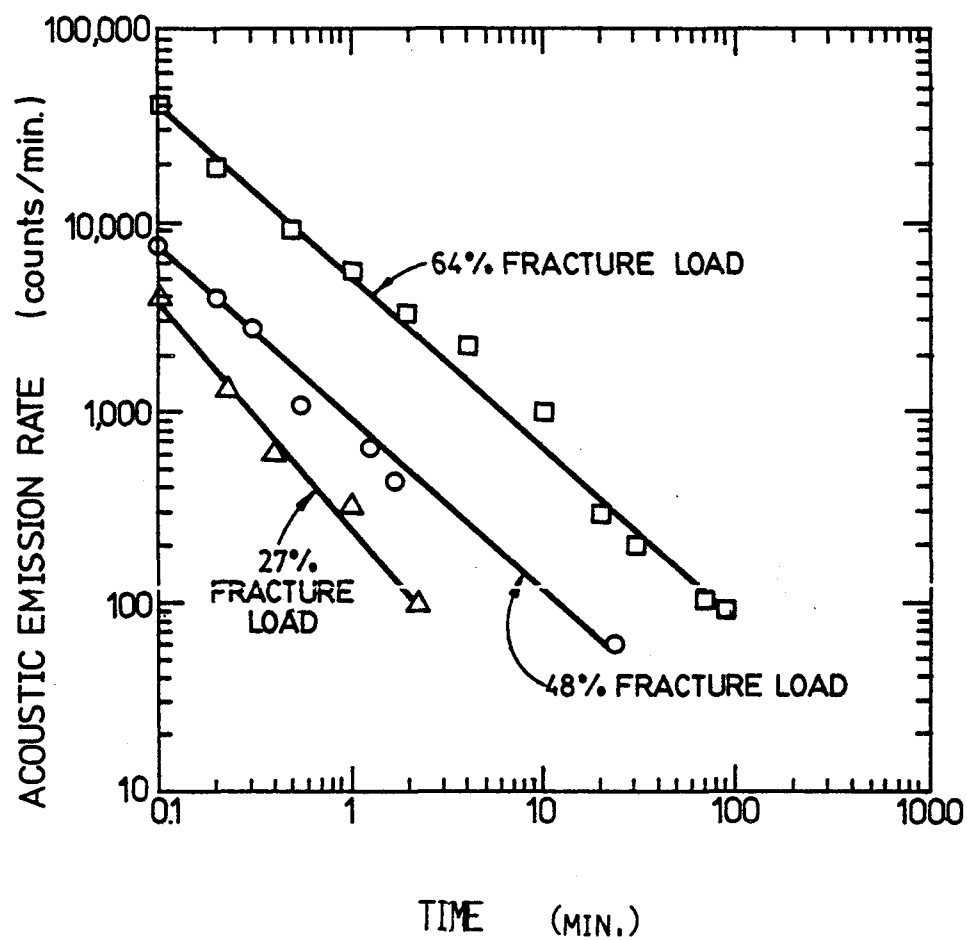


Figure E-4. Acoustic emission rate versus time response for creep tests (sustained-load tests) at various percentages of ultimate failure load over long-term monitoring.

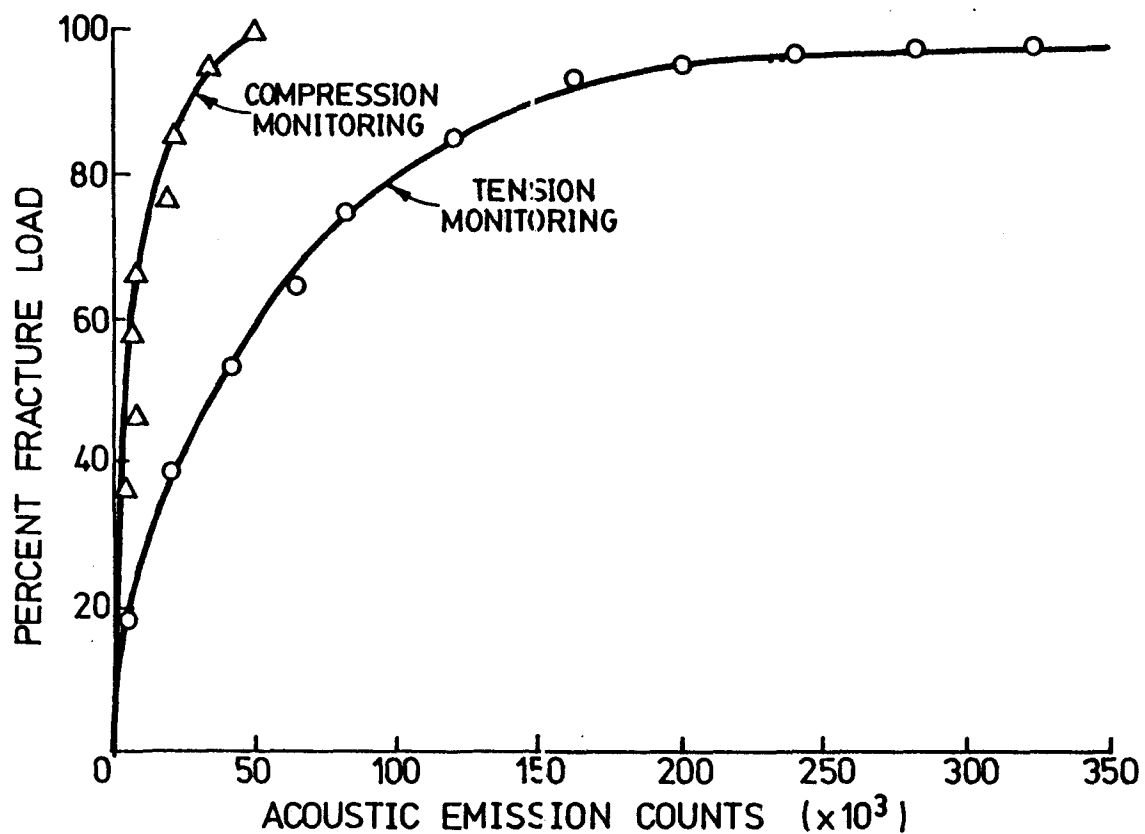


Figure E-5. Load versus acoustic emission response of concrete beams tested in three-point loading tests (flexure tests) with transducer mounted either on the compression face or on the tension face.

APPENDIX F

GLOSSARY

P-Waves - A P-wave is a longitudinal elastic wave (primary wave).

S-Waves - An S-wave is a shear elastic wave (secondary wave).

R-Waves - An R-wave is a Rayleigh surface elastic wave.

Angle of shear resistance - the same as the friction angle, ϕ (q.v.).

σ 's = stresses:

σ_1 = major principal stress

σ_2 = intermediate principal stress

σ_3 = minor principal stress

σ_0 = used when $\sigma_1 = \sigma_2 = \sigma_3 = \sigma_0$

Note that the stresses are normal to each other, and correspond to stresses in an orthogonal arrangement (x,y,z-axes).

Compression creep test - constant compressive stress is applied during the entire test (same stress top and bottom σ_1).

Deviator stress - $(\sigma_3 - \sigma_1)$, where σ_3 is the major principal stress and σ_1 is the minor principal stress.

Drained test - indicates that there is no excess pore water pressure.

Floating accelerometer - accelerometer embedded within sample.

Fixed accelerometer - accelerometer fixed in bottom end plate of compression test unit.

Failure (bulldging)- the mass deforms some what as a rubber ball does when pressed against a support plate by a parallel moveable plate to which stress is applied.

Failure (shear plane development) - the material yields by having one portion move in a plane at a sidewise angle (slope) to the other portion.

Friction angle - The friction angle is defined as:

$$\tau ("tau") = c + \sigma_n (\tan \phi),$$

where "tau" = shear stress (kN/m²)

c = cohesion (kN/m²) (may equal zero in sand)

σ_n = normal stress on shear plane (kN/m²)

ϕ = friction angle

Isostatic compression tests - the external stresses (σ_1, σ_2 , and σ_3) are all equal. $\sigma_1 = \sigma_2 = \sigma_3$ and the stress is usually designated as σ_0 .

Oedometer (consolidation) - a confined compression device in which strain (movement, change in a dimension per unit dimension) can be measured as a function of time to determine the compression characteristics of soil (as these change with time).

Triaxial Shear Creep Test - constant stress is applied to all surfaces and an extra stress is applied in one direction.

Unconfined compression test - axial (but not lateral) stress is applied during the entire test.

TECHNICAL REPORT DATA
(Please read instructions on the reverse before completing)

1. REPORT NO.		2.		3. RECIPIENT'S ACCESSION NO.	
4. TITLE AND SUBTITLE Spill Alert Device for Earth Dam Failure Warning				5. REPORT DATE	
				6. PERFORMING ORGANIZATION CODE	
7. AUTHOR(S) Robert M. Koerner Arthur E. Lord, Jr.				8. PERFORMING ORGANIZATION REPORT NO.	
9. PERFORMING ORGANIZATION NAME AND ADDRESS Drexel University Philadelphia, PA 19104				10. PROGRAM ELEMENT NO. CBRD1A	
				11. CONTRACT/GRANT NO. R-802511	
12. SPONSORING AGENCY NAME AND ADDRESS Municipal Environmental Research Laboratory--Cin, OH Office of Research and Development U.S. Environmental Protection Agency Cincinnati, OH 45268				13. TYPE OF REPORT AND PERIOD COVERED Final	
				14. SPONSORING AGENCY CODE EPA/600/14	
15. SUPPLEMENTARY NOTES Project Officer: John E. Brugger (201)321-6634					
16. ABSTRACT A spill alert device for determining earth dam safety based on the monitoring of the acoustic emissions generated in a deforming soil mass was developed and field tested. The acoustic emissions are related to the basic mechanisms from which soils derive their strength. Laboratory feasibility tests, conducted under widely varying conditions, have resulted in an instrument package consisting of a wave guide (an iron rod projecting into the earth mass), a transducer (to convert the mechanical waves transmitted from the deforming soil into an electrical signal), an amplifier (to increase the signal level), and a counter (to quantify the signal). The resulting monitoring system has been field tested at 19 sites and found to portray accurately the stability of the particular site in question. Additional detail has been added that enables the following categorization of the relative stability of the soil mass being monitored: No emissions: soil mass is at equilibrium and safe. Low emissions: continue to monitor soil mass. High emissions: soil mass requires remedial work. Very high emissions: this situation requires evacuation of downstream residents. This report was submitted in fulfillment of EPA Grant No. R-802511 by Drexel University under the sponsorship of the U. S. Environmental Protection Agency. This report covers the period from July 1, 1973, to June 30, 1979, and work was completed as of June 30, 1979.					
17. KEY WORDS AND DOCUMENT ANALYSIS					
A. DESCRIPTORS		B. IDENTIFIERS/OPEN ENDED TERMS		C. COSATI Field/Group	
18. DISTRIBUTION STATEMENT Release to Public		19. SECURITY CLASS (This Report) Unclassified		21. NO. OF PAGES	
		20. SECURITY CLASS (This page) Unclassified		22. PRICE	